Dissertation

submitted to the
Combined Faculties for the Natural Sciences and for Mathematics
of the Ruperto-Carola University of Heidelberg, Germany
for the degree of
Doctor of Natural Sciences

presented by

Diplom-Biochemikerin Julie Bachmann

born in Mainz, Germany

oral examination: …….

Dynamic Modeling of the JAK2/STAT5 Signal Transduction Pathway to Dissect the Specific Roles of Negative Feedback Regulators

Referees: PD Dr. Ursula Klingmüller

Prof. Dr. Michael Brunner

Acknowledgements

Many thanks to all the people who supported me during my work.

First of all, I would like to thank my supervisor PD Dr. Ursula Klingmüller for giving me the opportunity to work on this exciting interdisciplinary project and for her advice and guidance.

I thank Prof. Dr. Michael Brunner for being the second referee for this thesis.

I am grateful to all current and former members of our group for their continuous support, for the nice atmosphere and the stimulating working environment. I would like to thank Dr. Marcel Schilling for his computational support and fruitful discussions on mathematical modeling, Dr. Verena Becker for the joint work and scientific contributions as well as Ute Baumann and Sandra Manthey for all the technical help provided. I thank Dr. Andrea C. Pfeifer for advice as a member of my PhD committee and Dr. Alexandra Kienast for the collaboration on protein arrays. Many thanks to Dr. Lorenza D´Alessandro, Dr. Peter Nickel and Stephanie Müller for being such harmonious benchmates.

I would like to thank all the people being part of fruitful collaborations. Prof. Dr. Jens Timmer for stimulating discussions and continuous support, Andreas Raue for providing vital contributions on mathematical modeling as well as Stefan Hengl and Thomas Maiwald (FDM Freiburg) for helpful advice. Many thanks to all the members of the COSBICS project, especially Prof. Dr. Olaf Wolkenhauer and Dr. Julio Vera for the joint project on amplification.

I would like to thank Prof. Dr. Bujard (ZMBH, Heidelberg) for providing the Tet-On constructs and Lars Weingarten for stimulating discussions on the Tet-On system.

I acknowledge funding by the European Commission 6th Framework Program (FP6) as part of the COSBICS project under contract no. LSHG-CT-2004-512060.

Finally, I am deeply grateful to my friends, my sister, my brother and Frank Risse for giving me support, motivation and encouragement in their very own ways. Most of all, I thank my parents to whom I dedicate this work.

Table of Contents

Summary

Erythropoietin (Epo) acts as the key regulator of red blood cell development in mammals. During erythropoiesis, Epo initiates the JAK2/STAT5 signal transduction pathway that elicits pro-survival signals in erythroid progenitor cells. Therefore, the tight regulation of JAK2/STAT5 signaling is crucial for the fine-tuned balance of erythrocyte production. Recently, several factors regulating Epo-induced JAK2/STAT5 signaling have been identified. However, their relative contribution in controlling the dynamic behavior of JAK2/STAT5 signaling is poorly understood. To elucidate the specific roles of these negative regulators in attenuating the pathway, data-based mathematical modeling was employed.

In this study, standardized protocols were established facilitating the generation of quantitative time-resolved data of Epo-induced JAK2/STAT5 pathway activation in primary erythroid progenitor cells and the hematopoietic cell line BaF3-EpoR, which is a frequently used model system to study EpoR signaling. For the fine-tuned overexpression of negative regulators in hematopoietic cells, an inducible Tet-On retroviral vector system was developed. Systematic comparison of stoichiometries and activation dynamics of Epo-induced JAK2/STAT5 signaling in CFU-E and BaF3-EpoR cells revealed fundamental differences between both cell types, emphasizing the importance of the use of primary cells in the investigation of EpoR signaling. Genome-wide expression profiling identified potential feedback regulators of Epo-induced JAK2/STAT5 signaling in CFU-E cells. To dissect the complex roles of negative regulators that employ different mechanisms to attenuate JAK2/STAT5 signaling, a data-based dynamic pathway model was established. Calibration of the mathematical model was performed using multiple experimental data sets of Epo-induced JAK2/STAT5 signaling monitored under different conditions. The estimated parameters were fully identifiable and displayed small confidence intervals, which are required for accurate simulations. Comprehensive model analysis identified the rapid recruitment of the phosphatase SHP-1 as major mechanism controlling the early-phase kinetics of pathway activation, while the two transcriptionally induced regulators SOCS3 and CIS were elucidated as modulators of the STAT5 steady-state phosphorylation level. Furthermore, global sensitivity analysis uncovered the concentrations of SHP-1 and JAK2 as well as the parameter *SOCS3 expression* as critical to control the integral signal strength of nuclear phosphorylated STAT5, which is proportionally linked to the survival of erythroid progenitor cells.

In conclusion, by combining mathematical modeling with experimental data, the crucial regulators enabling the tight control of Epo-induced JAK2/STAT5 signaling were elucidated. The detailed understanding of the molecular processes and regulatory mechanisms of Epo-induced signaling during normal erythropoiesis can be further exploited to gain insights into alterations promoting erythroleukemia and related malignant hematopoietic diseases.

Zusammenfassung

Erythropoetin (Epo) ist der zentrale Regulator der Bildung roter Blutzellen in Säugetieren. Während der Erythropoese aktiviert Epo den JAK2/STAT5 Signalweg, der Überlebenssignale in erythropoetischen Vorläuferzellen auslöst. Daher ist die präzise Regulation des JAK2/STAT5 Signalweges wichtig für das feinabgestimmte Gleichgewicht der Produktion von Erythrozyten. Kürzlich wurden mehrere Faktoren identifiziert, die den Epo-induzierten JAK2/STAT5 Signalweg regulieren. Eine wesentliche Frage ist, zu welchem Anteil diese Modulatoren das dynamische Verhalten des JAK2/STAT5 Signalweges steuern. Um die spezifische Rolle der negativen Regulatoren bei der Abschaltung des Signalweges zu identifizieren, wurde ein datenbasierter mathematischer Modellierungsansatz gewählt.
Zur Erzeugung quantitativer und zeitaufgelöster Daten der Aktivierung des Epo-induzierten JAK2/STAT5 Signalweges in primären erythroiden Vorläuferzellen und der hematopoetischen Zellinie BaF3-EpoR, die ein häufig genutztes Modellsystem für die Untersuchung von EpoR-Signalwegen ist, wurden standardisierte Protokolle etabliert. Desweiteren wurde ein induzierbares retrovirales *Tet-On* Vektorsystem entwickelt, um eine feinregulierte Überexpression von negativen Regulatoren in hematopoetischen Zellen zu ermöglichen. Der systematische Vergleich von Stöchiometrien und der Aktivierungsdynamik des Epo-induzierten JAK2/STAT5 Signalweges in CFU-E und BaF3-EpoR Zellen zeigte grundlegende Unterschiede zwischen beiden Zelltypen auf und verdeutlichte die Bedeutung von Primärzellen in der Untersuchung von EpoR-abhängigen Signalwegen. Durch eine genomweite Expressionsanalyse konnten potentielle negative Regulatoren des Epo-induzierten JAK2/STAT5 Signalweges in CFU-E Zellen identifiziert werden. Zur Untersuchung der komplexen Rolle von negativen Rückkopplungs-(*feedback*) Regulatoren, die den JAK2/STAT5 Signalweg durch unterschiedliche Mechanismen abschalten, wurde ein datenbasiertes Modell des JAK2/STAT5 Signalweges erstellt. Die Kalibrierung des Modells erfolgte mittels umfangreicher quantitativer Daten, die unter unterschiedlichen Bedingungen generiert wurden. Die bestimmten Parameter waren vollständig identifizierbar und wiesen kleine Konfidenzintervalle auf, die wichtig für akkurate Simulationen sind. Eine umfassende Modellanalyse identifizierte die schnelle Rekrutierung der Phosphatase SHP-1 als einen zentralen Mechanismus zur Regulierung der frühen Aktivierungsphase, während die zwei transkriptionell induzierten Regulatoren CIS und SOCS3 als Modulatoren der Phosphorylierung von STAT5 in der *steady state*-Phase nachgewiesen wurden. Darüber hinaus konnten durch eine globale Sensitivitätsanalyse die Konzentration von SHP-1 und JAK2 sowie der Parameter *SOCS3 Expression* als kritische Faktoren bei der Kontrolle der integralen Signalstärke des nukleären phosphorylierten STAT5 identifiziert werden, die proportional mit der Überlebensrate von erythropoetische Vorläuferzellen verknüpft ist.
Zusammenfassend konnte durch die Kombination von mathematischer Modellierung und quantitativen experimentellen Daten die zentralen Regulatoren identifiziert werden, die eine präzise Kontrolle des Epo-induzierten JAK2/STAT5 Signalweges ermöglichen. Die detaillierten Erkenntnisse der regulatorischen Mechanismen von Epo-induzierten Signalwegen während der Erythropoese können weiterhin genutzt werden, um Einblicke in molekulare Prozesse zu gewinnen, die Erythroleukämien und verwandte hematopoetische Krankheiten induzieren.

1 Introduction

Eukaryotic cells communicate via extracellular signaling molecules to control multiple cellular processes within an organism. By interacting with specific cell surface receptors on target cells these messengers trigger cytoplasmic signal transduction pathways, which lead to the modification of gene expression and thus regulate cellular decisions. Depending on the specific cell context and stimulus the response involves proliferation, differentiation, migration or survival.

1.1 Signaling through cytokine receptors

An important group of extracellular signaling molecules are small secreted glycoproteins, called cytokines, that operate at very low concentrations. Cytokines include interferons (IFNs), interleukines (ILs), chemokines, and factors that induce the formation of blood cells. They are primarily involved in the development and regulation of the immune system, hematopoiesis and developmental processes during embryogenesis. Secreted by a wide variety of cells, their mode of action may be endocrine, paracrine or autocrine. To initiate their specific functions, they interact with cell surface receptors of the cytokine receptor superfamily, which are classified in type I, e.g. IL2-6, erythropoietin (Epo), prolactin (PR), growth hormone (GH), and type II, e.g. IFN-α, -β, -γ receptors. Functional receptors consist of a signal-receiving extracellular domain, a single transmembrane domain, and a signal-transducing cytoplasmic domain that lacks intrinsic enzymatic activity and therefore associates with members of the Janus kinase (JAK) family to initiate intracellular signal transduction pathways (Aaronson and Horvath, 2002). Although many different signaling cascades are activated by cytokine receptors, the JAK/ signal transducer and activator of transcription (STAT) pathway plays a central role in transmitting and processing the information received from cytokines within eukaryotic cells.

1.1.1 The JAK/STAT signaling pathway

JAKs have first been described by studies of transcriptional activation in response to interferon α (IFNα) and interferon γ (IFNγ) (Schindler et al., 1992). They represent a family of four non-receptor tyrosine kinases, JAK1, JAK2, JAK3 and Tyk2. Being pre-associated with the cytoplasmic domain of cytokine receptors, these kinases are activated by trans-phosphorylation upon cytokine-induced receptor dimerization or re-organization. Activated JAKs subsequently phosphorylate tyrosine residues within the cytoplasmic tail of the

receptor, providing docking sites for SH2 domain containing STATs (Aaronson et al., 2002). STATs comprise a family of seven structurally and functionally related proteins: STAT1, STAT2, STAT3, STAT4, STAT5a, STAT5b and STAT6. As latent transcription factors, STATs reside in the cytoplasm until they become activated by tyrosine phosphorylation (Fig. 1). Phosphorylated STATs rapidly dimerize and translocate into the nucleus to activate gene transcription (Levy and Darnell, 2002). For this purpose, they bind to gamma-activated sequence (GAS) elements in the promoter regions of their target genes that are characterized by the consensus sequence TTNCNNNAA (Horvath, 2000; Xu et al., 1996). The precise mechanism of STAT entry into the nucleus still remains unknown. The large size of these protein complexes (~180 kD for the STAT dimer) implies that they require facilitated transport in the nucleus (Mattaj and Englmeier, 1998). Binding of STAT to importin, one of the subunits of the nucleocytoplasmic transport machinery, has been described and, in at least some cells, also unphosphorylated STATs can enter the nucleus (Reich and Liu, 2006). Dephosphorylation of STAT occurs in the nucleus and is an important signal for the export into the cytoplasm, which may be mediated by Crm1, a nuclear export protein (Marg et al., 2004).

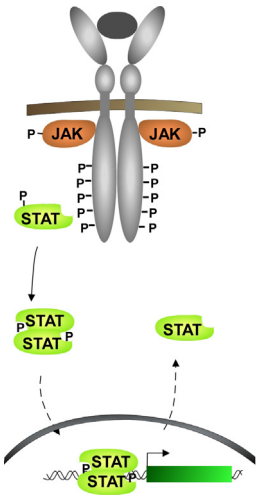

Fig. 1. The JAK/STAT signal transduction pathway. Cytokine-induced receptor oligomerization or reorganization activates pre-associated JAKs by tyrosine trans-phosphorylation. Activated JAKs phosphorylate tyrosine residues of the cytoplasmic domain of cytokine receptors, thereby providing binding sites for SH2-domain containing STATs. STAT molecules become tyrosine-phosphorylated by JAKs, dissociate from the receptor and dimerize. STAT dimers translocate to the nucleus and induce target gene expression. After dephosphorylation in the nucleus, the dimers dissociate and monomeric STATs re-enter the cytoplasm.

1.1.2 Structure and function of JAKs and STATs

The unique structure of JAKs clearly distinguishes them from other members of protein tyrosine kinase families. The most intriguing feature of these proteins are two adjacent domains: a C-terminal kinase domain (JAK homology 1, JH1) and a catalytically inactive pseudokinase domain (JH2), which has a kinase domain fold but lacks crucial residues for catalytic activity and for nucleotide binding (Baker et al., 2007) (Fig. 2). This characteristic structure gives the family their name after Janus, the Roman God of gates and doors who is represented by a double-faced head looking in opposite directions. Growing evidence indicates that the JH2 domain is required for inhibiting the basal activity of the kinase domain (Saharinen and Silvennoinen, 2002; Saharinen et al., 2003). The N-terminal half of JAKs

contains two motifs, a region (JH3-4) resembling a src-homology (SH2) domain and a four-point-one, Ezrin, Radixin, Moesin (FERM) domain. Despite of the homology to SH2 sequences, the SH2-like domain does not appear to bind phosphotyrosine residues and its function still remains to be defined (Higgins et al., 1996; Radtke et al., 2005). The FERM domain (JH6-7) has been shown to mediate association with receptors by binding to the box1/proline-rich membrane proximal region of cytokine receptors (Pellegrini and Dusanter-Fourt, 1997). Moreover, recent studies suggested that residues within the FERM domain are important for hydrophobic core stabilization and also catalytic function (Haan et al., 2008).

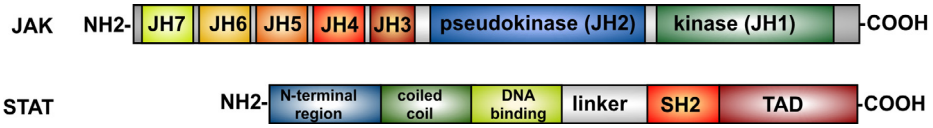

Fig. 2. Domain structure of Janus kinases (JAKs) and signal transducers and activators of transcription (STATs). Sequence analysis indicated conserved domains for JAKs and STATs. JAKs contain seven JAK homology domains (JH1-7). The catalytic activity of the kinase domain JH1 is regulated by interaction with the pseudo-kinase domain JH2. JH3-JH7 mediate protein-protein interactions, e.g. receptor association. STATs contain six defined domains. The N-terminal region is critical for STAT function, i.e. nuclear import and export. The coiled domain is involved in receptor binding and association with regulatory proteins. The SH2 domain binds to specific phospho-tyrosine residues of other STATs or of receptors. The C-terminal transactivation domain (TAD) varies among family members and its detailed function is not fully understood. Abbreviations see text.

Similar to most transcription factors, STATs exhibit a modular structure with six well-defined domains, including an N-terminal conserved domain, a coiled-coil domain, a DNA binding domain, a linker region, a SH2 domain and a C-terminal transactivation domain (TAD). This structure was defined by homology studies and crystallographic analysis of the core amino acids (130-710) of either dimeric STAT1 or dimeric STAT3 bound to DNA (Chen et al., 1998). The N-terminal region of STATs is well conserved among all family members and appears to be critical for STAT function, i.e. nuclear import, export or receptor binding. The coiled-coil domain adopts an alpha-helical conformation, functions in receptor binding and associates with regulatory proteins (Kisseleva et al., 2002). The DNA-binding domain is highly conserved among STATs. The linker domain functions as a spacer to maintain proper conformation between the dimerization and the DNA-binding domains. The SH2 domain is critical for the recruitment of STATs to activated receptor complexes and for STAT dimerization. Directly downstream of the SH2 domain around position 700, all STATs contain a tyrosine residue that has been found to be essential for the activation and dimerization of STATs (Darnell, 1997; Schindler and Darnell, 1995). In addition to tyrosine phosphorylation, several STATs are regulated by serine phosphorylation that is mediated by serine/threonine kinases including p38 or JNK (Khwaja, 2006). The transactivation domain varies among family members and its detailed function and specificity in transcriptional regulation of different STAT isoforms remains to be determined.

1.2 Negative regulation of cytokine signaling

Regulation of the initiation, strength and duration of JAK/STAT signaling is crucial for the control and fine-tuning of cytokine responses. Recently, several mechanisms of negative feedback inhibition have been suggested to be involved in the attenuation of cytokine responses at multiple levels (Fig. 3). These include protein tyrosine phosphatases (PTPs), suppressors of cytokine signaling (SOCS), protein inhibitors of activated STATs (PIAS), and degradation of JAK/receptor complexes through receptor-mediated endocytosis (O'Sullivan et al., 2007). Although a large number of negative regulators have been identified, the specificity and timing of these negative regulators in downregulation of distinct cytokine-induced responses are still elusive. For instance, SOCS proteins are induced in response to cytokines whereas phosphatases are constitutively expressed and may act as very early response regulators.

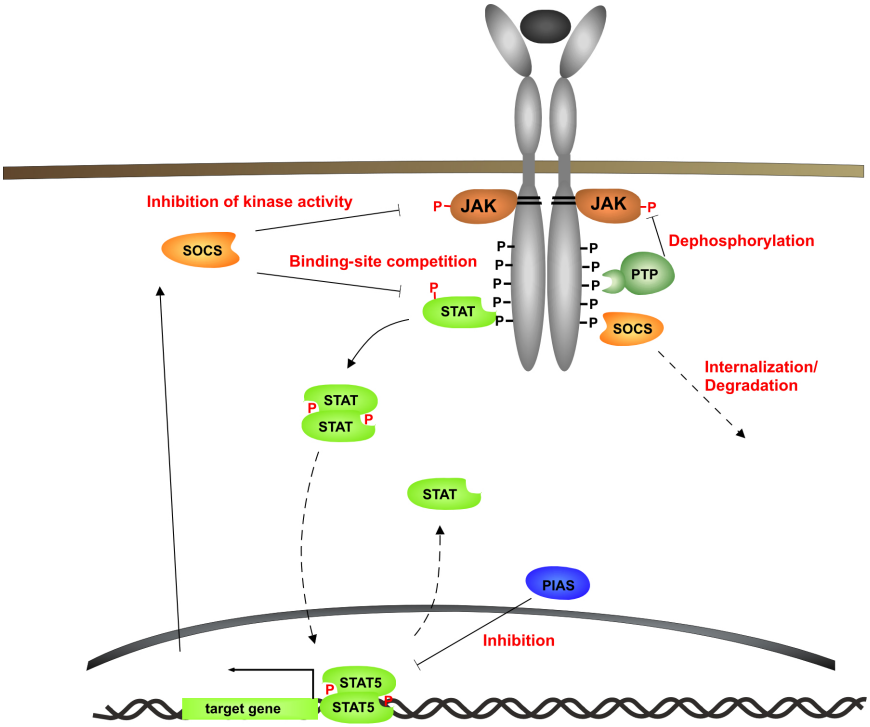

Fig. 3. Negative regulation of the JAK/STAT pathway. JAK/STAT signaling is regulated at various levels. Receptor internalization and degradation control the numbers of receptors at the cell surface. Phosphotyrosine phosphatases (PTPs) deactivate JAKs and receptors. Suppressors of cytokine signaling (SOCS) are induced upon cytokine stimulation and negatively regulate signaling by inhibition of kinase activity, by competing with STATs for phosphotyrosine binding sites on receptors and by promoting ubiquitination, and subsequent proteasome-mediated degradation of JAKs. Protein inhibitors of activated STATs (PIAS) bind to activated STAT dimers and inhibit transcription. Adapted from O'Sullivan et al., 2007.

1.2.1 Protein tyrosine phosphatases (PTPs)

Tyrosine phosphorylation levels are determined by the antagonistic actions of protein tyrosine kinases and protein tyrosine phosphatases (PTPs) (Pallen et al., 1992). In the JAK/STAT pathway three groups of PTPs have been proposed to regulate signaling. These

include (i) the SH2-containing phosphatases (SHPs) SHP-1 and SHP-2, (ii) the transmembrane tyrosine phosphatase CD45 as well as the (iii) phosphotyrosine phosphatase 1B (PTP1B) and the T-cell protein tyrosine phosphatase (TC-PTP).

SHPs SHP-1 and SHP-2 belong to a subfamily of non-transmembrane PTPs and are characterized by two N-terminal SH2 domains, a classic phosphatase domain and a C-terminal tail (Fig. 4). SHP-1 is predominantly expressed in hematopoietic cells, while expression of SHP2 is more ubiquitous (Banville et al., 1995). Recruitment of SHP-1 to activated receptors and JAKs via its SH2 domains causes dephosphorylation and inactivation of JAKs (Jiao et al., 1996; Ward et al., 2000). Importantly, mutation of the phosphotyrosine residues to which SHP-1 binds on the receptors for Epo, IL-3,-5 and GM-CSF results in sustained JAK activation (Klingmüller et al., 1995; Yi et al., 1993). In contrast, SHP-2 has been reported to function as both a positive and negative regulator of cytokine receptor signaling (Neel et al., 2003). Biochemical studies and the crystal structure of C-terminally truncated forms of SHP-1 and SHP-2 revealed an intramolecular regulatory mechanism that effectively links subcellular localization of SHPs with the phosphatase activity (Pao et al., 2007a). In the inactive state, the N-terminal SH2-domain blocks access of substrates to the active site and thereby inhibits the phosphatase domain. Binding of the N-terminal SH2-domain to a phosphotyrosine residue causes the release from the active site, leading to enzyme activation (Poole and Jones, 2005). Mice deficient for SHP-1 activity (*motheaten, me/me*) display severe immunological and hematopoietic dysfunctions (Shultz et al., 1993) and hyperphosphorylation of JAK1 and JAK2 following IFNα, GH or EPO treatment was observed (Jiao et al., 1996).

CD45 The second type of tyrosine phosphatase that was proposed to negatively regulate JAK/STAT signaling is the transmembrane tyrosine phosphatase CD45, which is expressed in hematopoietic cells and is a key regulator of T-cell and B-cell antigen receptor signaling in T- and B-lymphocytes. *In vitro*, CD45 directly binds to and dephosphorylates JAKs and negatively regulates IL-3 mediated cellular proliferation (Irie-Sasaki et al., 2001).

PTP1B and TC-PTP Phosphotyrosine phosphatase 1B (PTP1B) and T-cell protein tyrosine phosphatase (TC-PTP) share sequence similarities in their catalytic domains and comprise the third group of phosphatases that regulate JAK/STAT signaling. PTP1B is localized to the endoplasmic reticulum and is expressed in several tissues. TC-PTP, on the other hand, is primarily expressed in hematopoietic cell types and exists in two forms due to alternative splicing. The longer isoform (TC48) resides in the cytoplasm, whereas p45 (TC45) is localized to the nucleus. JAK2 and TYK2 are physiological substrates of PTP1B (Myers et al., 2001) whereas JAK1 and JAK3 are substrates of TC-PTP (Simoncic et al., 2002). TC45 also has been shown to inactivate STAT1 and STAT3 (ten Hoeve et al., 2002).

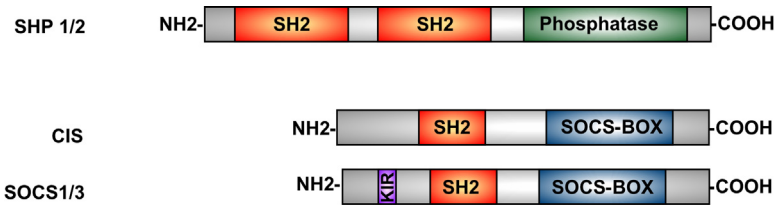

Fig. 4. Domain structure of exemplary negative regulators of JAK/STAT signaling. Sequence analysis indicated conserved domains for the tyrosine phosphatases SHP-1 and SHP-2 as well as for CIS and SOCS1/3. SHPs contain two C-terminal SH2 domains mediating protein-protein interactions. CIS/SOCS contain one SH2 domain and a SOCS box that associates with E3-ligase complexes, mediating proteasomal degradation. Additionally, SOCS1/3 contain a kinase inhibitory region (KIR) to bind to JAKs and block catalytic activity by acting as a pseudo-substrate.

1.2.2 Suppressors of cytokine signaling (SOCS)

In contrast to the constitutively expressed phosphatases, suppressors of cytokine signaling (SOCS) proteins are transcriptionally induced negative regulators. They comprise a family of at least eight members: the cytokine-inducible SH2 domain containing protein (CIS) and SOCS1-7 (Endo et al., 1997; Naka et al., 1997; Starr et al., 1997). They all contain a variable N-terminal region, a central SH2 domain and a C-terminal SOCS box that has been implicated in proteasomal degradation (Fig. 4). Following cytokine stimulation SOCS proteins are rapidly upregulated and the presence of STAT consensus sequences in their promoters suggests that their expression is regulated as part of a negative feedback loop (Matsumoto et al., 1997; Valentino and Pierre, 2006; Verdier et al., 1998b; Yoshimura et al., 1995). There are three general mechanisms by which SOCS proteins can regulate JAK/STAT activity. First, CIS and SOCS3 have been shown to compete with STATs for binding sites on receptors. Second, for SOCS1 and SOCS3 was reported that they can bind to JAKs directly via their kinase inhibitory region (KIR) that acts as a pseudosubstrate and thus prevent access of genuine substrates to the catalytic pocket (Elliott and Johnston, 2004). Third, SOCS proteins can downregulate JAK/STAT signaling by promoting ubiquitination and subsequent proteasome-mediated degradation of JAKs. Thereby, binding of elongin C to the SOCS box recruits an E3 ubiquitin ligase complex that targets bound proteins to proteolytic degradation (Ilangumaran et al., 2004). However, the physiological roles of specific SOCS proteins in controlling the different cytokine-induced signaling pathways as well as the timing and specificity of each of these mechanisms remain to be determined.

1.2.3 Protein inhibitors of activated STATs (PIAS)

Protein inhibitors of activated STATs (PIAS) family proteins were originally described as negative regulators of STATs, although they exhibit activity towards a variety of transcription factors. Five PIAS proteins including PIAS1, PIASx, PIASy, PIAS3α and PIASβ with various splicing isoforms have been described. They negatively regulate signaling by binding to

activated STAT dimers and inhibit transcription by distinct mechanisms. PIAS1 and PIAS3 associate with STAT1 and STAT3, respectively, and directly inhibit DNA binding. PIASx has been shown to regulate the recruitment of transcriptional repressors such as histone deacetylaes (HDACs) (Rakesh and Agrawal, 2005). Furthermore, recent studies have demonstrated that some PIAS family members possess small ubiquitin-like modifier (SUMO) E3-ligase activity and mediate the SUMOylation of STATs, which can modify the transcriptional activity (Ungureanu et al., 2005).

1.2.4 Dysregulated JAK/STAT signaling in hematopoietic diseases

Dysregulated JAK/STAT signaling has been associated with a number of hematological malignancies including chronic and acute leukemias as well as myeloproliferative diseases, i.e. polycytemia vera (PV), essential thrombocythemia (ET) and idiopathic myelofibrosis (IMF). Constitutive activation of STATs is a common characteristic that is caused by several mechanisms including downregulation of negative regulators, amplification of the JAK locus, JAK fusion proteins and activating point mutations in JAK2 (Khwaja, 2006).

The first direct evidence implicating dysregulation of the JAK/STAT pathway in hematopoietic malignancies was the identification of TEL-JAK2 fusions in lymphoid and myeloid leukemias (Lacronique et al., 1997). In this fusion protein the helix-loop-helix oligomerization domain of the transcription factor TEL is fused to the catalytic JH1 domain of JAK2, leading to constitutive association and activation of STAT proteins (Ho et al., 1999; Schwaller et al., 1998). Recently, several new JAK mutations have been identified that encode constitutively active or hyperactive JAK proteins. In particular, the constitutive active JAK2-V617F mutant has been identified in the majority of PV patients and in approximately 50 % of ET and IMF patients (Baxter et al., 2005; James et al., 2005; Kralovics et al., 2005; Levine et al., 2005). This mutation is believed to disrupt the inhibitory role of the JH2 pseudokinase domain. In addition, JAKs and STATs are also known to be constitutively activated in hematopoietic cells transformed by oncogenic tyrosine kinases such as Bcr-Abl (Chai et al., 1997). Although STAT mutations have not been found in cancer so far, certain STATs have oncogenic potential and therefore may play an important role in human tumors. In particular, a STAT3 mutant, denoted STAT3-C, in which two residues within the C-terminal loop of the SH2 domain are substituted by cysteines, is constitutive active and has oncogenic potential (Bromberg et al., 1999). Furthermore, using PCR driven mutagenesis, a constitutive active STAT5 mutant, termed STAT5 1*6, was isolated, that was found to render BaF3 cells cytokine-independent (Nosaka et al., 1999).

1.3 Erythropoietin receptor controlling erythropoiesis

1.3.1 Erythropoiesis

Hematopoietic cytokines tightly control the development of blood cells. Because most mature blood cells are short-lived, the different cell lineages are continuously renewed during embryogenesis and throughout lifetime by hematopoietic stem cells (HSCs) (Weissman, 2000). During hematopoiesis, the HSCs develop into progenitors that become progressively restricted to lineage precursors that further proliferate and differentiate into mature blood cells including erythrocytes, megacaryocytes, myeloid cells (monocytes/macrophage and neutrophils), and lymphocytes (Orkin and Zon, 2008). The process of differentation into hematopoietic lineages is regulated by pleiotropic cytokines or by a lineage specific cytokines.

In erythropoiesis, the development of red blood cells, erythropoietin (Epo) is the primary regulator. Erythrocytes are the most common type of blood cells and function as transporters of oxygen between lungs and tissue in the vertebrate body. Because they possess a short lifespan of approximately 120 days in human and 40 days in mice they undergo continuous renewal. In murine development, erythrocytes are being produced in stage-dependent distinct locations (Fig. 5).

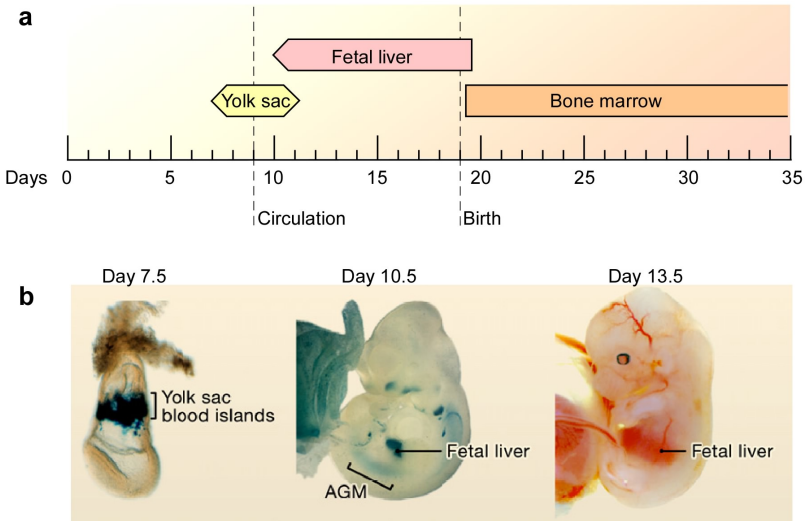

Fig. 5. Developmental regulation of erythropoiesis in the mouse. (a) Developmental time windows for distinct stages of erythropoiesis within the murine embryo. **(b)** Erythropoiesis first occurs in the yolk sac blood islands (primitive erythropoiesis) and later in the fetal liver (definitive erythropoiesis) before production shifts to the bone marrow. Yolk sac and fetal liver are visualized by LacZ staining. Adapted from Orkin et al., 2008

In the fetus, the first sites of erythrocyte production are the blood islands in the yolk sac. At this stage of primitive erythropoiesis, large nucleated erythrocytes are synthesized that express embryonic hemoglobin and are not dependent on Epo (Wu et al., 1995). Around day 12 of gestation (E12), the production of red blood cells shifts to the fetal liver, generating

non-nucleated definitive erythrocytes that express both embryonic and adult hemoglobins. Shortly before birth, definitive erythropoiesis relocates to the bone marrow and the spleen, which become the dominant sites of erythrocyte production throughout life (Hoffman, 1995).

During erythropoiesis in the fetal liver or the bone marrow (Fig. 6), the earliest committed progenitors identified *ex vivo* are the burst-forming units-erythroid (BFU-Es). In the presence of stem cell factor (SCF), interleukin-3 (IL-3), and erythropoietin (Epo), BFU-Es further progress into the colony-forming units-erythroid (CFU-E). The two types of progenitors are identified *in vitro* by the colonies they produce in colony-formation assays. Murine BFU-E colonies require 7-10 days to form in culture whereas CFU-E colonies require 2 days of cultivation in semi-solid medium (Gregory and Eaves, 1977).

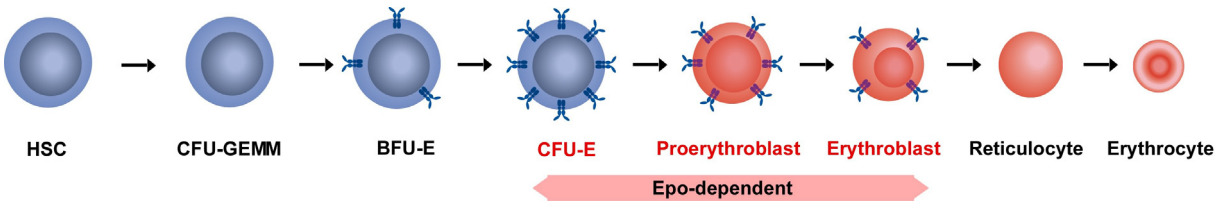

Fig. 6. Schematic overview depicting the formation of erythrocytes from the HSC during murine definitive erythropoiesis. The HSC gives rise to the colony forming unit-granulocyte-erythroid-makrophage-megakaryocyte (CFU-GEMM), which develops to the BFU-E after commitment to the erythroid lineage. Under the influence of SCF, IL-3, and Epo, the cells progress from the BFU-E stage to the CFU-E stage which is strictly Epo-dependent. The CFU-E further develop into erythroblasts under tight control of Epo signaling. After ejection of the nucleus, the reticulocytes enter the blood stream and mature to erythrocytes. Adapted from U. Klingmüller, 1997. Abbreviations see text.

In the presence of Epo, CFU-Es mature progressively through four different stages: pro-erythroblasts, basophilic, polychromatophilic and orthochromatophilic erythroblasts. When differentiation proceeds, erythroblasts display a gradual decrease in cell size, increase in chromatin condensation and increase in hemoglobin content. Finally, the nucleus is extruded and reticulocytes are formed that detach from their environment to enter the blood stream. By further expelling all organelles they mature to oxygen-carrying erythrocytes (Hoffman, 1995). The Epo receptor (EpoR) is first expressed at the BFU-E stage and most strongly in cells of the CFU-E stage. Beyond the late erythroblast stages, the expression of the receptor decreases and these cells are no longer dependent on Epo.

1.3.2 Erythropoietin and erythropoietin receptor

The physiological role of Epo and EpoR in erythropoiesis has been primarily determined using mice harboring null mutations in genes encoding either Epo or the EpoR. These knockout mice die during embryogenesis at day E12.5-E13.5, which is the stage of massive erythroid expansion. Fetal livers of these mice contain normal numbers of committed CFU-E, indicating that Epo signaling is dispensable at earlier stages of hematopoiesis (Richmond et al., 2005). During embryogenesis, Epo is produced in the fetal liver whereas in the adult, Epo

is primarily expressed in the tubular, juxtatubular endothelial, and interstitial cells of the kidney as well as extrarenally in hepatocytes and Kupffer cells (Krantz, 1991). Low oxygen tension in the tissue due to blood loss or high altitude strongly induces expression of the Epo gene by means of the hypoxia-inducible transcription factors HIF-1 and HIF-2 (Ebert and Bunn, 1999). As typical cytokine, Epo consists of four α-helices that are folded into a compact globular structure. The carbohydrate chains of the glycoprotein are required for full biological activity *in vivo*.

The murine EpoR belongs to the family of type I cytokine receptors that is composed of an extracellular N-terminal ligand-binding domain, one single transmembrane domain and a cytosolic domain that lacks enzymatic activity (D'Andrea et al., 1989). The extracellular domain contains two fibronectin type II domains, D1 and D2. Each subdomain contains two conserved cysteine residues that form disulfid bonds. The amino acid motif WSXWS that is conserved among the hematopoietic cytokine receptor superfamily, is located in proximity to the transmembrane domain (Bazan, 1990; Cosman et al., 1990). The signal-transducing cytoplasmic domain contains two proline-rich motifs Box1 and Box 2 that are required for JAK2 function (Huang et al., 2001). Mutations of the EpoR that cause expression of truncated EpoR variants have been implicated in primary familial polycythemias (de la Chapelle et al., 1993; Kralovics et al., 1997). This benign erythrocytosis is characterized by elevated red blood cell mass and low serum Epo level. Cultured erythroid progenitors from these patients show increased Epo-sensitivity compared to cells expressing the wild-type EpoR.

1.3.3 Signaling through the erythropoietin receptor

Signaling through the EpoR promotes cell survival, enhances proliferation and supports differentiation in erythropoiesis at the BFU-E stage through the CFU-E stage to late erythroblasts. Over the past decade, the major signaling proteins activated by Epo have been identified. As a typical cytokine receptor, the EpoR lacks intrinsic kinase activity and associates with the tyrosine kinase JAK2 that is involved in the activation of downstream pathways. The absolute requirement for JAK2 to transduce EpoR signals was substantiated by analyses of JAK2 knockout mice that die between E13 and E15 from severe anemia, demonstrating an essential role of JAK2 in definitive erythropoiesis (Neubauer et al., 1998). Upon binding of Epo and structural rearrangements of the EpoR cytoplasmic domain, JAK2 is rapidly activated by transphosphorylation on tyrosine 1007 in its activation loop (Feng et al., 1997). In turn, JAK2 phosphorylates several tyrosine residues within the EpoR cytoplasmic domain which serve as docking sites for SH2 domain-containing effectors. The signaling molecules und pathways activated upon recruitment to the phosphorylated EpoR include STAT5, phosphatidylinositol 3-kinase (PI3-K), mitogen-activated protein kinase (MAPK) and protein kinase C (PKC).

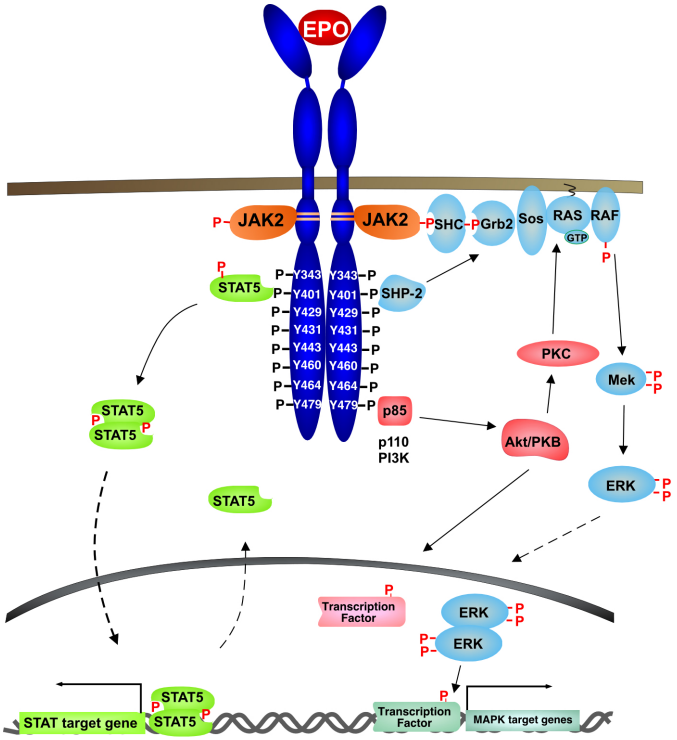

Fig. 7. Signaling pathways activated by the EpoR. Upon Epo binding to the preformed receptor dimer, JAK2 gets activated by transphosphorylation and in turn phosphorylates the EpoR on several cytoplasmic tyrosine residues. Several signaling pathways emanate from the EpoR, including the RAF/Mek/ERK and the Akt/PKB cascade. The most direct way of signal transduction through the EpoR is the activation of the transcription factor STAT5. Induction of CIS represents a negative feedback loop for STAT5 activity. In addition to SOCS proteins, downregulation of EpoR signaling is mediated by recruitment of protein tyrosine phosphatases including SHP-1. Abbreviations see text.

STAT5 signaling

The most direct way to transmit receptor stimulation to the nucleus is the activation of STAT5. The latent transcription factor associates with phosphorylated residues Y343 and Y401 on the activated EpoR which is sufficient for maximal STAT5 phosphorylation. The binding to phosphotyrosines 429 and 431 only results in partial STAT5 activation (Klingmüller et al., 1996). Upon phosphorylation, STAT5 dissociates from the receptor, dimerizes, translocates to the nucleus and binds to cognate elements in various promoters to activate transcription of target genes. These include the negative regulators CIS (Matsumoto et al., 1997) and SOCS-3 as well as targets such as Pim-1, c-myc, OncostatinM, Bcl-xL or D-type cyclins that are required for functional erythropoiesis (Menon et al., 2006; Silva et al., 1999; Socolovsky et al., 1999).

The physiological role of STAT5 in erythropoiesis has been extensively studied in the last years. Although discussed controversially, increasing evidence suggests that STAT5 promotes survival in erythroid progenitor cells by directly inducing the expression of the anti-apoptotic protein Bcl-xL (Garcon et al., 2006; Socolovsky et al., 1999). STAT5ab$^{-/-}$ mice display fetal anemia and elevated rates of apoptosis of erythroid progenitor cells as a result

of a failure in Bcl-xL up-regulation (Socolovsky et al., 2001). Recently, a second study generated knockout mice of STAT5ab$^{-/-}$ and these mice are perinatally lethal and highly anemic *in utero* (Cui et al., 2004) which further supports the essential function of STAT5 during erythropoiesis.

MAP kinase and PI3 kinase signaling

Besides phosphorylation of STAT5, Epo induces the activation of several mitogen-activated protein kinases (MAPK), including the extracellular-regulated kinase 1/2 (Erk1/2). For initiation of the MAPK cascade Grb2-Sos is recruited to the EpoR by several different routes. Grb2 can bind either directly to Y464 of the EpoR or indirectly by interacting with SHP-2 or SHIP-1 (Mason et al., 2000; Tauchi et al., 1996). Alternatively, SHC can bind to JAK2 and serve as adapter protein for Grb2 (He et al., 1995). Subsequently, Sos-catalyzed exchange of GDP for GTP on Ras results in activation of Ras which leads to the initiation of the MAPK cascade. An alternative route for MAPK has been proposed through activation of the protein kinase C (PKC) via the phosphatidylinositol 3 kinase (PI3-K) pathway (Karnitz and Abraham, 1995).

PI3-K is activated upon Epo stimulation via two possible mechanisms. In the direct way, the p85 regulatory domain of PI3-K is directly recruited to Y479 of the activated EpoR (Damen et al., 1995; Klingmüller, 1997). Additionally, PI3-K can be activated indirectly by recruitment of the Grb2-associated binder (Gab) (Bouscary et al., 2003; Ravichandran et al., 1995). Downstream of PI3-K, the protein kinase B (PKB/Akt) is activated. One of the PKB/Akt substrates includes the forkhead box O3A (Foxo3a) transcription factor that has been shown to play an important role in erythroid differentiation (Kashii et al., 2000).

Termination of EpoR signaling

Although the downstream signaling cascades induced by the activated EpoR are well studied, the mechanisms that terminate signaling are poorly understood. In the last decade several classic negative regulators of JAK/STAT signaling have been proposed to be involved in attenuation of EpoR signaling. In particular, recruitment of SHP-1 to phosphotyrosine Y429 and Y431 of the EpoR has been shown to dephosphorylate JAK2 (Klingmüller et al., 1995) and potentially the EpoR. Moreover, four SOCS proteins have been associated with Epo-induced signaling: CIS, SOCS-1, SOCS2 and SOCS-3 (Pircher et al., 2001; Starr et al., 1997; Yoshimura et al., 1995). CIS was identified to bind to the EpoR on phosphorylated Y401, thereby competing for receptor binding with STAT5 (Ketteler et al., 2003). Other studies indicated that CIS is involved in proteasome-mediated inactivation of the EpoR (Verdier et al., 1998a). SOCS-3 was proposed to bind to activated EpoR and JAK2 (Hortner et al., 2002; Sasaki et al., 2000) and both SOCS-1 and SOCS-3 have been

suggested to inhibit JAK2 activity by directly binding to the kinase activation loop (Sasaki et al., 1999; Ungureanu et al., 2002). However, most of these studies were performed in transformed cell lines, and the specific roles of these proteins in controlling EpoR signaling in erythropoiesis are still unclear.

1.3.4 *In vitro* cell models to study erythropoiesis

In the past years, the majorities of studies that investigated signaling pathways in erythropoiesis used transformed growth factor independent (erythro-) leukemia cell lines (Drexler et al., 2004). Moreover, partially transformed factor-dependent cell lines are a frequently used model system to study erythropoiesis. In particular, the IL-3 dependent murine pro-B cell line BaF3 is well established to study Epo-dependent signaling pathways by exogenously expressing the EpoR (Warmuth et al., 2007). However, cell lines may be genetically instable and exhibit major alterations in signaling pathways due to aberrant stoichiometries of signaling molecules, contributing to transformed cell growth (Wickrema and Crispino, 2007). For studying signaling pathways in erythropoiesis closely resembling the *in vivo* situation, the use of primary cells is indispensable. Erythroid progenitors at the CFU-E stage isolated from mouse fetal livers can be cultured under standardized conditions to investigate the regulation of proliferation, survival and the differentiation into mature erythrocytes. Nevertheless, the limited availability of primary erythroid progenitor cells and the short time span before they undergo differentiation is a major challenge for the investigation of molecular processes that are involved in the regulation of erythropoiesis.

1.4 Systems biology approach

1.4.1 Systems biology in signal transduction

An enormous amount of qualitative information about the components of signal transduction pathways and their interplay has accumulated in the past decades. However, in order to understand how signaling networks are regulated and which parameters determine their dynamics, a static representation of the pathway components is not sufficient (Heinrich et al., 2002). Mathematical modeling has emerged as a powerful tool in the last decade to analyze key features of signal transduction pathways involved in the regulation of systems behavior (Kholodenko, 2006; Kolch et al., 2005; Stelling et al., 2004). Progress in this area requires optimized quantitative data generation as well as advanced computational methods to make testable predictions and suggest experiments most informative for hypothesis-driven research in biology (Fig. 8).

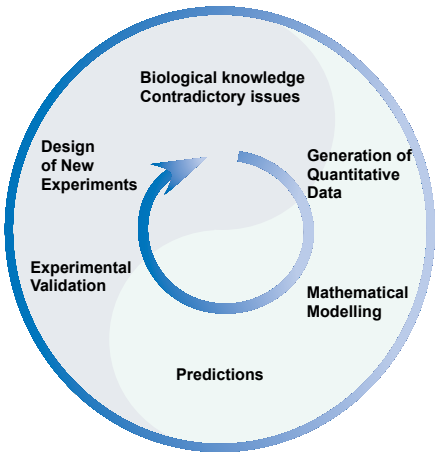

Fig. 8. Iterative cycle of systems biology. Biological issues are adressed by an iterative cycle of quantitative experimental data generation, mathematical modeling, *in silico* predictions, experimental validation and design of new experiments. Adapted from Kitano, 2002.

The pathways most extensively studied by systems biology approaches are the EGFR signaling network (Kholodenko et al., 1999; Kholodenko, 2007), the MAPK cascade (Orton et al., 2005) and NFkB signaling (Cheong and Levchenko, 2008; Nelson et al., 2004).

Recently, several kinetic models of JAK/STAT signaling pathways have been established. The majority of these studies rely on previously published data and simulations. They were focused on coordination principles and control mechanisms of the IFNγ activated JAK1/JAK2/STAT1 pathway (Soebiyanto et al., 2007; Yamada et al., 2003; Zi et al., 2005), robustness in the JAK/STAT1 pathway (Shudo et al., 2007) or IL-6 induced JAK/STAT signaling in hepatocytes (Singh et al., 2006). However, very few data-driven models exist that directly combine quantitative data with dynamic pathway modeling. One example is the data-based mathematical model of the JAK2/STAT5 pathway in BaF3-EpoR cells that identified nucleocytoplasmic shuttling of STAT5 as the most sensitive step in the core module of JAK/STAT signaling (Swameye et al., 2003). Nevertheless, to understand how signaling pathways and in particular the JAK/STAT pathway are controlled and which are the most important proteins that regulate the outcome of the pathway, mathematical models based on reliable time-resolved and quantitative data should be established.

1.4.2 Mathematical models

The form of a mathematical model depends on the properties of the studied system and the goal of the modeling effort (Aldridge et al., 2006). The most commonly used models to study signal transduction pathways are based on coupled ordinary differential equations (ODEs). An ODE network thereby represents the rate of production and consumption of individual protein species in terms of mass action kinetics. Thus, each reversible biochemical transformation is represented by an elementary reaction with forward and reverse rate constants. If changes of proteins or molecules have to be modelled explicitly with respect to spatial distributions, partial differential equations (PDEs) are employed. Both ODE and PDE models can be cast either in deterministic form or using stochastic equations that include effects arising from random fluctuation around the average behavior (Kholodenko, 2006).

A first challenge in constructing a mathematical model of signal transduction pathways is specifying the scope and level of abstraction. If the scope of a model is too small, the predictive power is lost, whereas for too complex models with numerous species the uncertainty of predictions increases. Thus, an optimal compromise between complexity and oversimplification has to be made. After establishing the structure of the model, the parameters can be estimated using quantitative experimental data. In this process of model calibration, the values of parameters are computed to give the best fit to a set of experimental data using global optimizations methods (Banga, 2008). To validate the model experimentally, predictions are performed that can be subjected to experimental tests. Moreover, to improve the identifiability of parameters and to constrict the parameter space, an experimental design approach can be applied to systematically select the most informative experimental conditions by computational analysis (Maiwald et al., 2007).
When the topology and parameters of the mathematical models have been determined and the parameter values are identifiable, the model can be applied to perform simulations of the dynamic behavior to gain insight into control and regulatory mechanisms and to suggest new experiments. Furthermore, sensitivity analysis can be applied that is a powerful tool for systematically determining which concentrations and rate constants in a given model have the largest impact on the behavior of signaling species or the output of the system (Westerhoff, 2008).

1.4.3 Experimental technique for targeted perturbation - the Tet-inducible system

When studying biological processes, the dynamics can only be identified from experimental data through systematic perturbations and subsequent response analysis. The observation of a system under altered conditions may also help to improve and validate mathematical models. However, one major difficulty in biological experiments is the targeted perturbation of cellular systems. Generally, unspecific inhibitors such as the generic inhibitor of transcription, actinomycin D can be employed. Other frequently used methods to challenge the dynamic behavior are the increase of protein levels by overexpression or knockdown by RNA interference (siRNA). An advanced tool facilitating the dose- and time-dependent overexpression of signaling components is the Tetracycline-inducible (Tet-) system.
Tet-systems have been widely applied to control gene expression in eukaryotes (Baron and Bujard, 2000). The principle of these regulatory systems is based on the *E.coli* tetracycline resistance operon (Tn10) consisting of the tetracycline repressor protein (TetR) and its specific DNA binding site, the tetracycline operator sequence (tetO). In the original system, TetR blocks transcription of resistance-mediating genes by binding to the tetO sequences. In the presence of tetracycline, TetR dissociates from tetO and gene transcription is induced. For optimized application in mammalian organisms and cell lines the synthetic Tet-Off (Gossen and Bujard, 1992) and Tet-On (Gossen et al., 1995) systems were developed. The

key component of the first established Tet-Off system is the tetracycline-controlled transactivator (tTA). This fusion protein consists of the DNA binding domain of the bacterial TetR and the transcriptional activation domain of herpes simplex virus VP16 protein that allows interaction with the eukaryotic transcription machinery. The second component, the synthetic Tet-response element (TRE), consists of a fusion between a minimal CMV promoter and an array of seven tetO sequences. Because the Tet-Off system requires persistent administration of tetracycline or its derivative doxycycline (Dox) to suppress gene expression that my trigger undesirable side-effects, the Tet-On system was developed. This system is based on the reverse transactivator (rtTA) that contains four specific mutations in the TetR domain and therefore shows reverse binding properties. Thus, in the presence of Dox rtTA binds to the TRE and activates transcription of target genes. In the absence of Dox rtTA cannot bind to TRE and target gene expression is abolished (Fig. 9).

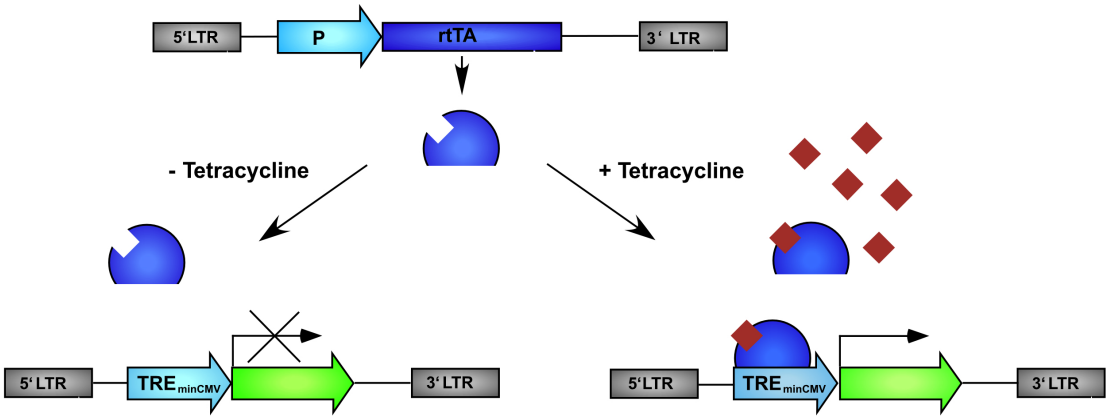

Fig. 9. Schematic representation of the Tetracycline inducible system (Tet-On). The Tet-On system consists of the reverse tetracycline-controlled transactivator (rtTA) and the Tet-responsive element (TRE). If tetracycline is absent, target gene expression is abolished. In contrast, binding of tetracycline to rtTA causes a conformational change in rtTA leading to association with DNA and activation of gene transcription. *P* promoter, *LTR* long terminal repeats.

A major bottle-neck of tetracycline-inducible (Tet) systems is the basal transcriptional activity in the off-state of the system. This leakiness is due to intrinsic residual activity of the minimal CMV promoter and low residual affinity of the reverse tetracycline transactivator (rtTA) to the tetracycline response element (TRE) in the absence of Tet. To circumvent these limitations, improved rtTA proteins and several redesigned and optimized TRE sequences have been developed (Baron et al., 2000; Urlinger et al., 2000) that exhibit improved sensitivity to Tet and lower basal activity in the off-state. Despite the generation of novel Tet-components the efficacy of tetracycline-dependent gene expression is strongly dependent on the cell type and the vector systems harboring the TRE and the rtTA. In particular, efficient Tet-regulatable expression vectors for the use in hematopoietic cells should be developed.

1.5 Objectives

The tight control of the duration and magnitude of JAK2/STAT5 signal transduction through the EpoR is crucial for the controlled balance of erythrocyte production. In the past years, a large number of factors regulating Epo-induced JAK2/STAT5 signaling have been identified. However, the importance and complex roles of these negative regulators in controlling the strength and dynamic behavior of the signal outcome are poorly understood. Moreover, little is known about differences in regulatory mechanisms of EpoR-signaling between primary erythroid progenitors at the CFU-E stage and cell lines that are frequently used as model system to study the Epo-induced JAK2/STAT5 pathway. Furthermore, key properties of the pathway that facilitate rapid information processing and sensitivity such as signal amplification are largely unknown in Epo-induced JAK/STAT signaling.

The goal of this work was to establish a mathematical pathway model of Epo-induced JAK2/STAT5 signaling in primary erythroid progenitor cells based on quantitative, time-resolved experimental data to identify the critical negative feedback regulators that attenuate EpoR signaling. Employing analytic tools of the mathematical model, the distinct temporal characteristics of negative regulators modulating the signal strength and duration of JAK2/STAT5 signaling should be elucidated. Additionally, this work aimed at understanding, how signaling dynamics are linked to the regulation of survival of erythroid progenitor cells.

2 Results

2.1 Mathematical model to study signal amplification in the JAK2/STAT5 pathway

The JAK2/STAT5 pathway rapidly transmits Epo signals from the cell membrane into the nucleus to activate gene transcription. To investigate key properties of the pathway allowing signal amplification between the EpoR and STAT5 and sensitivity of the system to different Epo concentrations, a data-based mathematical model was established. Computational modeling was performed in collaboration with Julio Vera (University of Rostock). The mathematical model representing the Epo-induced JAK/STAT5 pathway (Fig. 10a) was implemented using two different strategies that were compared in this study: (i) a conventional ordinary differential equation (ODE) model based on mass action kinetics and (ii) a power-law formulation that allows non-integer kinetic orders of the reactions (Vera, Bachmann et al., 2008). The model topology was based on a previous data-based mathematical model of the JAK2/STAT5 pathway that revealed nucleocytoplasmic cycling as an essential building principle of this cascade (Swameye et al., 2003). In order to relate Epo stimuli to STAT5 signaling responses, Epo was used as input function. Receptor dynamics were simplified by EpoR/JAK2 complexes that are deactivated by phosphatases or internalization. STAT5 was considered to have three different states: non-activated STAT5 in the cytosol, activated STAT5 in the cytosol and activated STAT5 in the nucleus. (see – *Appendix 6.1 Ordinary differential equations model to study JAK2/STAT5* amplification).

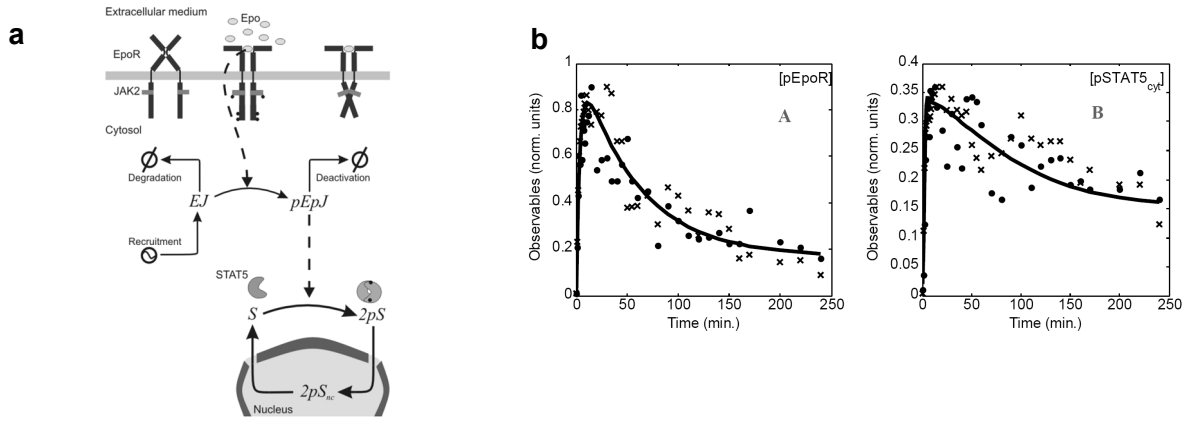

Fig. 10. Calibrated JAK2/STAT5 pathway model in BaF3-EpoR cells. (a) Schematic representation of the JAK2/STAT5 model. Upon Epo binding, the pre-associated EpoR-JAK2 (EJ) complex is phosphorylated. The activated EpoR-JAK (pEpJ) complex recruits STAT5 (S) that is phosphorylated. STAT5 dimers (2pS) translocate to the nucleus to activate transcription (2pSnc). After deactivation STAT5 returns into the cytosol. **(b)** Model calibration with experimental data. BaF3-EpoR cells were stimulated with 5 U/ml Epo and cellular lysates were subjected to immunoprecipitation with antibodies against EpoR and STAT5 and subsequently analyzed by quantitative immunoblotting. Data obtained from two experiments (1: crosses; 2: circles) are compared with the solution of the model trajectories (lines) (Vera, Bachmann et al., 2008)

To calibrate the mathematical model, time series of EpoR and STAT5 phosphorylation dynamics in BaF3-EpoR cells were generated by quantitative immunoblotting (Fig. 10b). When comparing the conventional model with fixed integer kinetic orders and models with an increasing number of variable non-integer kinetic orders, the best compromise between accurate data fitting and a suitable number of estimated parameters was observed for the model with fixed integer kinetic orders. This suggests that power law formulations are not required for describing the data. After parameter estimation, the calibrated model was employed to investigate the responsiveness of the system. Therefore, the amount of phosphorylated STAT5 in the nucleus was simulated for different Epo concentrations.
Fig. 11 shows the computed response of phosphorylated STAT5 values related to logarithmically scaled Epo concentrations.

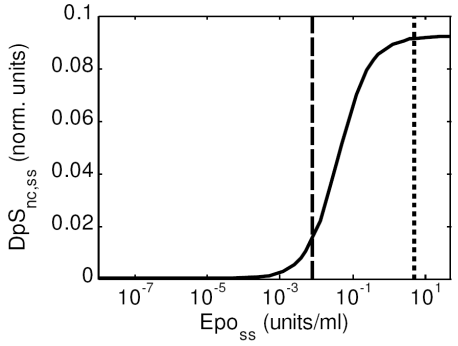

Fig. 11. Responsiveness of JAK2/STAT5 signaling for different Epo concentrations. The response of the system is represented by steady-state values of pSTAT5 in the nucleus and analyzed for different values of constant Epo concentrations ranging from 10-8 U/ml to 50 U/ml. The physiological serum concentration of Epo, (7.9×10-3 U/ml: long-dashed line) and the concentration of Epo used in the experiments (5 U/ml: short-dashed line) are indicated. DpSnc,ss: dimerized phosphorylated STAT5 in the nucleus, Eposs: Epo (Vera, Bachmann et al., 2008).

The sigmoidal behavior of the signal response demonstrates that the system is maximally sensitive to changes of Epo concentrations in the interval of 10^{-3}-10^{-1} U/ml. Interestingly, this range includes the physiological serum concentration in mice of approximately 7.9×10^{-3} U/ml Epo (Noe et al., 1999). For stimuli smaller than 10^{-4} U/ml the system is not significantly activated while upon stimuli beyond 5 U/ml the system becomes saturated to any further increase of the stimulus. This behavior has been previously described as a typical feature of amplifying signal transduction pathways (Barkai and Leibler, 1997). Furthermore, to quantify the ability of the system to amplify the signal, the logarithmic amplification was defined as the logarithm of the ratio between the total amount of activated STAT5 in the nucleus and the activated EpoR (see – *Appendix 6.1 Ordinary differential equations model to study JAK2/STAT5* amplification). The amplification factor showed maximal increase of amplification in the interval 10^{-4}-10^{-1} U/ml of Epo which also includes the physiological value of Epo.
In conclusion, the mathematical model showed that the JAK2/STAT5 system acts as efficient amplifier. The sensitivity for input signals is maximal for the range of physiological values and reaches saturation for very intense Epo stimuli.

2.2 Genome-wide analysis of Epo-induced transcriptional regulators

The activation of JAK2/STAT5 signaling is counterbalanced by signal terminating events that regulate signal duration and magnitude. To obtain a comprehensive overview of Epo-mediated induction of negative feedback regulators genome-wide expression profiling was performed. Exogenous expression of the EpoR in the factor-dependent murine pro-B cell line BaF3-EpoR is a well established tool to study Epo-dependent JAK2/STAT5 signaling. However, little is known about differences in the regulation of the signaling pathway between this cell line and primary erythroid progenitor cells at the CFU-E stage that endogenously express the EpoR and are strictly Epo-dependent for proliferation, survival and differentiation. To compare negative feedback regulation in BaF3-EpoR and CFU-E cells time-resolved genome wide expression profiling was performed for both cell types. CFU-E cells isolated from murine fetal livers were stimulated with 0.5 U/ml Epo for 24 h and total RNA was extracted at timepoints 0, 1, 2, 3, 4, 5, 6, 7, 8, 14, 19, 24 h. Control cells were left unstimulated and RNA was isolated every hour between 0 and 8 h. This shortened time frame was chosen since CFU-E cells are Epo-dependent and undergo apoptosis beyond 8 h without stimulation. BaF3-EpoR cells were starved and either stimulated with 0.5 U/ml Epo or left untreated for 24 h and total RNA was extracted at timepoints 0, 1, 2, 3, 4, 5, 6, 7, 8, 20, 24 h. Processing of samples and data analysis was performed in collaboration with Norbert Gretz (University Hospital of Heidelberg in Mannheim) and Hauke Busch (University of Heidelberg). For hybridization, the GeneChip Mouse Genome 430 2.0 Array (Affymetrix) was used that comprises 45,100 probe sets representing 20,700 genes. Data analysis was performed by calculating the logarithmic fold change with respect to gene expression at 0 h.

In order to gain systematic insights into negative feedback regulation the genes encoding known negative regulators of JAK/STAT signaling were compiled. Based on literature information these genes were grouped into the following protein families: SOCS proteins, protein tyrosine phosphatases and PIAS proteins. The expression profiles of CFU-E and BaF3-EpoR cells without stimulation showed no up- or downregulation of mRNA levels of the selected negative regulators demonstrating that up- or downregulation in stimulated cells is Epo-specific. In CFU-E cells the mRNA levels of the two SOCS proteins CIS and SOCS3 were rapidly upregulated within one hour after stimulation and remained at a constant high level within 24 h of observation (Fig. 12a). These results were validated with qPCR and the same kinetics with a rapid induction were observed (see – *Appendix 6.2 Validation of time-resolved mRNA induction of SOCS3 and CIS*). SOCS1, which has also been reported as negative feedback regulator in EpoR signaling showed no significant modulation in CFU-E cells. In BaF3-EpoR cells (Fig. 12b) various SOCS proteins showed rapid induction after stimulation with Epo including CIS, SOCS1, SOCS3 and SOCS6.

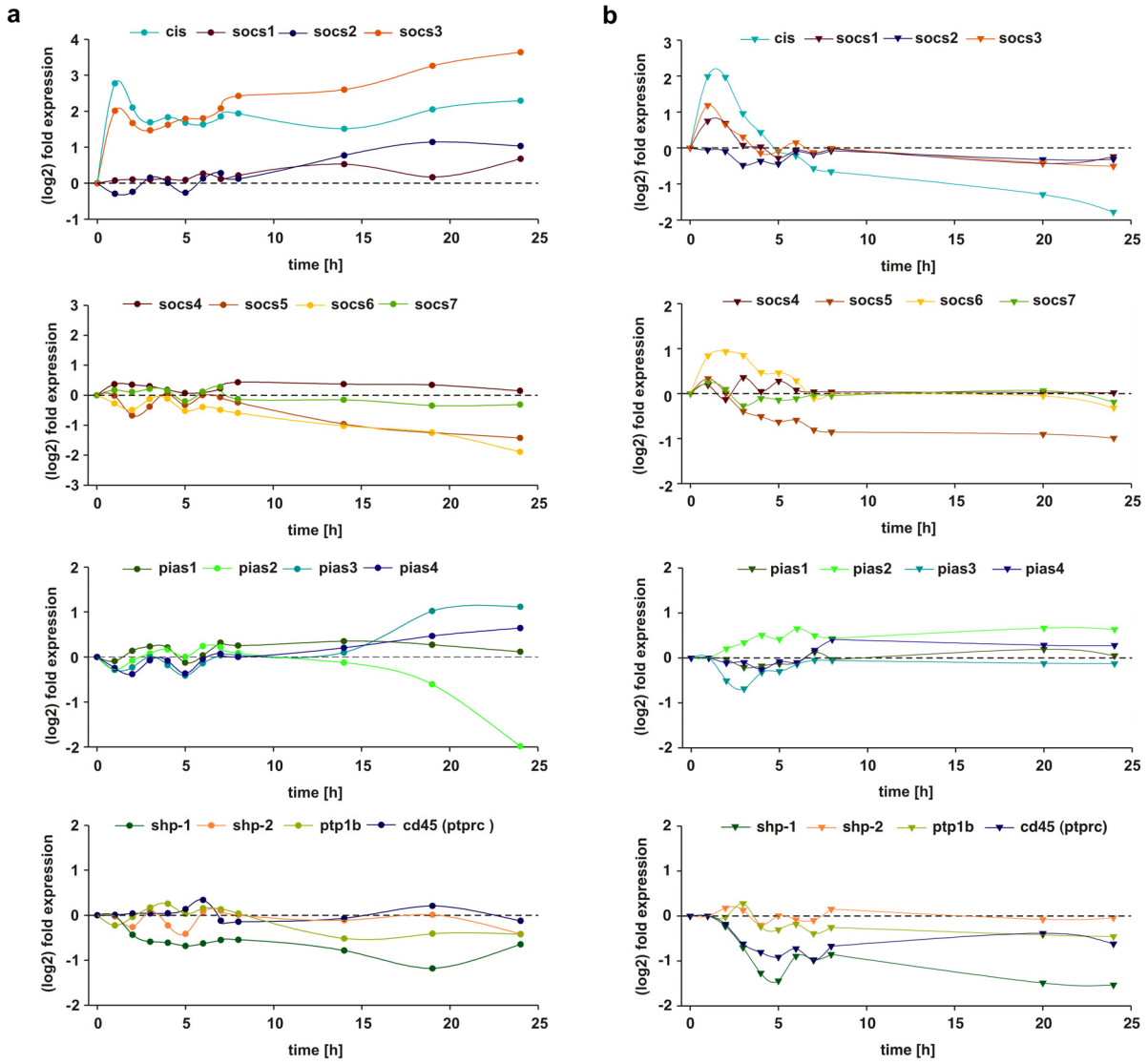

Fig. 12. Time-resolved expression profiling (Affymetrix microarray) of Epo-induced negative regulators in CFU-E cells and BaF3-EpoR cells. Log2-fold change of mRNA levels relative to timepoint t = 0 min after stimulation with Epo in **(a)** CFU-E cells and **(b)** BaF3-EpoR cells. Raw data were processed using the R environment together with the Bioconductor toolbox. The logarithmic gene fold expression was calculated with respect to the gene expression at 0 h.

However, the induction of these transcripts was only transient and declined to basal or even below basal level after 3-4 h. The time-resolved expression profiles of PIAS proteins and phosphatases showed only little Epo-dependent regulation of transcript levels over the entire period of observation in the two cell types. Solely the mRNA level of tyrosine phosphatase SHP-1 was weakly downmodulated upon stimulation with Epo. The half-life of SH2-domain containing phosphatases, however, has been estimated to range between 18-20 h (Siewert et al., 1999) suggesting that transcriptional regulation of SHP-1 does not significantly affect SHP-1 protein level in the first hours after Epo stimulation.

In summary, the microarray analysis indicated an Epo-dependent upregulation of CIS and SOCS3 in CFU-E cells. Their mRNA levels showed a rapid and strong induction suggesting an important role of the two proteins in the regulation of JAK2/STAT5 signaling in primary

erythroid cells. Furthermore, both transcripts were most strongly upregulated in BaF3-EpoR in comparison to other SOCS genes. Therefore, the following studies of transcriptional feedback regulation in JAK2/STAT5 signaling were focused on these two proteins.

2.3 Generation of quantitative and time-resolved data on JAK2/STAT5 signaling

2.3.1 Quantification of JAK2/STAT5 pathway components and negative regulators

Based on genome-wide transcriptional profiling the two SOCS proteins CIS and SOCS3 were identified as putative negative regulators of Epo-induced signaling which is in line with other studies indicating the involvement of SOCS proteins in this pathway. Additionally, the tyrosine phosphatase SHP1 that is constitutively expressed in hematopoietic cells was proposed in previous studies as a major negative regulator of Epo-induced signaling (Klingmüller, 1997). To dissect the complex roles of these three proteins that function by different mechanisms to attenuate JAK2/STAT5 signaling, a mathematical modelling approach provides useful tools that may help to gain deeper insight into negative feedback regulation of this pathway. However, establishing a mathematical model requires quantitative information about the protein species involved.

In order to analyze stoichiometric ratios and start values of the signaling components that are important for the mathematical model, the negative regulators were quantified at the protein level. Since CIS and SOCS3 are not constitutively expressed, cells were stimulated with 5 U/ml Epo and protein levels were determined at maximum activation (t = 120 min). SHP-1 levels remained constant over time (Fig. 14) and were therefore estimated in untreated cells.

To quantify endogenous protein levels, calibration curves of recombinant proteins were used in combination with quantitative immunoblotting (Schilling et al., 2005b). Therefore, recombinant proteins (calibrators) consisting of the protein of interest tagged with either streptavidine binding peptide (SBP) or glutathione S-transferase (GST) for purification were generated in *E.coli*. The concentration of these calibrators was determined by means of a known BSA standard. To determine endogenous protein levels, serial dilutions of the respective calibrators were added to cellular lysates prior to immunoprecipitation. After quantification of immunoblotting signals by chemiluminescence detection, calibration curves were calculated from dilution series. Based on the assumption that antibodies used for immunoprecipitation and immunoblotting possess the same affinity for the recombinant and the endogenous protein species, absolute endogenous protein concentrations could be estimated. Fig. 13 shows the quantifications of the negative regulators CIS, SHP-1 and SOCS3 in BaF3-EpoR and CFU-E cells that were analyzed by applying the recombinant proteins SBP-CIS, SBP-SOCS3 and GST-SHP-1.

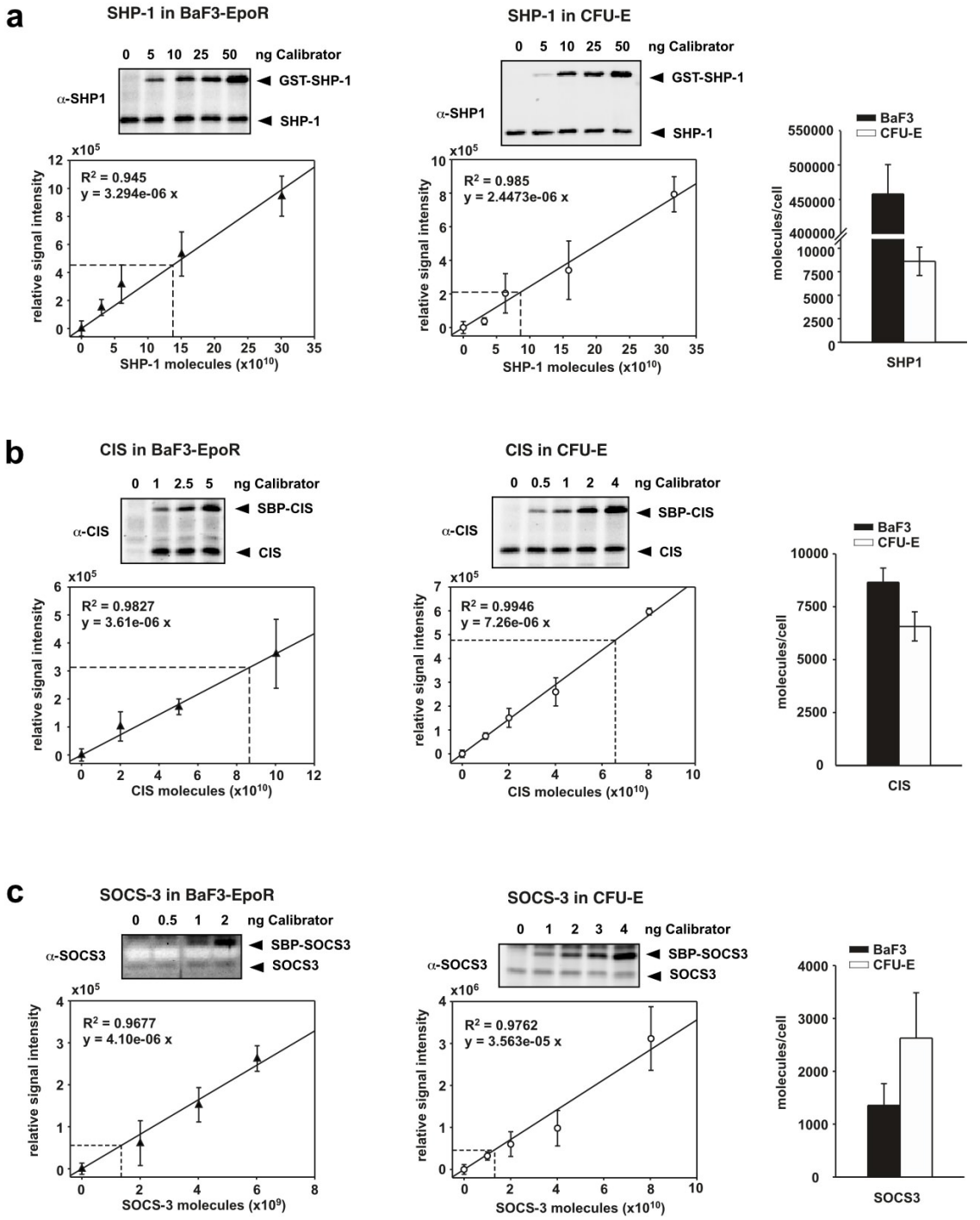

Fig. 13. Protein quantification of negative regulators of the JAK2/STAT5 pathway. Endogenous protein levels of SHP-1, CIS and SOCS3 were estimated in cellular lysates of BaF3-EpoR and CFU-E cells by means of dilution series (n=3) of added recombinant calibrator proteins SBP-CIS, GST-SHP-1 and SBP-SOCS, respectively. For quantification of CIS and SOCS3, cells were stimulated with 5 U/ml Epo for 2 h and subsequently lysed. Proteins were immunoprecipitated and analyzed by quantitative immunoblotting based on chemiluminescence detection. Dilution series of recombinant proteins were plotted with respective linear regression functions (solid lines) **(a)** for SHP-1 in BaF3-EpoR (3×10^5) and in CFU-E (1×10^7) cells, **(b)** for CIS in BaF3-EpoR (1×10^7) and CFU-E (1×10^7) cells, and **(c)** SOCS3 in BaF3-EpoR (1×10^7) and CFU-E (5×10^6) cells. Molecules per cell were calculated by means of the respective regression function. Bar plots show estimated molecules per cell of SHP-1, CIS and SOCS3 in BaF3-EpoR cells (black bars) and CFU-E cells (white bars).

For an overview of the results see Table 1. The endogenous levels of CIS were observed to be within the same range in BaF3-EpoR of approximately 8,600 molecules per cell and in CFU-E cells of 6,500 molecules per cell. Similarly, the levels of SOCS3 in BaF3-EpoR cells of approximately 1,300 molecules per cell were comparable with levels in CFU-E cells of 2,600 molecules per cell.

	BaF3-EpoR		CFU-E	
	molecules/cell	concentration*	molecules/cell	concentration*
EpoR on surface	15,700 ± 1300	21.6 ± 13.3 /μm^2	~ 1000	32.3 ± 6.7 /μm^2
JAK2	13,700 ± 3,300	16.3 ± 4.0 nM	23,700 ± 13,000	98.4 ± 54.0 nM
Stat5	175,000 ± 75,000	207.6 ± 89.0 nM	20,000 ± 10,000	83.0 ± 41.5 nM
SHP-1	450,000 ± 90,000	385.5 ± 90.0 nM	8,500 ± 1,700	27.0 ± 6.2 nM
CIS	8,600 ± 700	7.1 ± 2.4 nM	6,500 ± 700	24.9 ± 8.3 nM
SOCS3	1,300 ± 500	1.78 ± 0.7 nM	2,600 ± 900	10.39 ± 4.3 nM

Table 1. Molecules per cell of JAK2/STAT5 pathway components estimated in BaF3-EpoR and CFU-E cells. Protein numbers were estimated as described. To calculate the concentrations different volumes and surface areas were considered for BaF3-EpoR (cytoplasm: 1400 μm^3, nucleus: 450 μm^3, surface area: 729 μm^2) and CFU-E cells (cytoplasm: 400 μm^3, nucleus; 275 μm^3, surface area: 372 729 μm^2). Numbers of EpoR, JAK2, STAT5 were kindly provided by Marcel Schilling and Andrea C. Pfeifer (DKFZ, Heidelberg). Molecules per cell for EpoR on the surface of CFU-E cells was reported previously (D'Andrea and Zon, 1990). *In the case of EpoR the density on the surface is displayed instead of the concentration.

Interestingly, the endogenous level of SHP-1 in BaF3-EpoR cells with 450,000 molecules per cell was estimated to be more than 50-fold higher compared to the level in the primary cells with approximately 8,500 molecules per cell. The results of the quantifications are summarized in Table 1, including endogenous levels of the EpoR, JAK2 and STAT5 (kindly provided by Andrea C. Pfeifer and Marcel Schilling, DKFZ Heidelberg).

The comparison of JAK2 and STAT5 levels revealed also remarkable differences in both cell types. In particular, the numbers of STAT5 in BaF3 cells are almost 10-fold higher than in CFU-E cells. By estimating the absolute protein concentrations of SHP-1, CIS, SOCS3, STAT5 and JAK2 parameter ranges of initial values could be defined for each of the measured protein species in the mathematical model of the JAK2/STAT5 pathway in CFU-E cells (see *Results - 2.5 Implementation of dynamic JAK2/STAT5 pathway model*).

2.3.2 Cell type-specific activation profile of the Epo-induced JAK2/STAT5 pathway

When studying the dynamic behavior of signal transduction pathways by mathematical modeling, the major prerequisite is the availability of reliable quantitative and time-resolved data. Thus, a standardized protocol was established to measure time-course experiments of JAK2/STAT5 pathway activation in BaF3-EpoR and CFU-E cells that ensures experimental reproducibility. Preliminary tests and dose-response experiments revealed that a starvation

time of 4 hours in BaF3-EpoR and 2 hours in CFU-E cells as well as a dose of 5 U/ml Epo is appropriate for maximal signal activation. Hence, these conditions were used in all time-course experiments.

The activation kinetics of EpoR, JAK2 and STAT5 phosphorylation, the level of total proteins as well as the levels of SHP-1 were determined by immunoprecipitation and subsequent quantitative immunoblotting in both BaF3-EpoR and CFU-E cells. As CIS was induced more strongly at protein level compared to SOCS3 in both cell-types, only CIS expression was recorded. For computational data processing, constant amounts of recombinant calibrator proteins were added to cellular lysates prior to immunoprecipitation. SDS-PAGE samples were loaded in a randomized, non-chronological order (Schilling et al., 2005a). Representative examples of original immunoblotting data are depicted (Fig. 14). Because of the limited availability of primary CFU-E cells, the time-course consisted of only 14 time-points while in BaF3-EpoR cells 18 timepoints were recorded.

As the time-course data demonstrated, the initial activation dynamics of EpoR, JAK2 and STAT5 in BaF3-EpoR and CFU-E (Fig. 15) cells resemble each other in respect to the time-resolution of sample intervals. Induction of phosphorylation occurred within the first minutes upon Epo stimulation and all three proteins showed maximal peak activation at approximately 10 min followed by a sharp decline. Following pathway activation, expression of the negative regulatory protein CIS was induced after 30-60 min in both cell types. The tyrosine phosphatase SHP-1 is constitutively expressed and remained constant over the entire period of observation. However, after approximately 2 h of Epo stimulation, the phosphorylation kinetics of JAK2/STAT5 pathway components showed significant differences between the two cell types. In BaF3-EpoR cells, the activation curves of EpoR and STAT5 returned to basal level, whereas in primary cells a residual steady-state phosphorylation level remained over 4 h of observation. Furthermore, the expression profile of the negative regulatory protein CIS differed in the two cell types. CIS expression in BaF3-EpoR cells reached a transient maximum after approximately 2 h of Epo stimulation followed by a decline to basal levels. In contrast, in primary cells CIS expression reached a sustained plateau within 4 h. Finally, the levels of total proteins showed remarkable differences. While JAK2 and EpoR remained constant in CFU-E cells, their levels in BaF3-EpoR cells decreased during the time of observation.

Taken together, the discrepancies in the kinetic behavior of the JAK2/STAT5 pathway between BaF3-EpoR and CFU-E cells suggested fundamental differences in the deactivation processes and further emphasized the importance of studies that compare the mechanisms of negative regulation of JAK2/STAT5 signaling in cell lines versus primary cells.

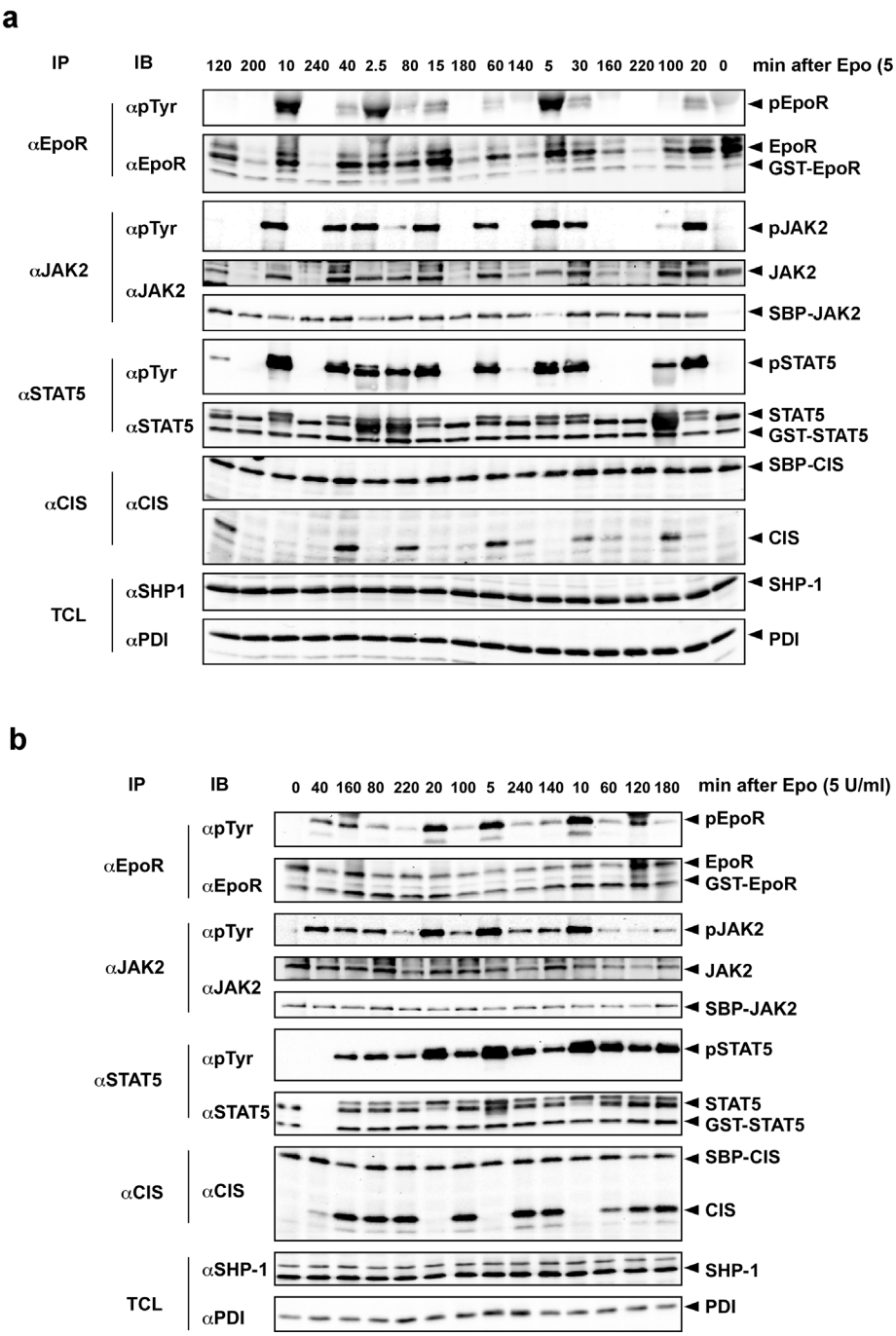

Fig. 14. Immunoblotting data of time-course experiments in BaF3-EpoR and CFU-E cells. Densely sampled time-course in Epo-induced **(a)** BaF3-EpoR and **(b)** CFU-E cells. Either BaF3-EpoR (1×10^7) or CFU-E cells (5×10^6) were stimulated with 5 U/ml Epo. At the indicated time points, cellular lysates were subjected to immunoprecipitation with antibodies against JAK2, EpoR, STAT5 and CIS and subsequently analyzed by quantitative immunoblotting based on chemiluminescence detection. All experiments were performed at least in triplicates and one representative example is shown.

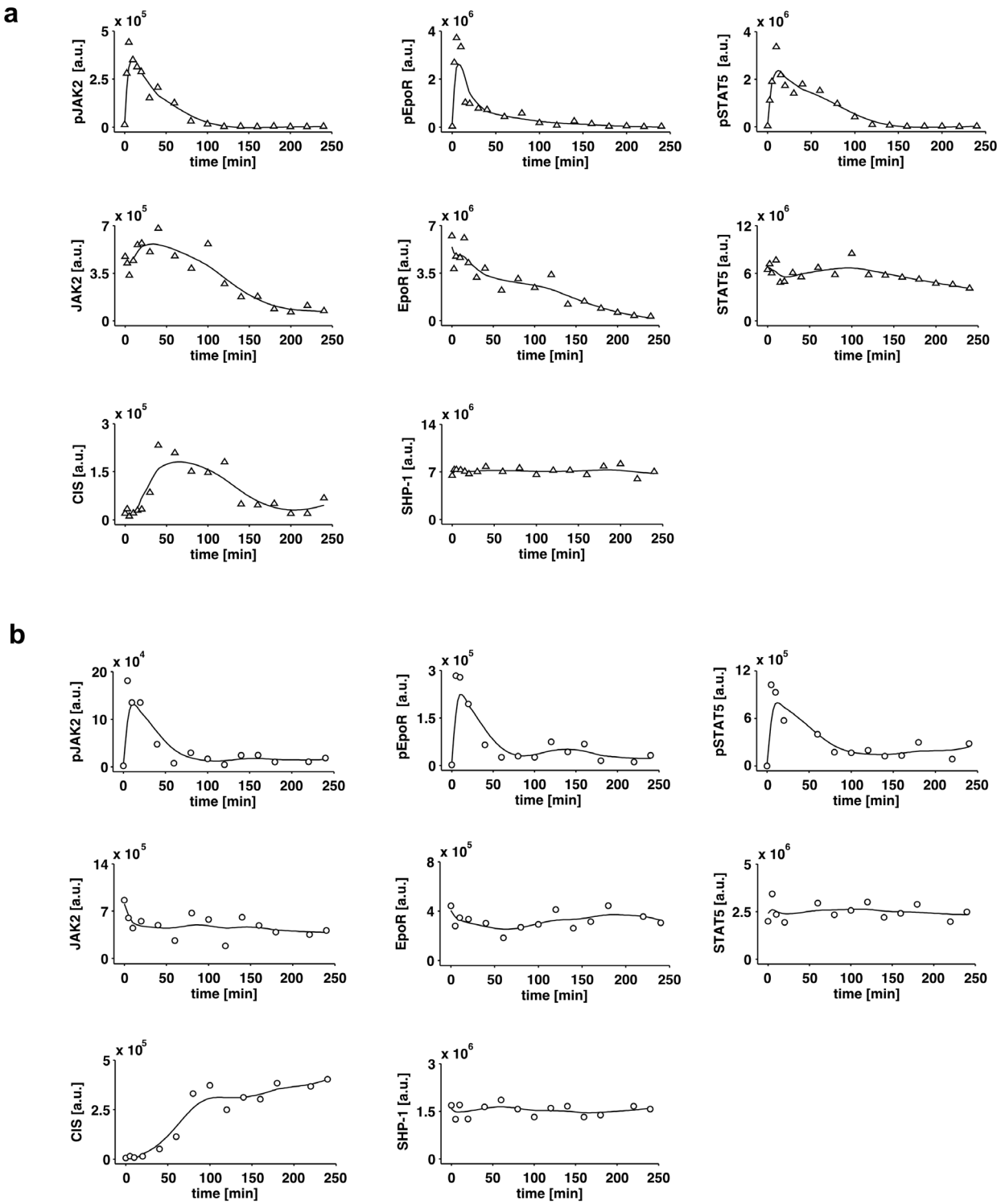

Fig. 15. Time series of Epo-induced JAK2/STAT5 pathway activation in BaF3-EpoR and CFU-E cells. Starved **(a)** BaF3-EpoR cells (1×10^7) or **(b)** CFU-E (5×10^6) were stimulated with 5 U/ml Epo and analyzed for relative levels of phosphorylated JAK2, EpoR and STAT5 as well as for relative expression levels of total proteins CIS, SHP-1, EpoR, JAK2 and STAT5. Data generated in BaF3-EpoR (triangles) or CFU-E (circles) cells were processed using GelInspector software and plotted with splines (solid lines). Time-course experiments were performed three times and a representative analysis is shown.

2.4 Targeted perturbation of negative feedback components

To gain insight into the potential role of the three negative feedback regulators SHP-1, CIS and SOCS3 in the cell line BaF3-EpoR and primary CFU-E cells, two strategies were employed. The Tet-inducible system was established to facilitate inducible dose-dependent overexpression of SHP-1 in BaF3-EpoR cells. By employing this technique the consequences of temporally controlled upregulated negative feedback loops on the dynamic behavior of the JAK2/STAT5 signaling pathway in BaF3-EpoR cells could be investigated. However, for CFU-E cells, the Tet-system is not applicable since these primary cells start to differentiate after approximately one day in culture. In the second strategy, the general inhibitor of transcription, actinomycin D, was used to block expression of induced transcriptional regulators.

2.4.1 Establishing the Tet-inducible system in BaF3 cells

To establish the Tet-system in BaF3 cells, the improved transactivator variant rtTA-M2 (Urlinger et al., 2000) as well as two different tet-response elements (TREs) have been employed. The first one, designated as TRE-L, contained the original heptamerized Tet-operator sequence P_{tet-1} with the CMV minimal promoter. The second one, denoted as TRE-T in this study, consists of a modified Tet-operator sequence and a shortened CMV promoter and was proposed to display tight control of gene expression with significantly less background activity than the original system (H. Bujard, ZMBH).

Besides the Tet-system components, an appropriate retroviral vector system is essential to achieve maximal induction rates and low background levels in hematopoietic cells which are difficult to transfect. Therefore, various retroviral vectors were tested and the two most efficient were selected. For the delivery of the gene of interest under the control of the TRE, a self-inactivating (SIN) retroviral vector (pMOWSIN) was used. This SIN-vector lacked the promoter and enhancer region of the U3 sequence in the 3'proviral longterminal repeats (LTRs) and thus prevented potential cross talk between the strong viral promoter and the inducible TRE that otherwise may cause increased background expression of the gene of interest. The rtTA was delivered by a second retroviral vector pMOWS (Ketteler et al., 2002) that was identified to produce the highest level of transgene expression in BaF3 cells.

In order to establish and evaluate the Tet-system in BaF3 cells, green fluorescent protein (GFP) was used as a reporter in induction assays that allows for detection not only by immunoblotting but also by flow cytometric analysis. BaF3 cells were co-transduced with both vectors and induced with increasing amounts of Dox ranging from 1 to 5000 ng/ml to compare the two different TRE variants, TRE-L and TRE-T. Relative expression levels of GFP were monitored by flow cytometric analysis as well as by immunoblotting of cellular lysates 24 h hours after Dox induction (Fig. 16).

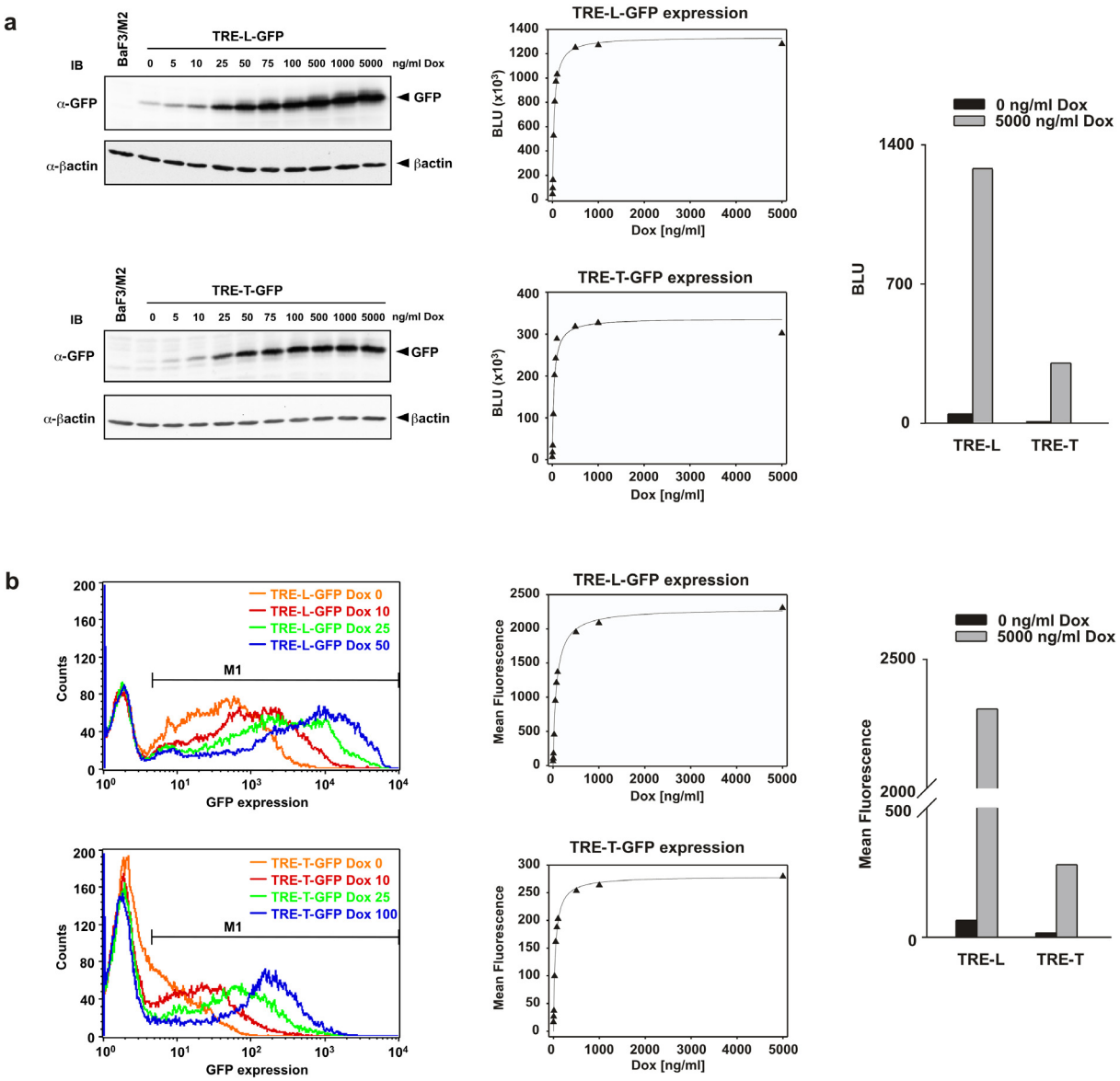

Fig. 16. Dose-dependent expression of GFP by the Tet-inducible system in BaF3 cells. BaF3 cells co-transduced with pMOWS-rtTA and pMOWSIN-TRE-GFP (variant TRE-T or TRE-L) were induced with increasing concentrations of Dox for 24 h. **(a)** Expression of GFP was subsequently determined in cellular lysates of 1×10^6 BaF3 cells by immunoblotting based on chemiluminescence detection. Quantification of immunoblot signals was plotted versus Dox concentrations (triangles) with a saturation regression function. Bars represent maximal fold induction of GFP with 5000 ng/ml Dox compared to background expression level with 0 ng/ml Dox. **(b)** A corresponding flow cytometry analysis was performed. The overlay histogram depicts four representative results of different doxycycline concentrations. The mean fluorescence was plotted versus Dox concentrations (triangles) with a saturation regression function. Bars represent maximal fold induction of GFP with 5000 ng/ml Dox compared to background expression level with 0 ng/ml Dox.

Quantification of GFP expression demonstrated that the system is particularly sensitive to low Dox concentrations between 5 and 500 ng/ml. In this range, the expression level of GFP followed the increasing concentrations of Dox almost linearly before saturation was reached at approximately 1000 ng/ml Dox. Interestingly, by comparing the flow cytometry analysis of

the two TRE variants, TRE-T showed significantly lower background activity at 0 ng/ml Dox which is in line with its proposed optimized efficacy. On the other hand, GFP expression under the control of the TRE-L variant achieved a remarkable higher range of overexpression up to 35-fold whereas the TRE-T variant only reached up to 20-fold GFP overexpression at highest Dox concentrations. Thus, exploiting the possibilities of the two TRE-variants, either tight control or high induction rates can be attained in BaF3 cells according to individual requirements.

2.4.2 Tet-inducible overexpression of SHP-1 in BaF3-EpoR cells

Next, the Tet-inducible expression system was used to overexpress SHP-1 in BaF3-EpoR cells and investigate the consequences on the dynamic behavior of the JAK2/STAT5 signaling pathway. Preliminary tests revealed that an induction of 8 h with Dox prior to Epo stimulation is sufficient to allow for high expression rates but avoid potential toxic artefacts of constitutively overexpressed negative regulators. In order to monitor the dynamic behavior of the JAK2/STAT5 signaling pathway in cells with upregulated SHP-1 levels, Dox-induced BaF3-EpoR cells were stimulated with 5 U/ml Epo and the kinetics of EpoR, JAK2 and STAT5 phosphorylation were determined by immunoprecipitation and subsequent quantitative immunoblotting based on chemiluminescence detection (Fig. 17). Surprisingly, the phosphorylation levels of EpoR, was altered only marginally. The phosphorylation of JAK2 which is suggested to be a substrate of SHP-1 showed no difference compared to the control while STAT5 phosphorylation was reduced slightly indicating that the effects taking place at the receptor level are transmitted to STAT5 level.

Taken together, the overexpression of SHP-1 had only little impact on the phosphorylation levels of the JAK2/STAT5 pathway components. This observation may be explained by the high endogenous expression level of SHP-1 in BaF3-EpoR cells and the comparable low overexpression level of only 2-fold. Moreover, previous studies reported that SHP-1 is not constitutively active but requires binding to a phosphorylated tyrosine residue i.e. on the EpoR to be activated (Pao et al., 2007b). Because of the limited numbers of EpoR in the cells, the activation of SHP-1 may reach saturation that renders further upregulation of SHP-1 levels ineffective.

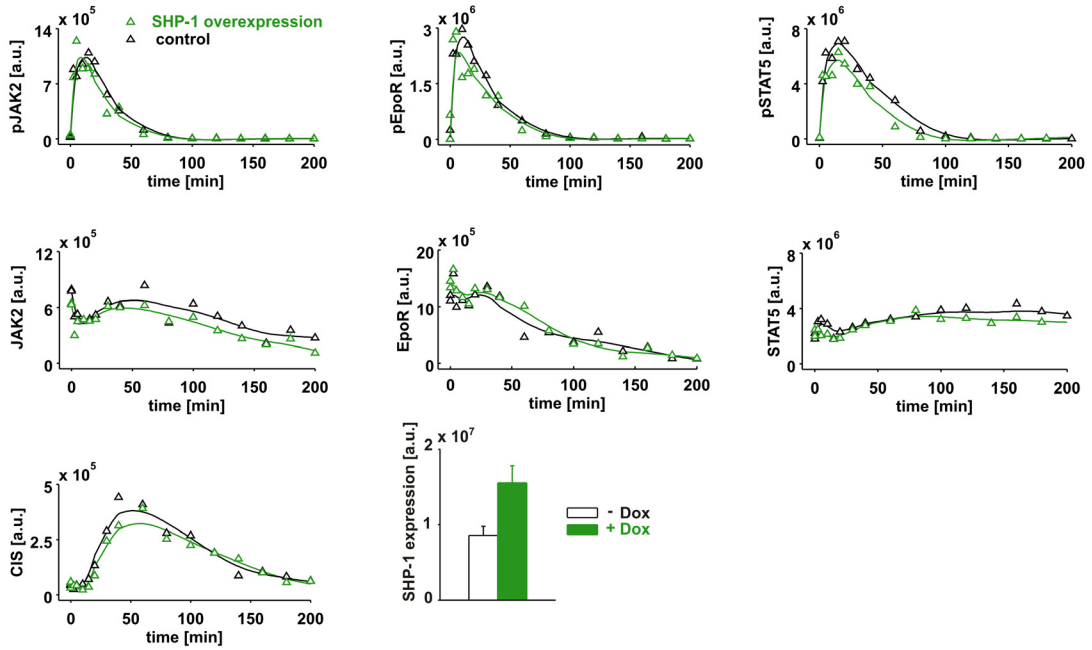

Fig. 17. Time series of Epo-induced JAK2/STAT5 pathway activation in BaF3-EpoR cells overexpressing SHP-1. BaF3-EpoR cells co-transduced with pMOWS-rtTA and pMOWS-TRE-L-SHP-1 were induced with 2 µg/ml Dox (green) or without addition (black) for 8 h prior to stimulation with Epo. Cellular lysates of 1×10^7 BaF3-EpoR cells were analyzed for relative levels of phosphorylated JAK2, EpoR, STAT5 and relative expression level of total proteins CIS, EpoR, JAK2, STAT5 and SHP1 upon stimulation with 5 U/ml Epo. At the indicated time points, stimulated cells were lysed and proteins were analyzed by immunoprecipitation and subsequent quantitative immunoblotting. Data (triangles) was processed using GelInspector software and plotted with smoothing splines (solid lines). Time-course experiments were performed three times and a representative analysis is shown.

2.4.3 Different impact of actinomycin D-mediated inhibition

Next, the generic inhibitor actinomycin D was used to inhibit transcription and observe the consequences on the dynamic behavior of JAK2/STAT5 signaling in BaF3-EpoR cells and primary CFU-E cells. Therefore, cells were treated with 1 µg/ml actinomycin for 10 min and the dynamic behavior of JAK2, EpoR and STAT5 activation was monitored as described before (see – *Results 2.4 Kinetic activation profile of JAK2/STAT5 signaling*). The original immunoblotting data are depicted in Fig. 18.

As control for the effectiveness of actinomycin D treatment on transcription, the kinetics of CIS expression in actinomycin D treated cells were compared to control cells. As demonstrated by the immunoblot of CIS in CFU-E and BaF3-EpoR cells (Fig. 18) 1 µg/ml actinomycin D was sufficient to completely block expression in both cells types. Interestingly, in BaF3-EpoR cells the kinetics of phosphorylation of EpoR, JAK2 and STAT5 between actinomycin D-treated cells and control cells showed no significant differences (Fig. 19a). These results indicate that induced transcriptional regulators seem to play no major role in attenuating signal transduction in BaF3-EpoR cells.

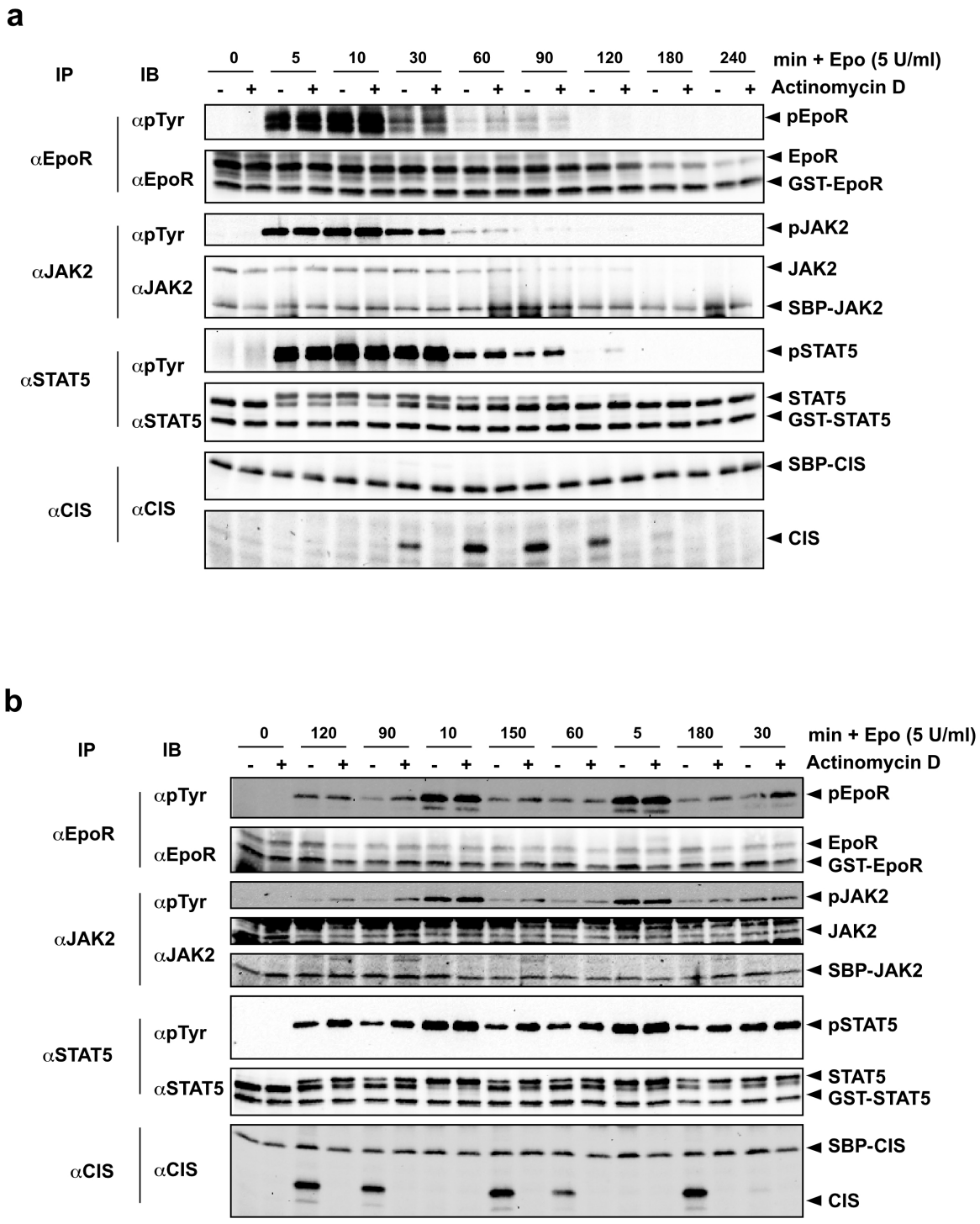

Fig. 18. Immunoblotting data of time-course experiments in untreated and in actinomycin D-treated BaF3-EpoR and CFU-E cells. (a) BaF3-EpoR or **(b)** CFU-E cells were treated with either 1 µg/ml actinomycin D or with vehicle (0.1 % dimethylsulfoxide) alone for 10 min. Subsequently, BaF3-EpoR (1×10^7) or CFU-E cells (5×10^6) were stimulated with 5 U/ml Epo. At the indicated time points and cellular lysates were subjected to immunoprecipitation with antibodies against JAK2, EpoR, STAT5 and CIS and analyzed by quantitative immunoblotting based on chemiluminescence detection. All experiments were performed at least in triplicates and one representative example is shown.

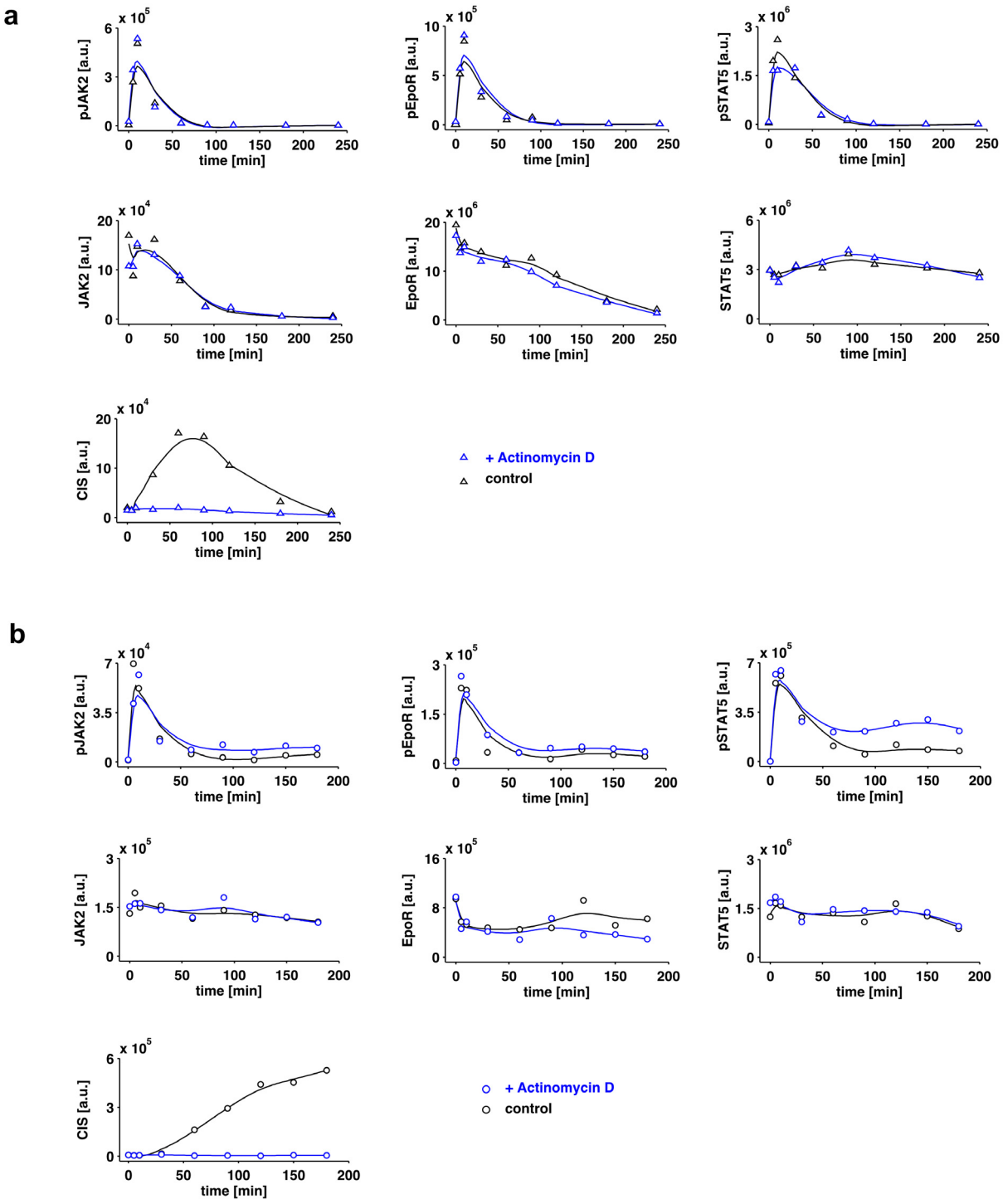

Fig. 19. Time series of Epo-induced JAK2/STAT5 pathway activation in untreated and in actinomycin D-treated BaF3-EpoR cells and CFU-E cells. (a) BaF3-EpoR or **(b)** CFU-E cells were treated with 1 µg/ml actinomycin D (blue) or with vehicle (0.1 % dimethylsulfoxide) alone (black) for 10 min. BaF3-EpoR or CFU-E cells were induced with 5 U/ml Epo and analyzed for relative levels of phosphorylated JAK2, EpoR, STAT5 and relative expression level of total proteins CIS, EpoR, JAK2 and STAT5 at the indicated time points. Generated data in BaF3-EpoR (triangles) was processed using GelInspector software and plotted with smoothing splines (solid lines). Time-course experiments were performed three times and a representative analysis is shown.

In CFU-E cells, however, the long-term phosphorylation level of STAT5 was significantly elevated in actinomycin D-treated cells. Hence, this result suggested a mechanism that involves induction of transcriptional regulators to control the long-term steady-state level of STAT5. The kinetics of EpoR and JAK2 differed only marginally from the control, indicating that downregulation of these species is predominantly regulated by other mechanisms.
In summary, the time-course experiments with actinomycin treatment demonstrated that the role of transcriptional regulators in the JAK2/STAT5 pathway differ in BaF3-EpoR cells and primary CFU-E cells. Thus, these observations underscore the importance of studying the effects of negative feedback loops in the relevant cellular context. For a deeper understanding of the situation *in vivo* it is essential to investigate the processes in primary CFU-E cells.

2.5 Implementation of dynamic JAK2/STAT5 pathway model in CFU-E cells

The three proteins SHP-1, SOCS3 and CIS have been identified in this work as putative negative regulators of the Epo-induced JAK2/STAT5 pathway which is in line with previous reports. Because of their overlapping functions, a major question was how these proteins control the JAK2/STAT5 pathway in respect to temporal aspects and effectiveness of signal inhibition. Employing the analytical tools of a mathematical modeling approach by systematically combining biological knowledge with quantitative experimental data a deeper insight into the control of the JAK2/STAT5 pathway can be attained. In particular, a dynamic model enables the identification and evaluation of the most important reactions and proteins involved in controlling the output of the system which is difficult to observe with classical experimental techniques.
In collaboration with Marcel Schilling (DKFZ, Heidelberg) and Andreas Raue (FDM, University of Freiburg) an ordinary differential equation (ODE) model of the Epo-induced JAK2/STAT5 pathway was implemented. All reactions of the network were modelled by mass-action kinetics or by Michaelis-Menten approximations. The general topology of the model was constructed based on prior biological knowledge and experimental data generated in this work. At first, a large model comprising all possible biological complexes and biochemical reactions was compiled. However, the major drawback of this very detailed model was the large number of free variables leading to unidentifiable parameters. Hence, in an iterative process the model was condensed by systematically abandoning short-lived protein-protein complexes and very rapid reactions that were proven not to be essential for describing the data as revealed by comparison of the model-data compliances. The final model comprised a total number of 13 variables and 17 parameters (Fig. 20). In this model, Epo was used as input function that directly triggered phosphorylation of JAK2. The activated kinase in turn mediated phosphorylation of the EpoR.

The tyrosine phosphatase SHP-1 has previously been shown to require binding to a phosphorylated tyrosine residue i.e. on the EpoR to activate phosphatase activity (Barford and Neel, 1998; Neel et al., 2003; Pei et al., 1996).

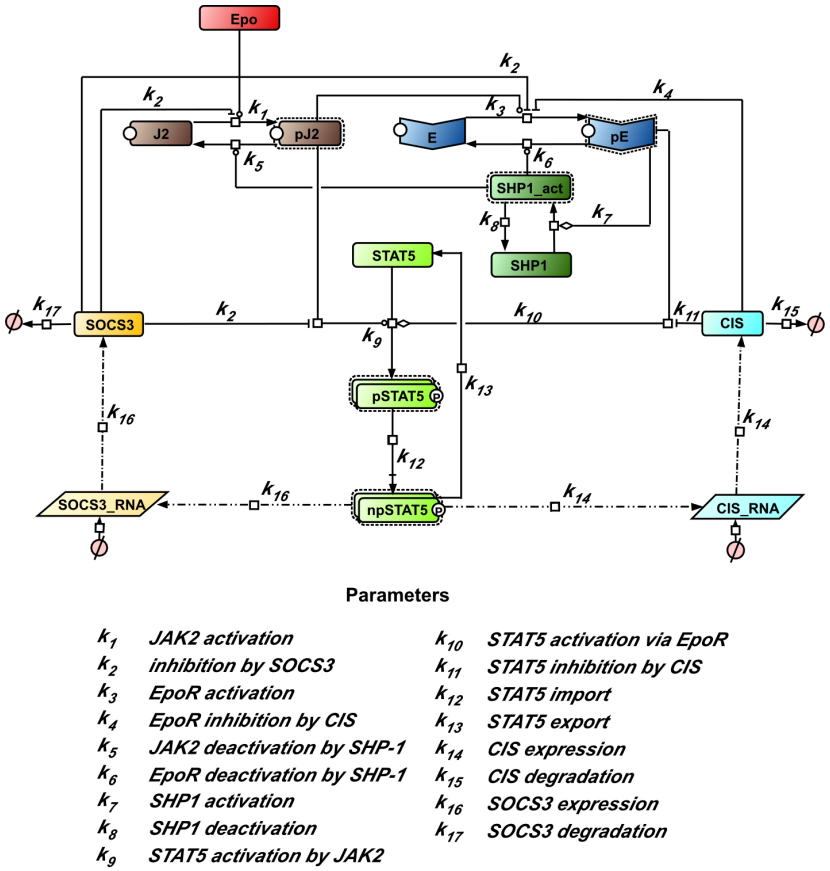

Fig. 20. Schematic representation of the JAK2/STAT5 pathway model with negative feedback regulators in CFU-E cells. The model consists of 17 parameters and 13 variables. Reactions were modelled assuming mass-action (solid arrows). Enzyme catalysis (circle-headed lines), inhibition (bar-headed lines) and modifiers (diamond-headed lines) are represented. Protein expression is indicated as pointed-dashed line. Prefix p represents phosphorylated species, n nuclear species. Graphical notation was adapted using Cell Designer (Version 4.0.1.).

Therefore, SHP-1 was considered to exist in two states in the model: one active and one inactive form. The transition of inactive to catalytically active SHP-1 is mediated by phosphorylated EpoR that reflects the recruitment to the specific phosphotyrosine residue. Because the number of EpoR is limited, activation of SHP-1 can reach saturation and thus was modelled by using a Michaelis-Menten approximation. The activated form of SHP-1 then can trigger dephosphorylation of JAK2 and the EpoR.

Phosphorylation of STAT5 by JAK2 is mediated by recruiting STAT5 to phosphotyrosine 343 and 401 of the EpoR cytoplasmic domain that functions as a scaffold (Barber et al., 2001; Gobert et al., 1996; Klingmüller et al., 1996). Thus, in the reaction of STAT5 activation both

proteins were included. Phosphorylated JAK2 was considered as enzyme and the phosphorylated EpoR as additional modifier. Dimerization of STAT5 is known to occur very rapidly after phosphorylation and could be neglected in the model. The phosphorylated and dimerized STAT5 shuttles into the nucleus and binds to consensus sequences of the DNA to activate gene transcription (Horvath, 2000). After a certain sojourn in the nucleus, dephosphorylated STAT5 translocates back into the cytoplasm to enter a new cycle of activation. This mechanism was revealed by a previous study that identified nucleocytoplasmic cycling of STAT5 as an important feature of the system to continuously monitor receptor activation (Swameye et al., 2003). The different forms of STAT5 were integrated in the model by three distinct variables: unphosphorylated STAT5 in the cytosol, phosphorylated STAT5 dimers in the cytosol and phosphorylated STAT5 dimers in the nucleus. Three parameters describe the transitions between these variables: STAT5 activation, the import rate into the nucleus and the export rate back into the cytosol.

The microarray analysis (Fig. 12) revealed that CIS and SOCS3 mRNA levels were rapidly and strongly upregulated in Epo-induced CFU-E cells (see *2.2 Genome-wide analysis of Epo-induced transcriptional regulators*). Thus, both proteins were included into the mathematical model as transcriptional feedback regulators. Previously, SOCS3 has been proposed to bind via its SH2 domain to activated EpoR and JAK2 and to inhibit JAK2 activity by directly binding to the kinase activation loop via its KIR domain (Hortner et al., 2002; Sasaki et al., 1999; Sasaki et al., 2000). CIS was identified as negative regulator of JAK/STAT signaling by binding to phosphotyrosine 401 of the EpoR, thereby competing for receptor binding with STAT5 (Ketteler et al., 2003; Yoshimura et al., 1995). Another study indicated that CIS is involved in proteasome-mediated degradation of the EpoR (Verdier et al., 1998a). Hence, SOCS3 and CIS were included in the model at different levels of signal transmission: CIS was considered as inhibitor only of STAT5 and EpoR activation and the impact of CIS on STAT5 activation was thereby exclusively related to the EpoR-mediated contribution of the reaction. In contrast, SOCS3 additionally inhibited JAK2 activation and downstream signals.

2.5.1 Generation of time-course data in CFU-E cells

To determine the parameters of the JAK2/STAT5 pathway model, various stimulation time-course experiments were performed in CFU-E cells monitoring the kinetics of several pathway components simultaneously by quantitative immunoblotting. Because CIS and SOCS3 have overlapping functions and thus are not structurally identifiable by the model, their role in negative regulation can only be dissected by perturbing the two proteins individually and observing the response of the system. Furthermore, to gain detailed information about the phosphatase also SHP-1 was altered directly. Consequently, five

different experimental conditions were selected to challenge the network and monitor the dynamic behavior experimentally upon Epo stimulation: (i) CFU-E cells (dense sampling and SOCS3 time-course) (ii) CFU-E cells treated with actinomycin D, (iii) CFU-E cells overexpressing CIS, (iv) CFU-E cells overexpressing SOCS3, (v) CFU-E cells overexpressing SHP-1.

The generation of time-course data in Epo-stimulated CFU-E cells and additionally Epo-stimulated CFU-E cells treated with actinomycin D has been described before (see - *2.3.2 Cell type-specific activation profile of the Epo-induced JAK2/STAT5* pathway). To determine the kinetic of SOCS3 expression, time-course experiments were performed in Epo stimulated CFU-E cells (Fig. 21). The time-resolved expression profile of SOCS3 resembles the behavior of its mRNA kinetic. After approximately 30 min the endogenous protein level increases and reaches its maximum level at 120 min. Within the entire time of observation SOCS3 remains at this constant high level.

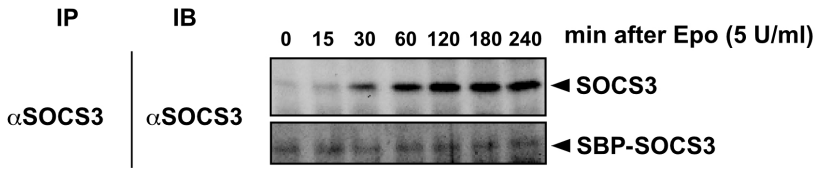

Fig. 21. Time-course experiment of SOCS3 expression in CFU-E cells. Starved CFU-E cells (5×10^6) were stimulated with 5 U/ml Epo and analyzed for relative levels of total protein SOCS3. At the indicated time points cellular lysates were subjected to immunoprecipitation with anti-SOCS3 and subsequently analyzed by quantitative immunoblotting based on chemiluminescence detection. Time-course experiments were performed in duplicates and a representative analysis is shown.

In order to perform time-course experiments in CFU-E cells overexpressing SOCS3, CIS or SHP-1, freshly isolated primary erythroid progenitor cells were retrovirally transduced. The low transduction efficiency in primary erythroid cells yielded only 10-20% positive cells. These cells were sorted by the magnetic cell separation system (MACSselect, Miltenyi Biotec) and directly used for the experiment. Fig. 22 depicts representative examples of unprocessed immunoblotting data.

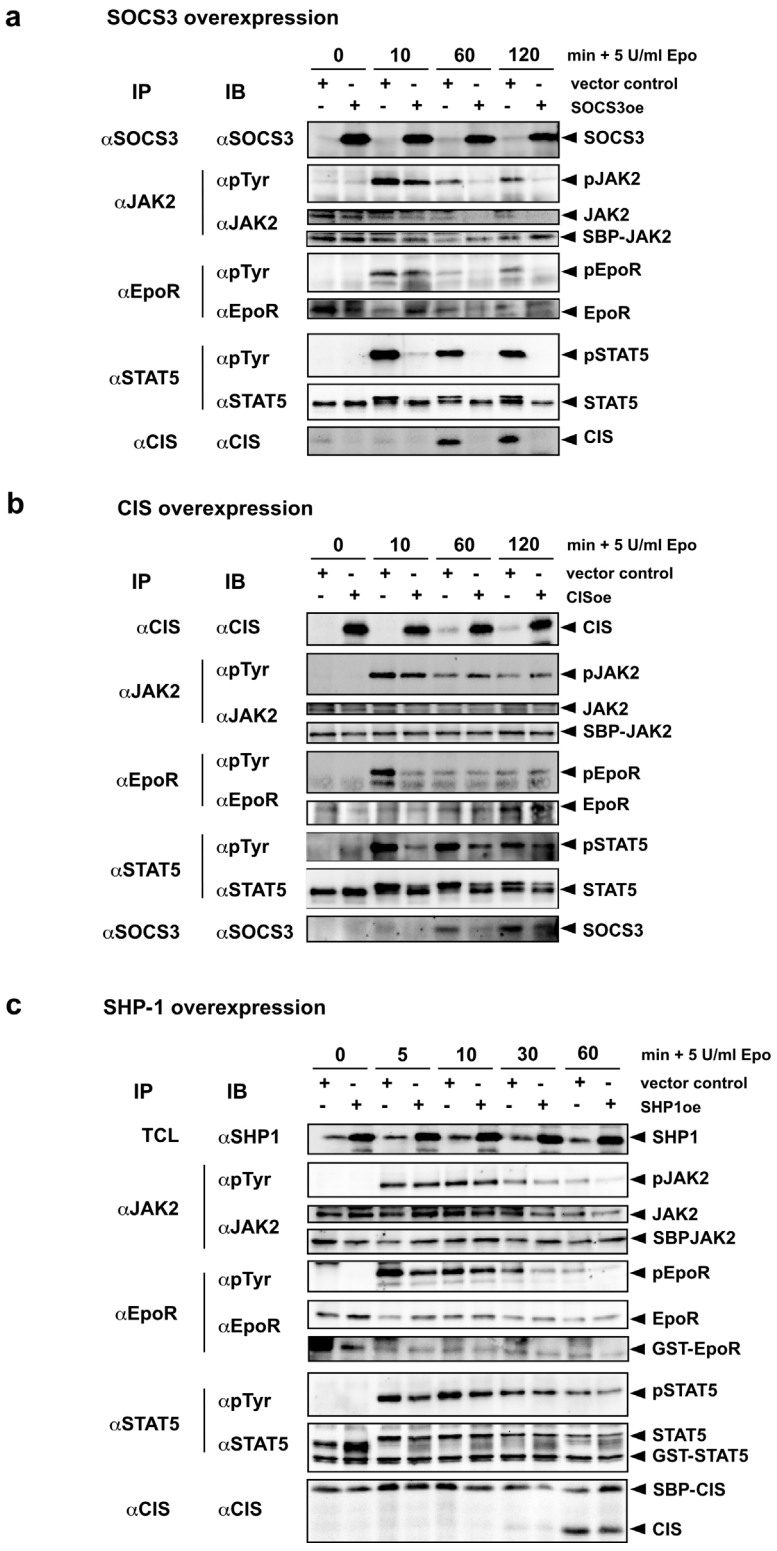

Fig. 22. Immunoblotting data of time-course experiments in CFU-E cells for multiple perturbation conditions. Freshly isolated CFU-E cells were retrovirally transduced with **(a)** SOCS3, **(b)** CIS or **(c)** SHP-1. After sorting of positive cells, CFU-E cells (5×10^6) were induced with 5 U/ml Epo. At the indicated time points cellular lysates were subjected to immunoprecipitation with antibodies against JAK2, EpoR, STAT5, CIS and SOCS3 and subsequently analyzed by quantitative immunoblotting based on chemiluminescence detection. All experiments were performed in at least duplicates and one representative example is shown.

Due to the limited availability of primary cells experiments consisted of only 4-6 timepoints. Overexpression of SOCS3 in CFU-E cells strongly inhibited the phosphorylation of JAK2, EpoR and STAT5 as well as the expression of CIS. CIS overexpression in CFU-E cells led to reduced activation of STAT5 and EpoR phosphorylation and caused decreased expression of SOCS3. In cells overexpressing SHP-1, the peak amplitude of EpoR and STAT5 activation were decreased considerably whereas CIS and JAK2 were reduced only marginally.

2.5.2 Model calibration by multi-experiment fitting

Parameter estimation was performed by multi-experiment fitting of all data sets (Fig. 14,Fig. 18, Fig. 21, Fig. 22) simultaneously using the software PottersWheel (Maiwald and Timmer, 2008). Six observables were defined for calibration of the mathematical model: phosphorylated EpoR, phosphorylated JAK2, STAT5 in the cytoplasm, phosphorylated STAT5 in the cytoplasm, CIS and SOCS3. The levels of total proteins of JAK2 and EpoR remained fairly constant over the entire period of observation and thus mass conservation was assumed for these proteins. The start values of the different species in the model were defined as described (see – *2.4 Quantifications of negative feedback regulators of the JAK2/STAT5 pathway*). The concentrations of CIS and SOCS3 were set to zero at t = 0 min and the amounts determined at maximal activation t = 120 min were included in the model. Trajectories of the best fit are depicted (Fig. 23 - Fig. 25).

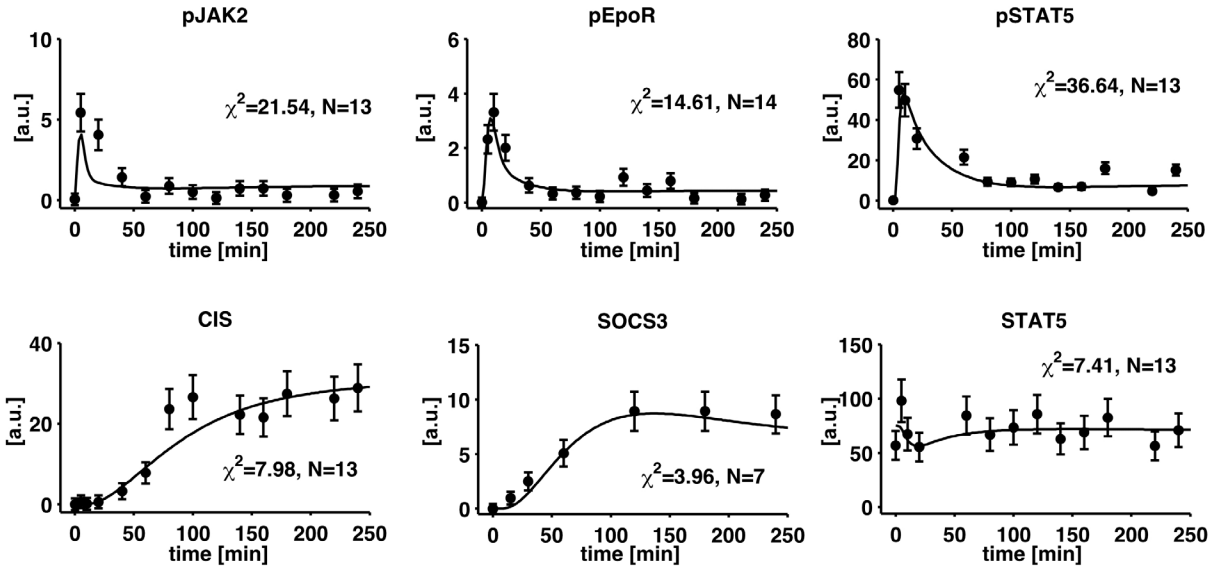

Fig. 23. Model calibration by multi-experiment fitting (I): Time-course with dense sampling and SOCS3 in CFU-E cells. For generation of data refer to Fig. 14 and Fig. 21. Trajectories of the best fit are indicated by solid lines and experimental data are represented by black circles with standard deviations. Parameter estimation was performed simultaneously for five different data sets. χ^2-values lower than N (number of data points) indicate accurate description of the data.

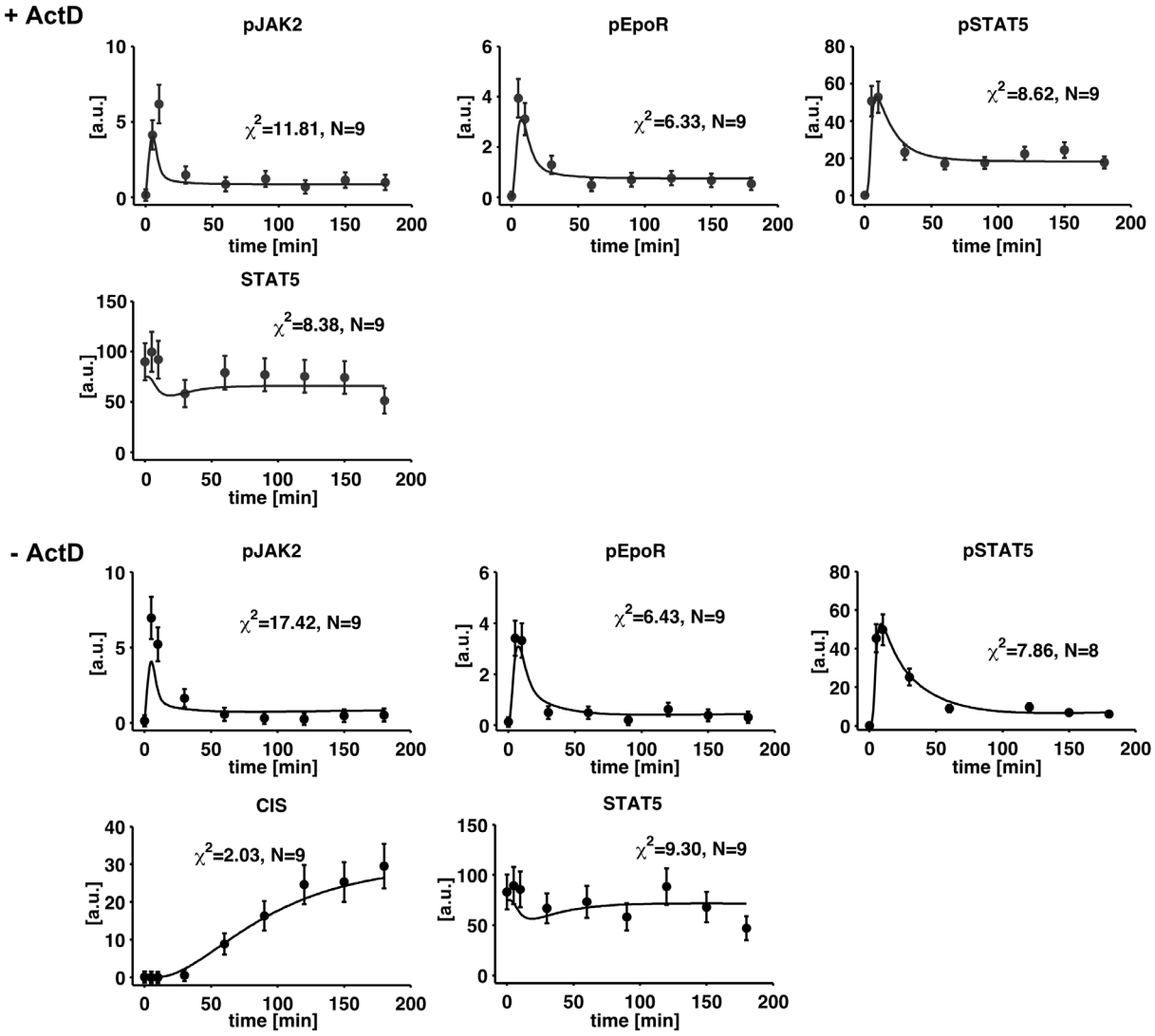

Fig. 24. Model calibration by multi-experiment fitting (II): Time-course in CFU-E cells treated with actinomycin D. For generation of the data refer to Fig. 18. Trajectories of the best fit are indicated by solid lines and experimental data are represented by black circles with standard deviations. Parameter estimation was performed simultaneously for five different data sets. χ^2-values lower than N (number of data points) indicate accurate description of the data.

The total χ^2 = 241.82 that is defined as the model deviation from the data normalized to the measurement error, indicates an accurate description of the data in respect to the total number of N = 213 datapoints. For detailed information on parameter values refer to *Appendix - 6.3 Ordinary differential equation model of the JAK2/STAT5 pathway in CFU-E cells*.

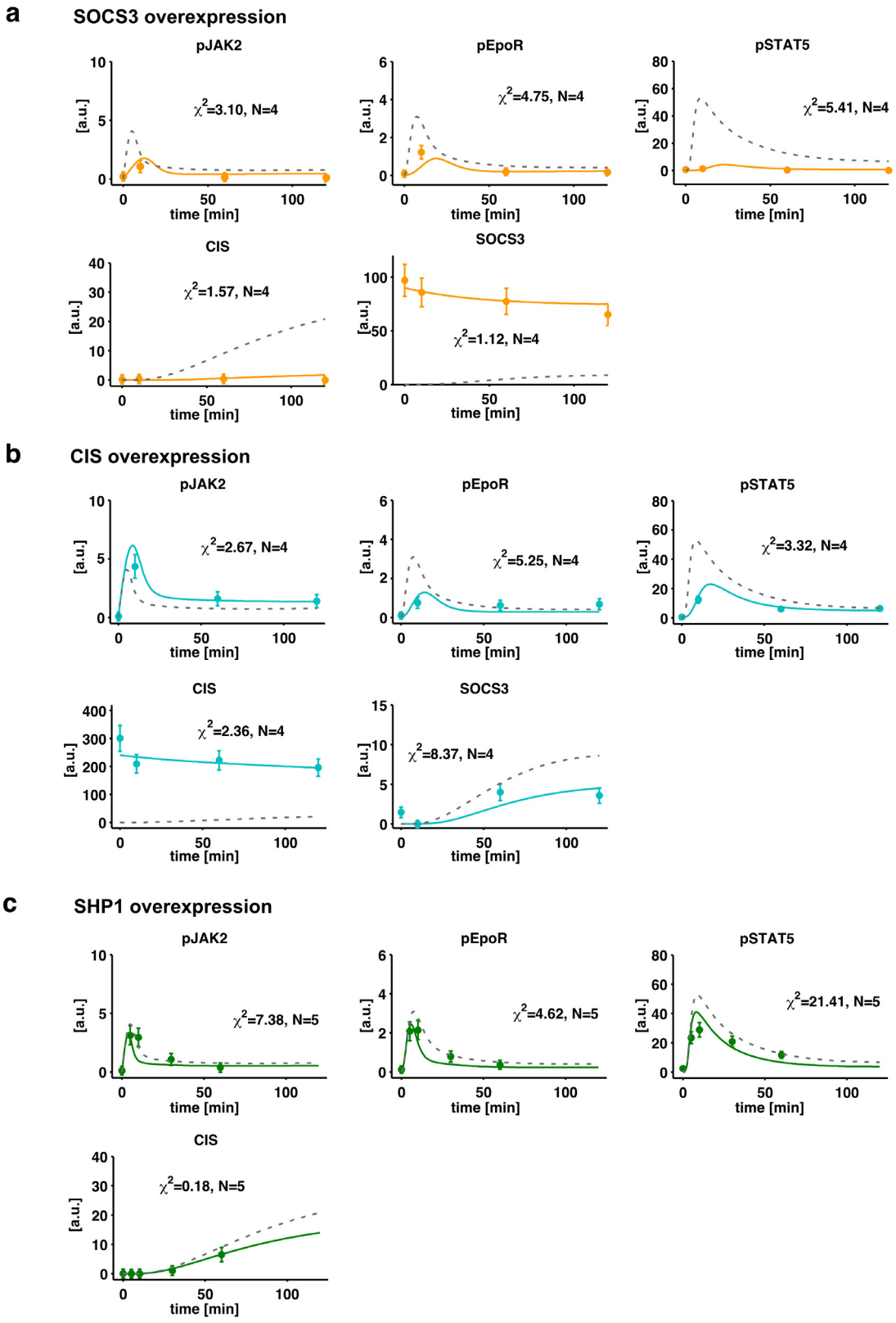

Fig. 25. Model calibration by multi-experiment fitting (III): Time-course in CFU-E cells overexpressing SOCS3, CIS or SHP-1. For generation of data refer to Fig. 22. Trajectories of the best fit are indicated by solid lines and experimental data are represented by circles with standard deviations for **(a)** SOCS overexpression (orange), **(b)** CIS overexpression (blue) and **(c)** SHP-1 overexpression (green). For visualization, simulated trajectories of control cells are indicated (dashed lines). Parameter estimation was performed simultaneously for five different data sets. χ^2-values lower than N (number of data points) indicate accurate description of the data.

2.5.3 Identifiability of estimated parameters and confidence intervals

For a good accuracy of model simulations, the estimated parameters are required to display small confidence intervals. Furthermore, to calculate the confidence intervals the model parameters have to be identifiable. Therefore, the estimated parameter values were investigated by a fit sequence analysis. Fits to experimental data were performed for 5000 runs with varying initial guesses of parameters and the distribution of the calibrated parameter values of 4% of the best 5000 fits were plotted (see *Appendix - 6.4 Identifiability analysis*). Only three out of 17 parameters exhibited a large distribution of values indicating a non-identifiability. Detailed scatter plots of parameter dependencies revealed a strong correlation between these three parameters. The fixation of one of the three parameters resulted in a narrowed relative distribution of all parameters below 35% and thus all parameters could be defined as identifiable. Next, point-wise confidence intervals (68%) on the estimated parameter values were calculated. As represented in Fig. 26 sufficiently small confidence intervals were found for all parameters demonstrating good accuracy of model predictions.

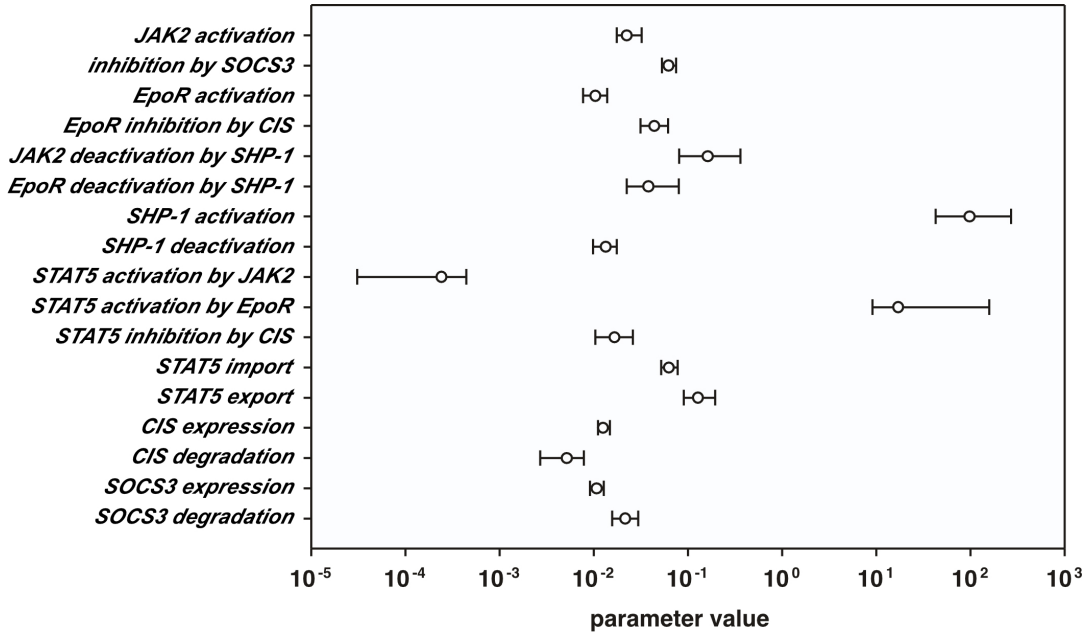

Fig. 26. Point-wise 1σ confidence intervals for estimated parameters. The best fit with smallest total χ^2 = 241.82 was used to calculate the confidence intervals of all estimated parameters. In collaboration with Andreas Raue (University of Freiburg).

2.6 Control analysis of the JAK2/STAT5 pathway

2.6.1 Effects of altered SHP-1, SOCS3 and CIS levels on JAK2/STAT5 signaling

Statistical validation demonstrated a good model-data-compliance and adequate confidence intervals. Therefore, the calibrated model could be employed to investigate the impact of the negative feedback regulators SHP-1, SOCS3 and CIS on the kinetic behavior of the JAK2/STAT5 pathway. To address the question to what extent the magnitude as well as the duration of signaling are controlled by the phosphatase and the two SOCS proteins simulations with perturbed parameters controlling SHP-1, SOCS3 or CIS levels were performed (Fig. 27).

The initial value of SHP-1 was logarithmically incremented in 5 steps to 10-fold or decreased in 5 steps to 0.1-fold expression. Simulations of the kinetic behavior of phosphorylated EpoR, JAK2 and STAT5 showed a strong influence of SHP-1 on the peak amplitude and signal duration (Fig. 27a). Interestingly, a high expression level of SHP-1 had only small effects on the signal intensity, whereas downregulation of the SHP-1 level strongly increased the duration. All signaling molecules were similar sensitive towards changes of SHP-1 levels.

Parameters controlling SOCS3 and CIS expression were varied as described above for SHP-1 to compare the effect of perturbed SOCS proteins on the pathway components (Fig. 27b,c). Simulations showed that the influence of SOCS3 and CIS concentrated on the long-term steady-state level of the activated signaling components. The strongest alterations were observed for phosphorylation levels of STAT5 in the nucleus. Here, a significant effect on the steady-state value of STAT5 was predicted even for small parameter changes of SOCS3 and CIS expression. High expression of SOCS3 led to complete inactivation of the STAT5 phosphorylation level that recovered at later timepoints due to the negative feedback on pathway activation. The comparison of the impact of the two SOCS proteins on the modulation of STAT5 phosphorylation levels revealed that the control strength of SOCS3 exceeded that of CIS. This indicates that the inhibitory effect of SOCS3 on the level of JAK2 activity is more efficient than the inhibitory action of CIS on the level of EpoR in respect to the activation of STAT5.

Taken together, the simulations revealed that changing SHP-1 concentrations influence the initial signal magnitude and duration of JAK2/STAT5 signaling components, whereas the levels of the two SOCS proteins fine-tune the extent of the long-term steady-state level.

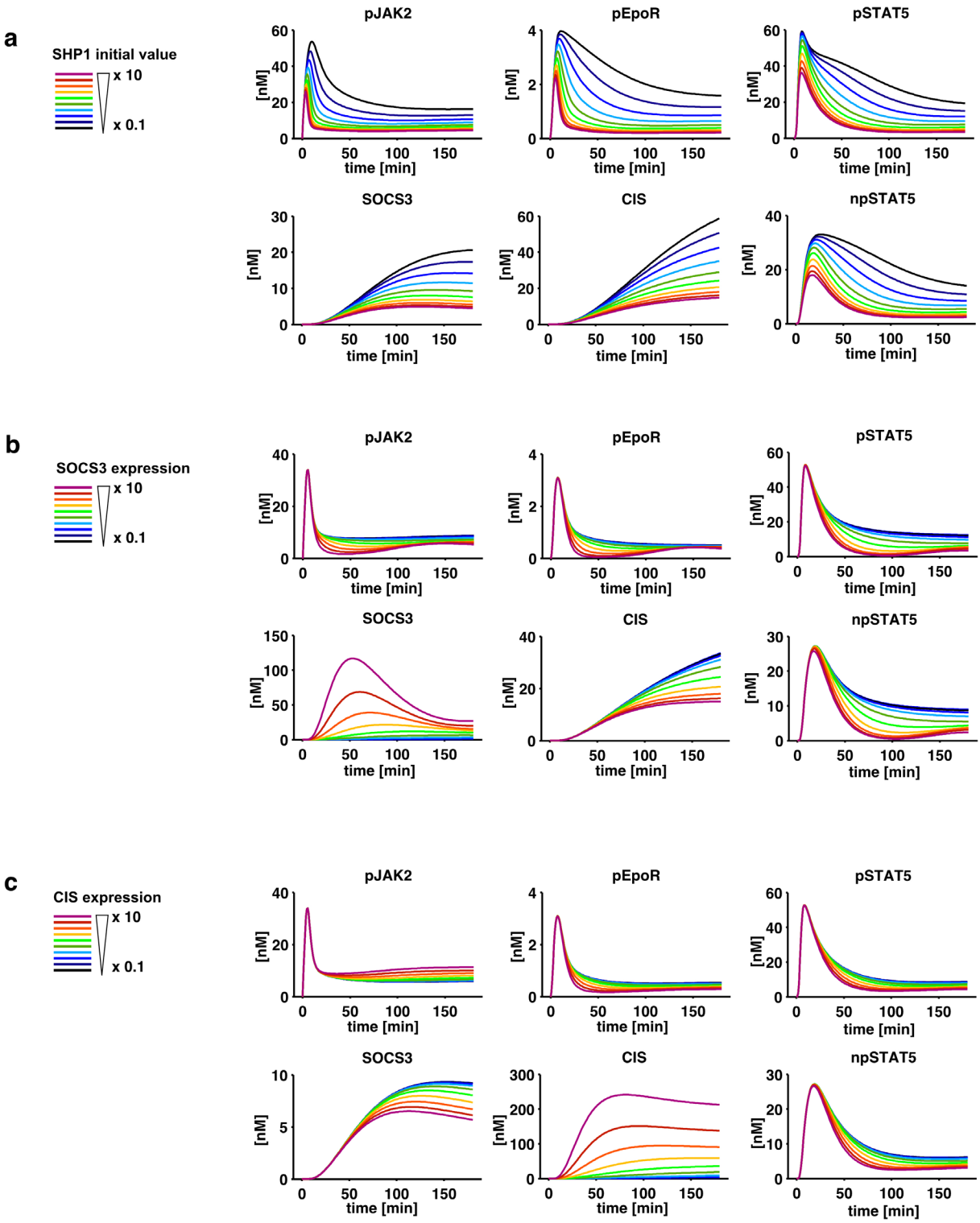

Fig. 27. Simulation of the effect of perturbed SHP-1, CIS and SOCS3 expression levels. Simulations were performed by perturbing the parameters controlling SHP-1, SOCS3 or CIS levels. The initial value of **(a)** SHP-1, and the parameters of either **(b)** SOCS3 or **(c)** CIS expression were incremented logarithmically in 5 steps to 10-fold (1.6, 2.5, 4.0, 6.3, 10) or decreased in 5 steps to 0.1-fold (0.63, 0.40, 0.25, 0.16, 0.1) and the simulated kinetic behavior of the pathway components were plotted. (npSTAT: nuclear phosphorylated STAT5)

Application of the CFU-E-derived JAK2/STAT5 pathway model on BaF3-EpoR cells

In addition to investigating the impact of negative regulators, the mathematical model was applied to elucidate the differences in regulatory mechanisms of JAK2/STAT5 signaling between BaF3-EpoR and CFU-E cells that were observed in time-course experiments upon actinomycin D treatment (Fig. 19). These results showed that in contrast to CFU-E cells, the dynamic behavior of the pathway components in BaF3-EpoR cells was not substantially affected by actinomycin D, suggesting that induced negative regulators are not involved in the attenuation of Epo-signaling in this cell line. This observation may have various reasons since numerous differences were observed between BaF3-EpoR cells and CFU-E cells. First, the stoichiometries of pathway components in BaF3-EpoR cells differed fundamentally from the numbers estimated in primary cells (Table 1). Second, the time-course in BaF3-EpoR cells showed a rapid degradation of EpoR and JAK2 (Fig. 15). Third, strong Epo degradation in the medium was observed after stimulation in BaF3-EpoR cells (provided by Verena Becker, DKFZ, Heidelberg). To systematically test whether one of these characteristics can explain the observed effects, the mathematical model was employed. First, the different stoichiometries of pathway components estimated in BaF3-EpoR cells were included in the mathematical model for CFU-E cells. However, the simulations of the dynamic behavior were inconclusive with the kinetics observed in BaF3-EpoR cells. To address this appropriately would require the estimation of parameters valid for the BaF3-EpoR cell system because of the different volume of BaF3-EpoR cells compared to CFU-E cells.

The next hypothesis testable with the model of CFU-E cells was the impact of the altered input function observed in BaF3-EpoR cells (in collaboration with Verena Becker, DKFZ, Heidelberg). Quantitative immunoblotting of Epo revealed that after stimulation of BaF3-EpoR cells with 5 U/ml Epo the ligand concentration in the medium showed an exponential decay due to receptor-mediated endocytosis. In contrast, the effect of Epo degradation in CFU-E cells at high doses was only marginal. These findings prompted us to apply the model and to simulate the dynamic behavior of JAK2/STAT5 signaling components considering the exponential decay and continuous input function that were experimentally observed for BaF3-EpoR and CFU-E cells, respectively. Additionally, the behavior of the system in the presence of actinomycin D was predicted (Fig. 28). Interestingly, when Epo degradation was included as input function, the phosphorylation level of STAT5 in presence or absence of actinomycin D was in line with the experimental data in BaF3-EpoR cells. In case of a constant Epo stimulus, the dynamic behavior reflected the kinetics observed in CFU-E cells.

The degradation of EpoR and JAK2 may be an additional process that contributes to attenuation of the pathway, potentially rendering transcriptional feedback regulators dispensable. However, testing whether these characteristic can explain the observed effects,

would require a further extension of the mathematical model and the estimation of new parameters for BaF3-EpoR cells.

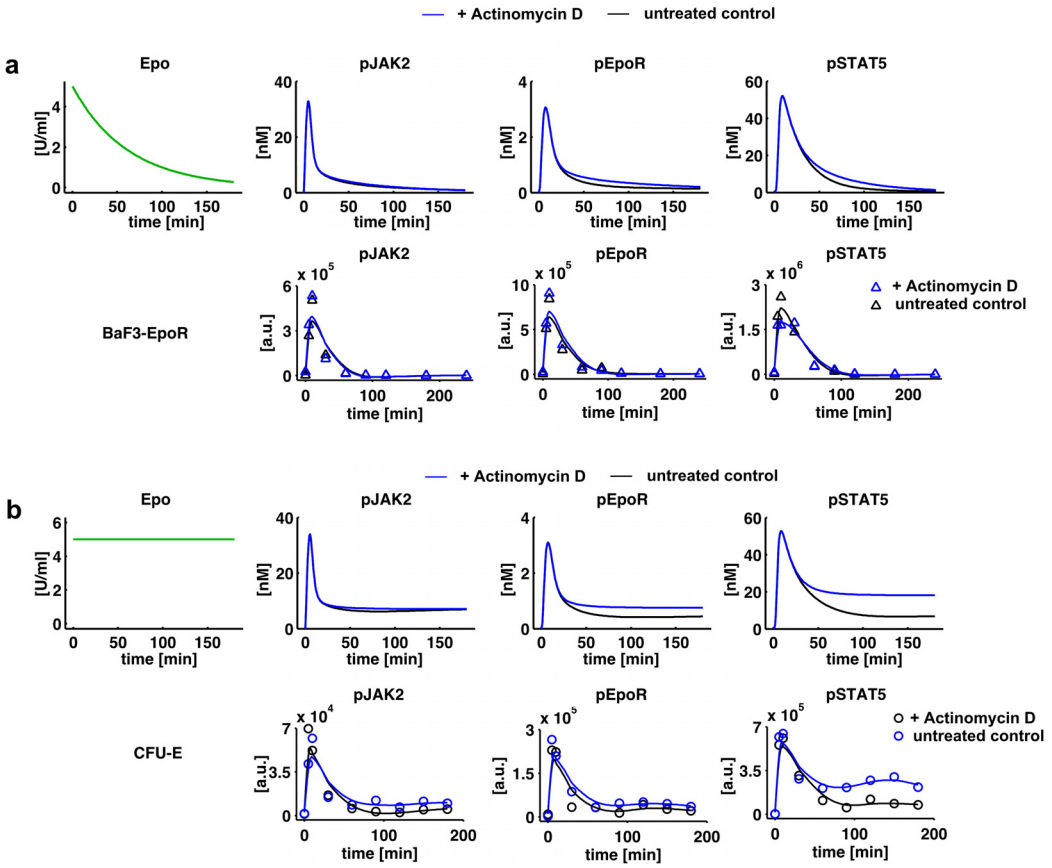

Fig. 28. Simulation of the dynamic behaviour of JAK2/STAT5 signaling in control cells or treated with actinomycin D dependent on different Epo stimuli. (a) Upper panel: Simulated kinetics of phosphorylated JAK2, EpoR and STAT considering Epo degradation for actinomycin D treated cells (blue) and untreated control cells (black). Lower panel**:** Time-course data in BaF3-EpoR cells in presence or absence of actinomycin D from Fig. 19 with spline approximations. **(b)** Upper panel: Simulated time course with constant Epo stimulus for actinomycin D treated cells (blue) and untreated control cells (black) as observed in CFU-E. Lower panel: Time-course data in CFU-E cells in presence or absence of actinomycin D from Fig. 19 with spline approximations.

In summary, the application of the mathematical model established for CFU-E cells proposed that rapid degradation of Epo in BaF3-EpoR cells may be a possible explanation for the different dynamic behavior of the two cell types upon actinomycin D treatment. However, further analysis with an extended mathematical model including all characteristics of BaF3-EpoR cells will be necessary to understand the distinct mechanisms of JAK2/STAT5 pathway attenuation in BaF3-EpoR and CFU-E cells.

2.6.2 Sensitivity analysis of the JAK2/STAT5 pathway

Besides studying the effect of parameter changes of negative feedback regulators, a global sensitivity analysis can provide a deeper insight into the most important processes and proteins that control the output of the pathway. Employing this analysis can lead to a better understanding of coordination in the pathway and explain why particular genes can be

converted to oncogenes but others not (Hornberg et al., 2005b). In our system, phosphorylated STAT5 in the nucleus (npSTAT5) was chosen as the target variable representing the output of the pathway as it is directly involved in the activation of gene transcription. Recently, various studies demonstrated that the signal magnitude and duration of transcription factor activity may control the specificity of cellular decisions. Hence, different characteristics of the dynamic STAT5 profile were defined and investigated individually: (i) peak amplitude, (ii) signal duration (total time until signal drops below 18% of the peak amplitude), (iii) integral signal strength (area under curve between 0 and 120 min) and (iv) steady-state level (last value at 180 min) (Fig. 29a).

To identify the steps that are most important for controlling these quantities, control coefficients were calculated. Positive control coefficients indicate that values for signal duration, peak amplitude, integral signal strength and steady-state level increase with higher parameter values, while negative control coefficients indicate that higher parameters lead to lower values for these quantities. Higher absolute values of control coefficients represent a larger influence of the parameter on the specific characteristic of npSTAT5 dynamics.

Remarkably, the peak amplitude of npSTAT5 is almost exclusively controlled by three parameters: the concentration of STAT5 in the cytoplasm as well as its import and export rates (Fig. 29b). This result implied that increasing amounts of STAT5 in the cytoplasm lead to a larger number of phosphorylated STAT5 in the nucleus at the peak time, while import and export parameters represent the rate-limiting steps. Furthermore, the concentration of SHP-1 is important for controlling the peak amplitude, although its influence is lower than that of STAT5 concentration.

In contrast to the peak amplitude, the control of integral signal strength, signal duration and steady-state level depended on a larger number of processes and all three characteristics showed a similar general control pattern. The concentration of SHP-1, *deactivation of SHP-1*, *SOCS3 expression* and *JAK2 inhibition* revealed the largest impact. The control coefficient of CIS was smaller compared to that of SOCS3 suggesting that CIS protein levels are less important for the control of npSTAT5 dynamics. Additionally, the concentration of JAK2 and the parameter *JAK2 activation* were identified to be critical. In contrast, changes of EpoR concentrations were predicted to not affect the npSTAT5 signal of the system. STAT5 concentration was important for the control of signal duration, but had less impact on the integral signal strength and steady-state level.

In summary, the control pattern of the peak amplitude of npSTAT5 differed significantly from that of signal duration, integral signal strength and steady-state level. Whereas the amplitude is controlled mainly by three parameters (STAT5 concentration and import as well as export rates), the control of the other characteristics yielded a broader distribution over various steps of the signaling cascade.

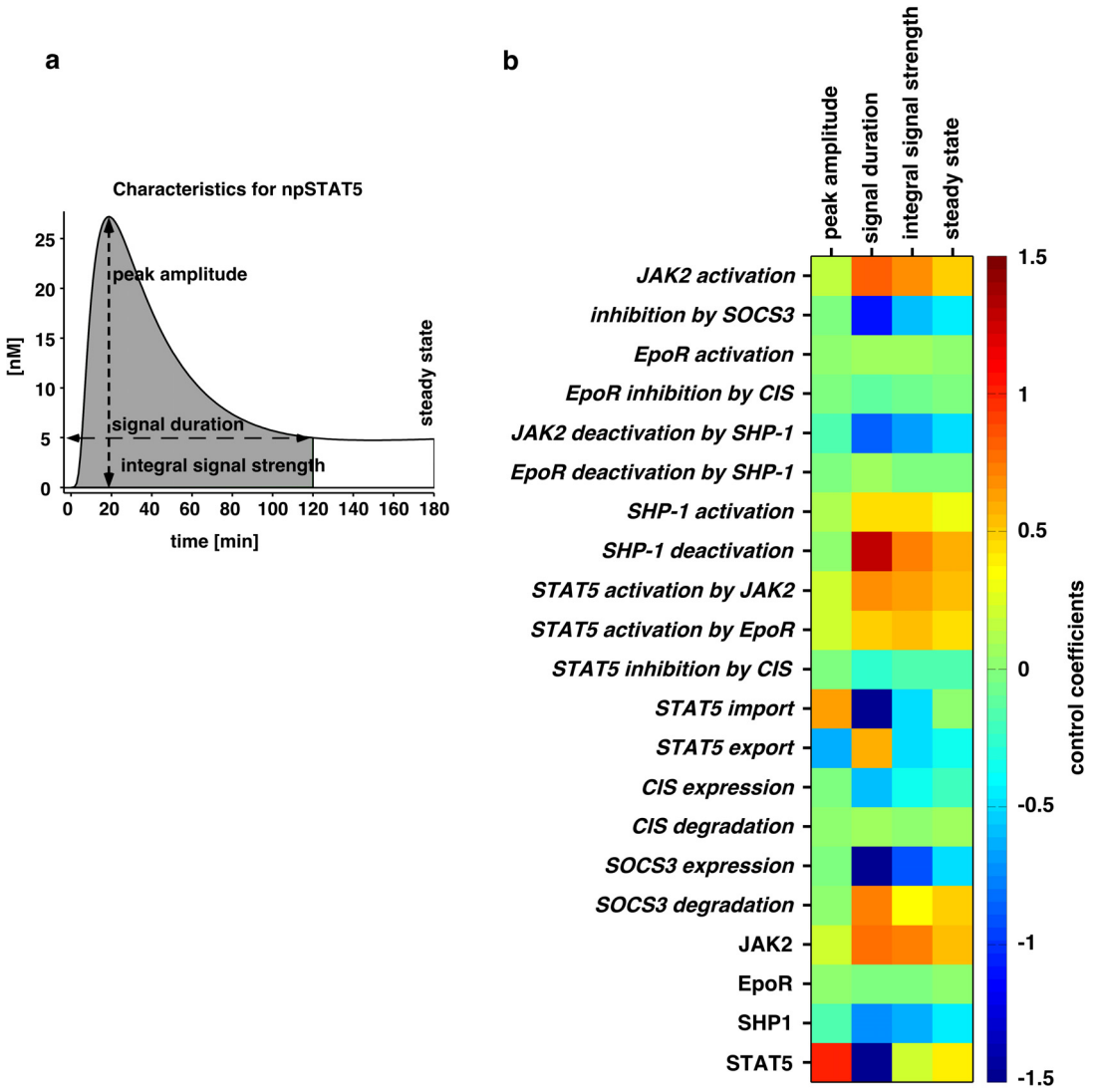

Fig. 29. Control coefficients for different characteristics of phosphorylated STAT5 in the nucleus (npSTAT5). (a) Definitions of the four quantities peak amplitude, signal duration, integral signal strength and steady-state that characterize the transient activation profile of phosphorylated STAT5 in the nucleus (npSTAT5). **(b)** Control coefficients of parameters calculated for the four characteristics of npSTAT5. Negative (blue); positive (red) and insignificant (green) values of control coefficients are represented by a heatmap.

To provide a visual overview of the sensitivity analysis, parameters that control the integral signal strength of npSTAT5 were ranked. Therefore, the control coefficients were classified to be significant if the absolute value is not smaller that 20% of the largest control coefficient. After applying these classification rules, three reactions and one protein with either the largest positive or largest negative values were identified (Fig. 30). *SOCS3 expression*, *JAK2 deactivation by SHP-1* and *SOCS3 inhibition* were identified as the parameters with the largest negative control coefficient whereas *SHP-1 deactivation*, *JAK2 activation* and *STAT5 activation by JAK2* were the reactions with the highest positive values. Furthermore, JAK2 and SHP-1 were revealed as the proteins with the largest impact.

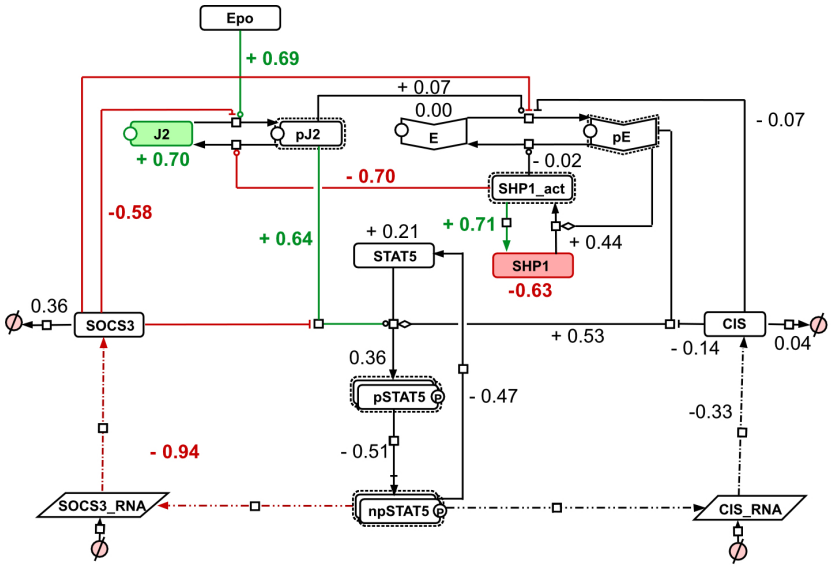

Fig. 30. Reactions and proteins displaying the largest control coefficients for the integral signal strength of phosphorylated STAT5 in the nucleus. Processes and proteins were classified to be essential for controlling the integral npSTAT5 signal by ranking the calculated control coefficients. The three reactions with the highest positive (green) control coefficient and highest negative (red) control coefficient were highlighted. Protein concentrations with the highest positive value (green) and highest negative value (red) of calculated control coefficients were indicated.

2.7 Effects of altered negative feedback loops on cellular decisions

Previous studies have demonstrated that STAT5 is involved in maintaining survival in erythroid progenitor cells. To study whether the integral signal strength of nuclear STAT5 (npSTAT5) correlated with survival, the effect of SHP-1, SOCS3 and CIS overexpression on the apoptosis rate of primary CFU-E cells was studied and compared with the simulated integral signal strength of npSTAT5 of the mathematical model. At this point, it is important to consider that in contrast to the simulations in Fig. 27, in this experiment, the proteins were constantly overexpressed and thus, CIS and SOCS3 overexpression is expected to reduce the initial peak amplitude.

Freshly isolated CFU-E cells were retrovirally transduced with either SHP-1, SOCS3 or CIS and stimulated with 0.5 U/ml Epo. The expression levels of these proteins in the CFU-E cells were quantified by using the LumiImager software (Roche Diagnostics, Mannheim). Because of the high level of the endogenous protein, SHP-1 reached only a level of 3.5 fold overexpression. SOCS3 and CIS reached 10-fold and 11-fold overexpression levels, respectively (Fig. 31a). After 24 h the number of apoptotic cells was analyzed using the TUNEL assay which detects DNA breaks. The results of this assay (Fig. 31b) showed that the highest rate of apoptosis was observed in cells overexpressing SOCS3. CFU-E cells overexpressing CIS showed a small but significant upregulation of apoptosis whereas for cells overexpressing SHP-1 no significant effect was observed.

To calculate the integral signal strength of STAT5 in the nucleus for all four conditions, the dynamic behavior of npSTAT5 was simulated considering the different levels of overexpression for CIS, SHP-1 and SOCS3 by using the mathematical model. The calculation revealed that in SHP-1 overexpressing cells this quantity was reduced only to a small extent. The strongest effect on the simulated integral response was calculated for cells overexpressing SOCS3 whereas the value calculated for 10-fold CIS overexpression level was intermediate. Hence, in the analysis that related the integral response of npSTAT5 to the survival rate a good correlation (R^2 = 0.9881) with a hyperbolic function was observed, indicating a strong dependency of the calculated amount of phosphorylated STAT5 in the nucleus and the survival rate of CFU-E cells.

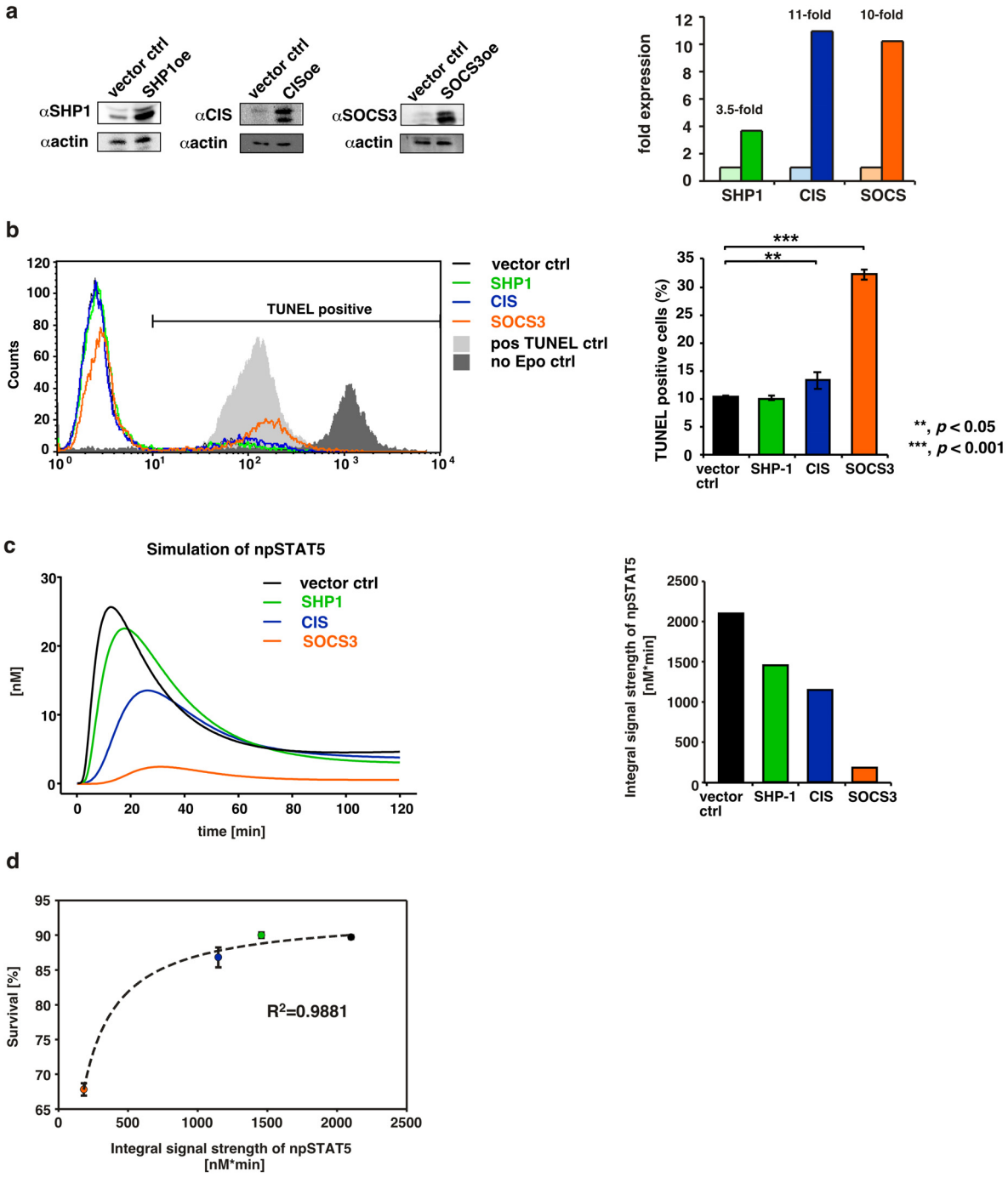

Fig. 31. Correlation of integral signal strength of phosphorylated STAT5 in the nucleus and survival of CFU-E cells. (a) CFU-E cells were retrovirally transduced with SHP-1, SOCS3 or CIS and sorted for positively transduced cells. Cellular lysates were subjected to immunoprecipitation with antibodies against SHP-1, CIS or SOCS3 to determine overexpression levels. Bars represent quantifications of vector control (light colour) and overexpression (dark colour) of different subsets. **(b)** CFU-E cells overexpressing SHP-1 CIS or SOCS3 were cultured 24 h in 0.5 U/ml Epo. Histograms show the representative result of a TUNEL assay used to detect DNA double-strand breaks indicative of apoptotic cells. Cells for positive control were treated with DNaseI for 10 min and subjected to the TUNEL assay. The bar plot shows the mean ± S.D. percentage of TUNEL positive cells in the different CFU-E subsets obtained in three independent experiments, ***P<0.001, **P<0.05 (paired *t*-test, two-sided). **(c)** The JAK2/STAT5 model was used to simulate the response of phosphorylated STAT5 in the nucleus (npSTAT5) for the indicated subsets. Bars represent calculated values of the integral signal strength (within 120 min) after stimulation with 0.5 U/ml Epo of phosphorylated STAT5 in the nucleus for cells overexpressing SHP-1, CIS or SOCS3. **(d)** Calculated values of integral signal strength of npSTAT5 were correlated to the survival rate of CFU-E cells determined by the TUNEL assay.

3 Discussion

In this study, a data-based dynamic pathway model was established to examine the different roles of negative feedback regulators attenuating the Epo-induced JAK2/STAT5 pathway during erythropoiesis. The tyrosine phosphatase SHP-1 was identified as the major negative regulator controlling the early phase kinetics of the signaling pathway, whereas the two transcriptionally induced regulators SOCS3 and CIS were elucidated as main modulators of the long-term steady state STAT5 phosphorylation level. Furthermore, signal amplification of Epo-induced JAK2/STAT5 pathway was revealed as a crucial characteristic enabling signal transmission at low concentrations of Epo.

3.1 Establishing standardized experimental techniques for systems biology

3.1.1 Quantitative techniques for studying EpoR signaling

The generation of reproducible, quantitative and time-resolved data suitable for systems biology approaches requires advanced techniques for data acquisition and processing as well as a standardized *in vitro* cell system (Schilling et al., 2008). Hence, for the implementation of a dynamic pathway model of Epo-induced JAK2/STAT5 signaling in primary murine erythroid progenitor cells at the CFU-E stage, standard operating procedures for the preparation and cultivation of CFU-E cells were established. These procedures included the exclusive use of the inbred mouse strain Balb/c for the isolation of erythroid progenitors from fetal livers of 13.5 days-old embryos. Furthermore, primary cells were routinely cultivated 12-14 h prior to experiments. Starvation time and Epo concentrations for the stimulation of CFU-E cells were optimized to induce maximal signal activation within the linear range, avoiding signal saturation. Besides establishing standardized protocols for the cultivation of primary erythroid progenitors, experimental methods were optimized to meet the quantitative requirements for mathematical modeling approaches.

The quality of data obtained from immunoblotting experiments were optimized by employing advanced strategies for error reduction and automated data processing (Schilling et al., 2005a). In particular, correlated errors typically originating from immunoblotting due to inhomogeneities in the gel or the transfer process were prevented by randomized gel loading. Data normalization and computational data processing was further improved by applying constant amounts of purified calibrator proteins to the cellular lysates. Since densitometric scanning of X-ray films displays a narrow linear detection range, a CCD-camera based LumiImager system was employed to avoid artificial signal saturation and to

yield immunoblotting data in digital format. By applying these strategies, a reliable experimental setup for the generation of highly reproducible time-resolved data of JAK2/STAT5 pathway activation dynamics was established that are suitable for mathematical modeling approaches.

Beyond the optimization of quantitative immunoblotting techniques, a number of novel strategies for the quantification of endogenous protein levels and post-translational modifications have recently been developed. Protein microarrays are a promising example allowing accurate quantification of low-level phosphoproteins in particular from limited biological material, such as primary CFU-E cells (Korf et al., 2008). Therefore, this technique is currently being optimized in collaboration with Alexandra Kienast, DKFZ Heidelberg to quantify the activation of JAK2/STAT5 pathway components. Alternatively, for the investigation of large-scale kinetics of proteomes, advanced mass spectrometry (MS) techniques based on isotope-coded protein labels (Schmidt et al., 2005) or stable isotope labeling with amino acids in cell culture (SILAC) (Mann, 2006) were developed. However, MS techniques still require large amounts of material and will need further optimization before they can be used for the generation of densely sampled time-course data appropriate for mathematical modeling.

3.1.2 A powerful tool for targeted perturbation - the Tet-On inducible system

In systems biology, the validation of mathematical models requires efficient experimental tools that allow the targeted perturbation of the investigated signaling network (Swameye et al., 2003). Hence, for the fine-tuned overexpression of pathway components, an efficient Tet-On inducible expression system was established that facilitates the tight control of transgene expression in a time- and dose-dependent manner.

Most of the previous Tet-On vector systems were restricted to the usage in transfectable adherent cells (Chenuaud et al., 2004; Nagarajan and Sinha, 2008; Urlinger et al., 2000), and only few studies described retro- or lentivirus vector-based systems appropriate for hematopoietic cells (Barde et al., 2006). Thus, a novel dual retroviral vector system for the particular use in hematopoietic cells was constructed that harbors newly developed Tet-On system components. Importantly, the two separate viral vectors ensure that the TRE is not juxtaposed with the promoter used to drive transactivator expression, thereby avoiding background expression in the non-induced state (Lee et al., 2005). For the optimized inducibility of the system, two different TREs, a first generation TRE-L (Baron et al., 2000) and the second generation TREtight (TRE-T) (H. Bujard, ZMBH Heidelberg) were compared in combination with the novel transactivator rtTA-M2. Due to the shortened CMV minimal promotor and the optimized TetO sequences, the TRE-T variant showed significantly lower background activity in the uninduced state compared to the TRE-L, thereby confirming previous reports (Backman et al., 2004). In contrast, the TRE-L variant reached a remarkably

higher induction rate in BaF3 cells. Similar results were obtained in a study that compared both TRE variants in a lentiviral vector system in human breast carcinoma cells (Pluta et al., 2005). Hence, both elements are ultimately useful depending on whether low background expression levels or high induced transgene expression levels are desired.

However, this system is not appropriate for the application in primary CFU-E cells, because these cells differentiate into erythroblasts after approximately one day in culture and this time frame is too short for the *ex vivo* delivery of the Tet-inducible system. Instead, the generation of transgenic mice expressing the rtTA under the control of an erythroid-lineage specific promotor will facilitate the investigation of dose-dependent upregulation of negative regulatory proteins *in vivo*.

3.2 Signal amplification in the Epo-induced JAK2/STAT5 pathway

Signal amplification is a well-known phenomenon in signal transduction pathways. However, only few studies have adressed this characteristic in mathematical terms (Heinrich et al., 2002; Legewie et al., 2005; Sourjik and Berg, 2002). By employing a data-based dynamic model of the core module of Epo-induced JAK2/STAT5 signaling, a sigmoidal behavior with maximal responsiveness of the pathway was observed for low Epo concentrations, while at high stimuli STAT5 levels become saturated (Vera, Bachmann et al, 2008). Interestingly, this behavior is in line with previous studies that described this characteristic as a typical feature of amplifying signal transduction pathways (Chaves, 2004). Heinrich et al. (2002) emphasized this issue in the analysis of the MAPK cascade, demonstrating that a weakly activated pathway leads to higher amplification, while for strong stimuli only lower levels of amplification are reached (Heinrich et al., 2002). To further quantify the ability of the JAK2/STAT5 pathway to amplify the Epo-induced signal, the logarithmic amplification factor (LA) was defined as the logarithm of the ratio between the total amount of activated STAT5 in the nucleus and activated EpoR. Consistent with the previous analysis, the LA factor demonstrated that the system acts as a strong amplifier between the activated pathway components EpoR and STAT5. Interestingly, maximal increase in amplification was observed for the levels of low stimuli including the physiological plasma concentrations of Epo at steady-state conditions (Jelkmann, 2004). This suggests that the system is designed to maximally amplify the signal at biologically relevant Epo concentrations, thereby facilitating efficient cellular responses (Vera, Bachmann et al, 2008).

3.3 Quantitative dynamic data on Epo-induced JAK2/STAT5 signaling

3.3.1 Quantitative analysis of JAK2/STAT5 pathway activation dynamics

Time-resolved quantitative data of pathway activation is an important requirement for mathematical modeling. In addition to the dynamic behavior, the knowledge of the stoichiometries of pathway components is useful to determine the initial values of species in the mathematical model. Therefore, by using serial dilutions of recombinant calibrator proteins, the absolute amounts of JAK2/STAT5 signaling components including the negative regulators SHP-1, CIS and SOCS3 were determined in primary CFU-E cells and in BaF3-EpoR cells, which exogeneously express the EpoR. Although BaF3-EpoR cells are a frequently used model system to study Epo-dependent signaling (Moucadel and Constantinescu, 2005), severe alterations in the stoichiometries between primary CFU-E cells and BaF3-EpoR cells were observed. In particular, BaF3-EpoR cells show higher amounts of STAT5 compared to primary cells and the SHP-1 level was with approximately 450.000 molecules per cell in BaF3-EpoR 50-fold higher than in CFU-E cells with approximately 8,500 molecules per cell. In a similar approach using serial dilutions of protein standards, SHP-1 levels were estimated to be 800,000 molecules per cell in naïve OT-1 T-cells (Altan-Bonnet and Germain, 2005), indicating that the amounts of SHP-1 differ considerably between cell-types. Moreover, the relative expression levels of STAT5 and SHP-1 are often dysregulated in leukemic cell lines (Pao et al., 2007b; Wu et al., 2003).

In addition to the altered stoichiometries, the dynamic behavior of JAK2/STAT5 signaling in BaF3-EpoR cells differed in multiple aspects from the kinetic observed in primary cells. In contrast to CFU-E cells, that showed constant levels of the proteins JAK2 and EpoR, in BaF3 cells the two proteins were strongly degraded after long-time stimulation with Epo. Moreover, attenuation of JAK2/STAT5 signaling was not dependent on *de novo* protein synthesis, indicating that induced transcriptional regulators such as SOCS3 and CIS play no major role in the regulation of JAK2/STAT5 signaling in this cell line. These findings emphasize the importance of the use of primary erythroid progenitor cells to gain a deeper insight into the regulation of EpoR signaling *in vivo* during erythropoiesis (Wickrema et al., 2007).

In primary CFU-E cells, the activation profile of EpoR, JAK2 and STAT5 followed a sharp peak that declined to a lower steady state level, typical for adaptive cytokine-induced responses (Tsuji-Takayama et al., 2006). CIS and SOCS3 were induced and remained at a constant high level similar to the kinetics of their respective mRNA levels. Since mRNA and proteins of SOCS family members have been reported to be very short-lived with a half-life of less than one hour (Wormald et al., 2006), either the level of phosphorylated STAT5 in the nucleus is sufficient to maintain these long-term expression or other factors may be involved that increase the mRNA stabilities (Ehlting et al., 2007). The tyrosine phosphatase SHP-1 is constitutively expressed and the protein level remained constant over the entire period of

observation. Because the catalytic activity of SHP-1 is regulated by an intramolecular conformational change (Barford et al., 1998; Jones et al., 2004; Neel et al., 2003; Pei et al., 1996; Zhang et al., 2003), the dynamics of SHP-1 activation could not be studied directly using our experimental setup. Previous studies analyzed the dynamics of SHP-1 activation *in vitro* using p-nitrophenyl phosphate as substrate and synthetic peptides mimetics of the EpoR phosphotyrosine residue Y429 to activate the catalytic activity (Pei et al., 1994). However, the activation dynamics determined *in vitro* often differ from the situation *in vivo* due to the specific subcellular environment. As an alternative strategy, mathematical modeling can provide useful tools to gain insight into the dynamic function of SHP-1 activity.

3.3.2 Differential upregulation of SOCS proteins

Several inducible negative feedback proteins of the SOCS family have been implicated in the attenuation of Epo-induced signaling including CIS, SOCS1, SOCS2 and SOCS3 (Sasaki et al., 2000; Starr et al., 1997; Yoshimura et al., 1995). However, the detailed contribution of the SOCS proteins involved in EpoR signaling during *in vivo* erythropoiesis remained unclear, since most of the previous studies used transformed erythroleukemic cell lines, such as R11 or J2E whose expression patterns differ considerably from normal erythroid progenitor cells (Sarna et al., 2003; Wickrema et al., 2007). For this reason, primary erythroid progenitor cells were employed to gain deeper insight into the role of SOCS proteins during normal erythropoiesis.

As evidenced by time-resolved expression profiling of primary erythroid cells at the CFU-E stage, only CIS and SOCS3 show rapid and permanent upregulation at the mRNA level upon stimulation with Epo. These findings are in line with the presence of STAT5 consensus sites in the promoters of CIS (Matsumoto et al., 1997) and SOCS3 (Barclay et al., 2007). In contrast, neither SOCS1 nor SOCS2 mRNA expression were detected in CFU-E cells suggesting that these SOCS proteins are either primarily expressed in transformed cell lines or as hypothesized by Sarna et al. (2003) may be induced in other stages during erythroid maturation. The analysis of SOCS expression in the hematopoietic cytokine-dependent cell line BaF3-EpoR, show the induction of SOCS1 and SOCS6 additionally to CIS and SOCS3. Similarly, Epo-dependent upregulation of CIS and SOCS1, -2, -3 has been reported in the cell lines 32D-EpoR and HCD57 (Jegalian and Wu, 2002). Hence, Epo-induced upregulation of SOCS genes occurs in a cell type-specific manner, emphasizing the importance of the use of primary cells in studies on Epo-dependent signaling during erythropoiesis.

3.4 Mathematical model of negative feedback regulation in the JAK2/STAT5 pathway

3.4.1 Evaluation of the dynamic JAK2/STAT5 model

Most of the previously published JAK/STAT models have a complex structure comprising a large number of variables and parameters (Soebiyanto et al., 2007; Yamada et al., 2003; Zi et al., 2005). Since these approaches frequently lack quantitative data for the appropriate calibration, the models often contain non-identifiabilities.

In this work, as an alternative modeling strategy, a reductionistic bottom-up approach was employed, which aims at fully identifiable parameters that are essential to obtain models with high predictive power (Aldridge et al., 2006; Bruggeman et al., 2002). The number of reactions in the mathematical model was reduced by introducing several assumptions and simplifications. The JAK2/STAT5 pathway was considered as an independent module, which is not influenced by other Epo-induced signaling pathways. Reactions and proteins were limited the core module of JAK2/STAT5 signaling, such as the EpoR, JAK2 and STAT5 as well as the three negative regulators SHP-1, CIS and SOCS3. Protein complexes and rapid reactions that were identified not to be essential for describing the data, as revealed by comparison of the respective model-data compliances were neglected. Moreover, alternative mechanisms that may be involved in the inactivation of Epo-induced signaling, such as receptor internalization (Walrafen et al., 2005) have not been included, since model versions considering EpoR endocytosis could not improve the model fits. The systematical condensation of the reactions and species in the mathematical model resulted in a total number of 13 ordinary differential equations and 17 parameters. This established model could simultaneously describe multiple different data sets of Epo-induced JAK2/STAT5 signaling monitored under five different conditions including total and phosphorylated levels of EpoR, JAK2, STAT5 and total levels of CIS and SOCS3. As demonstrated by fit sequence analysis a global parameter optimum of the multi-experiment fitting was determined showing that all parameters in the model are identifiable. Additionally, confidence intervals of all estimated parameters confirmed a high accuracy for model predictions.

3.4.2 Model-based elucidation of the temporal control of JAK2/STAT5 signaling

The temporal regulation of Epo-induced signal transduction is crucial for the controlled balance of erythrocyte production. Despite the administration of a sustained Epo stimulus, JAK2/STAT5 pathway activation is rapidly attenuated to a lower phosphorylation level, suggesting an effective inhibition via feedback mechanisms that lead to the long-term adaption of the system (Behar et al., 2007).

By data-based mathematical modeling, the rapid recruitment and fast activation of the constitutively expressed phosphatase SHP-1 was identified as the major mechanism controlling the early-phase kinetics of pathway activation. At later time points, negative

regulation by SHP-1 is accompanied by the two transcriptionally induced regulators SOCS3 and CIS, which fine-tune the extent of the STAT5 long-term phosphorylation level in primary erythroid progenitor cells (Fig. 32).

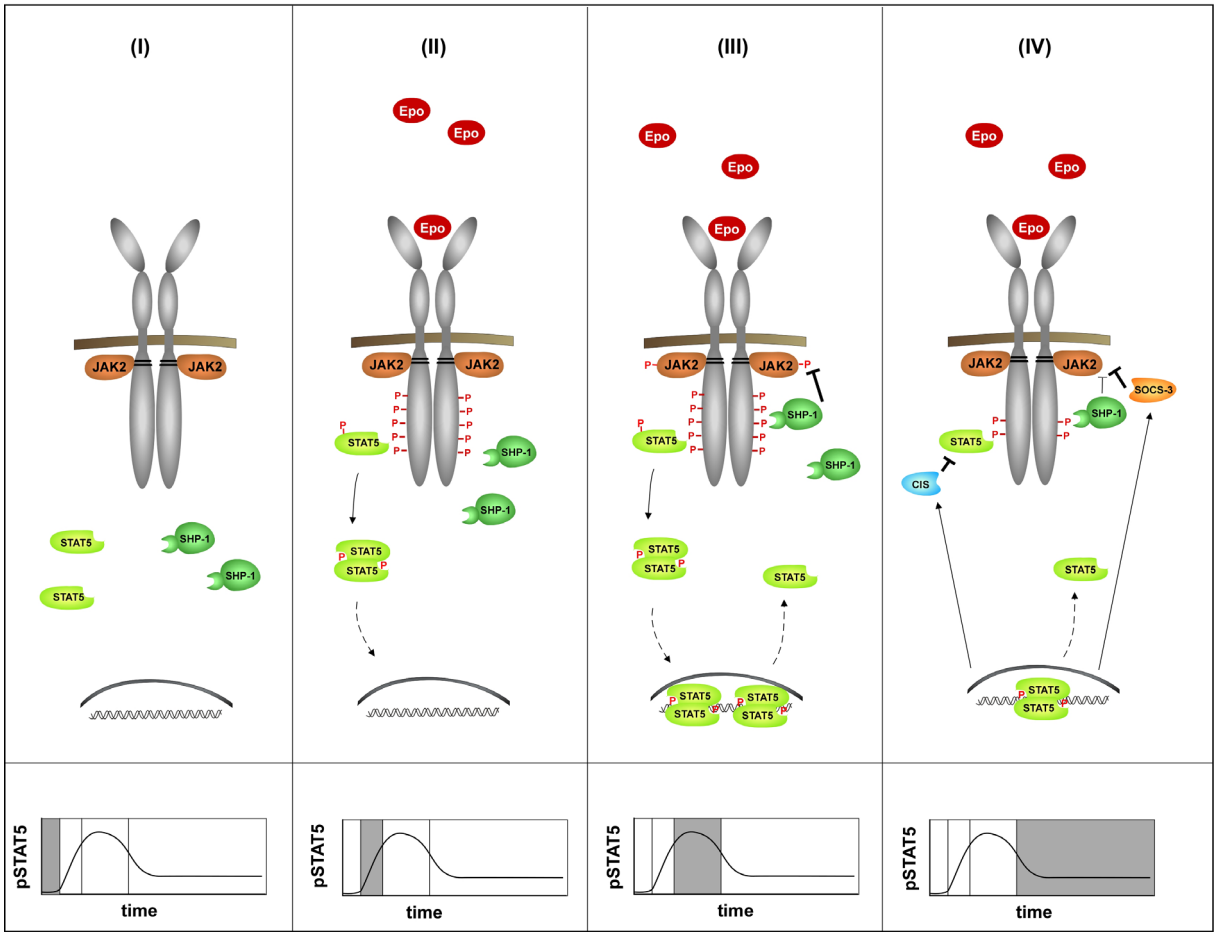

Fig. 32. Schematic overview of the temporal control of Epo-induced JAK2/STAT5 signaling by negative feedback loops in primary CFU-E cells. Schematic representation of the different phases (I-IV) of JAK2/STAT5 signal activation showing the EpoR (grey) with the associated tyrosine kinase JAK2 (orange), STAT5 (light green) and the tyrosine phosphatase SHP-1 (dark green) (upper level). (I) In the basal state, the constitutively expressed phosphatase SHP-1 is present in an inactive state in the cytoplasm. (II) Upon Epo binding, the receptor-associated JAK2 is activated and subsequently phosphorylates the EpoR on various cytoplasmic tyrosine residues, which recruits the SH2-domain containing proteins STAT5 and SHP-1. (III) The tyrosine phosphatase SHP-1 is activated by an intramolecular conformational change upon binding to the EpoR and controls the early-phase kinetic of pathway activation. (IV) During late-phase signaling, the transcriptionally induced feedback regulators CIS and SOCS3 fine-tune the long-term steady state phosphorylation level of STAT5 in addition to SHP-1, thereby enabling tight control of STAT5 induced responses. The corresponding phases of the activation profile of phosphorylated STAT5 in the nucleus (highlighted in grey) represent the basal state, initiation, early-phase STAT5 activation and late-phase steady state kinetic (lower level).

These findings are supported by several lines of experimental and theoretical evidence. First, only SOCS3 and CIS mRNA levels showed strong and persistent Epo-dependent upregulation in primary CFU-E cells, whereas other SOCS proteins such as SOCS1 or SOCS2 that have been previously associated with EpoR signaling were not responsive.

Second, Epo-induced CFU-E cells treated with actinomycin D showed elevated levels of STAT5 long-term phosphorylation indicating the involvement of *de novo* gene transcription in the regulation of late-phase signaling. In contrast, the kinetics of the initial phosphorylation maxima of EpoR, JAK2 and STAT5 in actinomycin D-treated cells were not altered compared to the control, thus suggesting that the initial response is regulated by post-transcriptional events. Third, time-course experiments in CFU-E cells overexpressing SOCS3, CIS, or SHP-1 demonstrated the effective and specific inhibition of EpoR signaling by these proteins at different levels of signal transmission. As an efficient inhibitor of JAK2, SOCS3 has been described to block enzymatic activity of the kinase by binding to the catalytic cleft via its kinase inhibitory domain (KIR) (Sasaki et al., 1999). Additionally, SOCS3 is recruited to the tyrosine-phosphorylated EpoR residue Y401 and competes with STAT5 for this receptor binding site (Hortner et al., 2002; Sasaki et al., 2000). In line with these reports, overexpression of SOCS3 in this study strongly inhibited the phosphorylation of JAK2, EpoR, and STAT5, supporting its proposed function to inhibit the pathway at multiple levels. Remarkably, the mechanism of STAT5 binding site competition on the tyrosine-phosphorylated EpoR residue Y401 has also been reported for CIS (Ketteler et al., 2003; Verdier et al., 1998a). However, in contrast to SOCS3, CIS does not contain a KIR domain for inhibiting JAK activity (Endo et al., 1997). Accordingly, diminished phosphorylation levels of STAT5 in CFU-E cells overexpressing CIS were observed, whereas JAK2 phosphorylation was not affected. As a prominent phosphatase in EpoR signaling, SHP-1 has been shown to be recruited to the phosphorylated tyrosine residues Y429 and Y431 of the EpoR and to subsequently inhibit JAK2 activation (Klingmüller et al., 1995; Yi et al., 1995). Consistent with these reports, our results for SHP-1 overexpression showed a modest but significant reduction of phosphorylation levels of JAK2 and EpoR as well as STAT5. Since STAT5 has been shown to be no direct substrate of SHP-1 in CFU-E cells by using substrate trapping mutants of SHP-1, the effect on STAT5 phosphorylation may be indirectly transmitted from JAK2 to the level of STAT5.

Finally, the central model hypothesis that SOCS3, CIS and SHP-1 differentially regulate Epo-induced JAK2/STAT5 was supported by the multi-experiment fitting results of diverse data-sets, which demonstrated a good compliance of the model trajectories and experimental data. Notably, initially tested model versions, lacking one of the three negative feedback proteins only poorly reflected the experimental data and were therefore rejected. Using the correctly calibrated mathematical model, simulations of the dynamic behavior of pathway components with varying parameters of SHP-1 expression levels demonstrated that duration and strength of the initial phosphorylation peak is controlled by the levels of phosphatase activity. Moreover, altered SOCS3 or CIS expression levels influenced the long-term phosphorylation level of STAT5.

This temporal regulation pattern, including short-term deactivation by constitutively expressed phosphatases and late-phase modulation by slow transcriptional feedbacks may evolve as a general paradigm for tightly controlled cytokine-induced signaling pathways (Legewie et al., 2008). The presence of multiple overlapping feedback regulation mechanisms, each with distinct temporal characteristics, thereby ensures the effective control of the signaling outcome to appropriately fine-tune cellular responses (Hao et al., 2007).

3.4.3 Attenuation of EpoR signaling is cell type-specific

Hematopoietic cell lines are a frequently used tool for studying JAK/STAT signaling pathways by mathematical modeling as they can be easily expanded in culture and are readily susceptible to retroviral expression systems. However, these cells harbor severe alterations in the signaling behavior compared to primary cells as revealed in this as well as in previous studies (Drexler et al., 2004; Wickrema et al., 2007).

By systematically comparing JAK2/STAT5 signaling in the cell line BaF3-EpoR and primary CFU-E cells, a number of striking differences were observed. First, the stoichiometries of signaling components determined for BaF3-EpoR and CFU-E cells differed considerably. Second, attenuation of JAK2/STAT5 signaling in BaF3-EpoR cells is not dependent on *de novo* protein synthesis despite the induction of four SOCS genes in these cells. This behavior could not be explained by the different stoichiometries determined for BaF3-EpoR cells using the mathematical model established for CFU-E cells. Presumably, alternative mechanisms are involved in the downregulation of JAK2/STAT5 signaling in BaF3-EpoR cells that may render SOCS proteins dispensable. These mechanisms may include receptor endocytosis, the degradation of the ligand Epo or the degradation of the tyrosine kinase JAK2.

Recently, receptor endocytosis followed by lysosomal and proteasomal degradation has been proposed to mediate the downregulation of activated EpoR complexes in the human myeloid cell line UT-7 (Walrafen et al., 2005). However, our studies in BaF3-EpoR cells revealed that the internalized receptor pool recovers at the cell surface while EpoR activation declines (Becker et al., *submitted*). This observation argues against the assumption that long-term attenuation of EpoR signaling is mediated by internalization and degradation of the EpoR. Instead, rapid clearance of the ligand Epo facilitated by constitutive receptor turnover was identified as an efficient mechanism to downregulate Epo signaling in BaF3-EpoR cells. Based on this observation, the behavior of JAK2/STAT5 signaling was simulated considering the experimentally determined exponential decay function of Epo using our mathematical model (kindly provided by V. Becker). Remarkably, the simulated kinetics of JAK2/STAT5 signaling showed rapid deactivation of EpoR signaling independent from the presence of

SOCS proteins. Hence, rapid degradation of the ligand Epo in BaF3-EpoR cells may be the dominant mechanism for attenuating EpoR signaling in this cell line.

Besides ligand degradation, recent studies in mouse embryonic fibroblasts proposed that upon Epo stimulation, JAK2 is autophosphorylated on a negatively regulating tyrosine within the receptor-binding FERM domain. This leads to dissociation from the EpoR and subsequent kinase degradation (Funakoshi-Tago et al., 2006). In line with this report, strong degradation of JAK2 was observed upon Epo stimulation in BaF3-EpoR cells. Notably, JAK2 levels in primary CFU-E cells remained stable over the entire period of observation. Considering the lower endogenous levels of JAK2 in BaF3-EpoR cells compared to CFU-E cells, the availability of JAK2 for receptor phosphorylation may be a limiting factor for long-term EpoR activity in BaF3-EpoR cells. To test this hypothesis, further analysis including JAK2 degradation in the mathematical model is desirable.

3.5 Physiological roles of SHP-1, SOCS3 and CIS

3.5.1 Potential redundant roles of SOCS3 and CIS during erythropoiesis

Based on our model analysis, the two proteins SOCS3 and CIS were identified as important feedback regulators modulating the STAT5 phosphorylation level in primary CFU-E cells. However, their specific roles in fetal liver erythropoiesis *in vivo* remain unclear.

STAT5 has been suggested in numerous studies to mediate protection from apoptosis by directly inducing the expression of the antiapoptotic protein Bcl-xL in erythroid and hematopoietic cells (Ariyoshi et al., 2000; Dumon et al., 1999; Garcon et al., 2006; Socolovsky et al., 1999). Importantly, decreased expression of Bcl-xL and increased apoptosis in adult and neonatal STAT5ab$^{-/-}$ knockout early erythroblasts correlates with the degree of anemia (Dolznig et al., 2006; Socolovsky et al., 2001). In this study, overexpression of SOCS3 as well as CIS resulted in a significant increase of apoptotic cells. The extent of the survival rate strongly correlated with the decreased STAT5 phosphorylation strength calculated for SOCS3 and CIS overexpression. This suggests that the amount of SOCS3 and CIS in erythroid progenitor cells sets a threshold to STAT5 survival signals to tightly control the production of erythroid progenitor cells. The fact that two SOCS members with redundant roles are involved in EpoR-signaling underscores the requirement to effectively and appropriately fine-tune STAT5-mediated responses. Notably, several other cytokine-induced signaling cascades have been reported to be controlled by more than one member of the SOCS family including JAK/STAT signaling through the GHR (Denson et al., 2003), IL-4Rα (Haque et al., 2000) and prolactin receptor (Pezet et al., 1999). Hence, the redundancy of SOCS proteins may be a common mechanism to ensure the tight control of cytokine-induced responses.

Interestingly, SOCS3 inhibits STAT5 phosphorylation more effectively than CIS as revealed by our sensitivity analysis and overexpression experiments in CFU-E cells. Presumably, the inhibition of the upstream kinase JAK2 by SOCS3 seems to be more effective than inhibiting STAT5 directly by binding site-competition at the EpoR cytoplasmic domain. Consistent with the role of SOCS3 as an effective inhibitor for EpoR signaling, SOCS3 transgenic mice have been previously reported to be embryonically lethal due to the suppression of fetal liver erythropoiesis (Marine et al., 1999). In the same study, the deletion of SOCS3 resulted in erythrocytosis and accumulation of nucleated cells in the fetal liver, indicating that SOCS3 is a critical regulator of normal erythropoiesis. In contrast to SOCS3, which may affect also other pathways elicited by the EpoR and JAK2 including the MAPK and PI3K cascade, CIS is a specific regulator of STAT5. In erythroid progenitor cells, forced expression of CIS has been previously shown to inhibit STAT5-mediated survival signals (Ketteler et al., 2003) and another study showed diminished expression levels of STAT5 target genes in hematopoietic cells overexpressing CIS (Matsumoto et al., 1997). The specific inhibition of STAT5 responses is in line with studies of CIS transgenic mice, which exhibit a remarkably similar phenotype to that observed in STAT5ab knockout mice (Matsumoto et al., 1999). Although mice deficient for CIS have not been studied in detail, it was reported that these mice show no significant abnormalities (Marine et al., 1999). This may be in part explained by the functional redundancy of SOCS3 and CIS and further studies will be necessary to dissect the physiological functions of these two SOCS proteins during *in vivo* erythropoiesis.

3.5.2 The role of SHP-1 in erythropoiesis

The modeling results propose a major role for SHP-1 in controlling the initial signal magnitude of EpoR signaling, however, their precise role in fetal liver erythropoiesis needs to be further addressed.

Two mouse strains with mutations in the SHP-1 gene have been extensively used to characterize the physiological function of SHP-1 in hematopoiesis. The murine motheaten mutation (*me*) results in a complete absence of SHP-1 activity, whereas the motheaten viable mutation (me^v) retains 10% to 20% of SHP-1 activity. These mice develop a multi-lineage hematopoietic disease that includes polycythemia, accumulation of macrophages and neutrophils in the lung and in the skin, causing the characteristic motheaten appearance of the coat (Shultz et al., 1997). The phenotypes of me/me and me^v/me^v differ only in severity, with me/me mice dying earlier (at 2-3 weeks) than me^v/me^v (at 9-12 weeks). Interestingly, CFU-E progenitors of me^v/me^v mice are stimulated by lower than the normal concentration of Epo (Van Zant and Shultz, 1989), supporting the model prediction that SHP-1 is the major negative regulator to control phosphorylation levels of EpoR and JAK2. Moreover, cells expressing EpoR mutants incapable of SHP-1 binding show prolonged phosphorylation in response to Epo (Klingmüller et al., 1995) which is in line with the

assumption that SHP-1 has to be activated by binding to the EpoR before it dephosphorylates its target proteins. To elucidate the role of SHP-1 in more detail, conditional knockout mice defective for SHP-1 specifically in the erythroid lineage are desirable to clarify the physiological relevance of this phosphatase during erythropoiesis.

3.6 Targeting JAK/STAT signaling in leukemia

Constitutive STAT activation has been associated with a number of hematological malignancies including chronic and acute leukemias and myeloproliferative disorders. To shed light on the critical components and reactions that control the output of a signaling pathway, sensitivity analysis of accurate mathematical models has been proposed to be a promising tool (Hornberg et al., 2005a).

In this study, sensitivity analysis was applied to calculate to what extent each process in the JAK2/STAT5 pathway controls the activation profile of phosphorylated STAT5 in the nucleus. The analysis revealed that the concentrations of JAK2 and SHP-1 as well as the parameter *SOCS3 expression* are most critical for controlling the integral signal strength of STAT5. Thereby, the concentration of JAK2 showed the highest positive control coefficient, implying that the system is in particular sensitive to higher expression levels of JAK2. In contrast, SHP-1 levels and the parameter controlling SOCS3 expression possess the two largest negative values, indicating that the reduction of these proteins severely alter the signaling outcome. Interestingly, these findings are in accordance with the experimentally verified observation that JAK2 is an oncogene (Baker et al., 2007) whereas SHP-1 was proposed as a candidate tumour suppressor gene (Wu et al., 2003). In particular, amplification of the JAK locus and constitutively active JAK2 mutants have been frequently identified in the majority of patients suffering from polycythemia (Baxter et al., 2005; James et al., 2005; Kralovics et al., 2005; Levine et al., 2005). Furthermore, inactivation of SHP-1 by promoter hypermethylation was described in various kinds of leukemia, lymphomas and multiple myeloma (Chim et al., 2004; Johan et al., 2005; Khoury et al., 2004; Oka et al., 2002; Zhang et al., 2000). The role of SOCS3 in transformed cells has not yet been studied in detail, but increasing evidence suggests that the expression of SOCS proteins is altered in a number of hematopoietic malignancies. Deletion of SOCS3 has been shown to result in polycythemia, a premalignant form of erythroid leukemia, demonstrating that a loss-of-function mutation may contribute to cellular transformation (Marine et al., 1999). Furthermore, SOCS-1, the most similar SOCS family member to SOCS3, has been recently identified as tumor suppressor that can counteract cell proliferation induced by the oncogenic TEL-JAK2 fusion protein (Rottapel et al., 2002). In support of this idea, two recent studies reported that the SOCS1 locus is epigenetically silenced by hypermethylation in hepatocellular carcinomas (Nagai et al., 2001; Yoshikawa et al., 2001).

In summary, the sensitivity analysis revealed that the control of the system output is distributed over several proteins and reactions. This indicates that a combination of events is involved in the pathogenesis of hematopoietic disorders. In fact, there are numerous recent studies showing that JAK activating mutations are complemented by SOCS and SHP-1 gene silencing in several malignant tumors (Chim et al., 2004; Johan et al., 2005; Jost et al., 2007). Thus, control analysis of accurate mathematical models is not only a tool to discover an new category of drug targets (Cascante et al., 2002), but also provides insights into the dynamic properties of signaling cascades.

3.7 Conclusions and outlook

In conclusion, a dynamic pathway model of Epo-induced JAK2/STAT5 signaling including negative feedback proteins in primary CFU-E cells was established based on quantitative, time-resolved experimental data. The mathematical model could simultaneously describe data derived from multiple experiments and comprised identifiable parameters with small confidence intervals important for accurate simulations. By extensive model analysis, the rapid recruitment of the phosphatase SHP-1 was identified to control the early-phase kinetics of pathway activation, while the two transcriptionally induced regulators SOCS3 and CIS were revealed as modulators that fine-tune the extent of the STAT5 long-term phosphorylation level. These results demonstrate that complementary negative feedback mechanisms have evolved that tightly control STAT5 survival signals in erythroid progenitor cells. Furthermore, signal amplification of Epo-induced JAK2/STAT5 pathway was revealed as a crucial characteristic enabling signal transmission at low concentrations of Epo. Moreover, systematic comparison of stoichiometries and activation dynamics of Epo-induced JAK2/STAT5 signaling in CFU-E and BaF3-EpoR cells revealed fundamental differences between both cell types, emphasizing the importance of the use of primary cells in the investigation of EpoR signaling

Based on the established model, the striking differences in Epo-induced signaling observed between primary CFU-E cells and the BaF3-EpoR cell line should be further elucidated. Therefore, to achieve this, the mathematical model needs to be extended by introducing several characteristics determined for BaF3-EpoR cells. After estimation of new parameters valid for BaF3-EpoR cells, sensitivity analysis can be applied to identify the crucial mechanisms that control JAK2/STAT5 pathway activation in the cell line and to compare these mechanisms with primary cells. This issue can be further addressed using an experimental design approach (Maiwald et al., 2007) that systematically selects the most informative experiments by means of computational simulations.

In CFU-E cells, SOCS3 and CIS have been identified as negative regulators of the long-term phosphorylation level of STAT5 using model simulations. To directly validate these findings

experimentally and to gain more insight into the specific roles of the two proteins controlling survival signals in erythroid progenitor cells, siRNA-mediated downregulation of SOCS3 and CIS is currently being established. However, conventional retro- and lentiviral vector systems for the delivery of small hairpin RNA (shRNA) only resulted in insufficient knockdown in CFU-E cells. Therefore, new vector systems need to be developed with optimized applicability in hematopoietic progenitor cells. As alternative strategy, conditional knockout mice defective for CIS or SOCS3 specifically in the erythroid lineage will be desirable to clarify the physiological relevance of these negative feedback regulators during erythropoiesis. Furthermore, global sensitivity analysis uncovered the parameter *SOCS3 inhibition* amongst others as critical to control the outcome of the JAK2/STAT5 pathway. This strong inhibitory effect of SOCS3 on JAK2 activation could be exploited to design peptide mimetics of the SOCS3 kinase inhibitory region (KIR) and examine whether these molecules can block aberrant activation of JAK2 in transformed leukemic cells.

The detailed understanding of the molecular processes and regulatory mechanisms of Epo-induced signaling during normal erythropoiesis in primary erythroid cells can be applied to gain insights into the alterations driving erythroleukemia and related malignant hematopoietic diseases. Considering the complex coordination and control distribution of JAK/STAT signaling, our mathematical model may assist in the identification of new drug targets and enable to theoretically estimate the effects of corresponding drugs prior to clinical application.

4 Materials and Methods

4.1 Molecular biology techniques

4.1.1 Generation of competent *E. coli* cells

For high-efficiency transformation of plasmid DNA, the *E. coli* strain Subcloning Efficiency™ DH5α™ Cells (Invitrogen) was used to prepare chemically competent bacteria. DH5α cells were cultured in 500 ml LB medium up to an optical density of 0.6-0.8 as measured at 600 nm. After incubation on ice for 10 min, cells were sedimented with 4,100 g for 5 min at 4°C and resuspended in 150 ml TFBI (100 mM RbCl, 50 mM $MnCl_2$, 10 mM $CaCl_2$, 30 mM potassium acetate, 15% glycerol, pH 5.3). Following 20 min of incubation on ice, cells were centrifuged for 5 min at 1,400 g and 4°C, resuspended in 10-15 ml TFBII (10 mM RbCl, 75 mM $CaCl_2$, 10 mM MOPS pH 7.0, 15% glycerol). Aliquots were stored at -80°C.

4.1.2 Purification of plasmid DNA

Plasmid DNA was amplified using *E. coli* cultures either on small analytic or large preparative scale. To isolate plasmid DNA on small scale, *E. coli* cells were cultured o/n at 37°C in 2 ml LB medium supplemented with 100 µg/ml ampicillin. The QIAprep® Spin Miniprep Kit (Qiagen) was used according to the manufacturer's instructions. To prepare plasmid DNA in large scale, a single colony or 50 µl of an *E. coli* culture were cultured in 200 ml LB medium supplemented with 100 µg/ml ampicillin for 16-18 h at 37°C. For purification, the JETSTAR 2.0 Maxi Kit (Genomed) was used according to the manufacturer's instructions.

4.1.3 Quantitative analysis of nucleic acids

The concentration of DNA solutions was determined by measuring the absorbance at 260nm (Ultrospec 3100 pro, GE Healthcare).

4.1.4 Automated DNA sequencing

All DNA sequences were verified by sequencing service of MWG Biotech AG, Martinsried, Germany. 1 µg of plasmid preparations were provided for this purpose.

4.1.5 Amplification of DNA fragments

For specific amplification of DNA by PCR a PTC-200 Thermo Cycler (MJ Research) was used. The number and duration of cycles as well as the annealing temperatures were optimized corresponding to the expected product length and primers. PCR amplification was performed in a 50 µl reaction volume containing 50 ng template DNA, 100 µM of each dNTP,

1 µM of forward and reverse primer, 10% of DMSO, 2.5 units Cloned *Pfu* DNA Polymerase (Stratagene) and buffer according to the manufacturer's manual.

4.1.6 Annealing of double-stranded DNA adapters

To produce double-stranded DNA adapters that contain specific restriction sites 100 pmol of complementary sense and anti-sense primers were heated in annealing buffer (10 mM Tris pH 8.0, 300 mM NaCl) for 5 min to 95°C. Subsequently, the mixture was cooled to RT during 30 min and subsequently used for ligation with the corresponding plasmid.

4.1.7 Molecular cloning of DNA fragments

To generate specific DNA sequences, restriction of DNA by type II endonucleases was performed in a 20 µl reaction volume containing 0.5-1 µg plasmid DNA, 5 U of the restriction enzyme, 2 µl of 10x buffer according to the manufacturer's protocol (New England Biolabs). The resulting DNA fragments were separated on a 1 % agarose gel (Invitrogen) supplemented with 100 ng/ml ethidiumbromide and excised from the gel using a scalpel. After elution and purification of the DNA fragments with the Qiaex®II Gel Extraction Kit (Qiagen), vector and an 2-3 fold excess of insert DNA were ligated for 30 min at RT using 1 µl of Quick T4 DNA Ligase (New England Biolabs) and subsequently transformed into competent *E. coli* DH5α cells. For transformation, competent DH5α dam+ cells were thawed on ice and 50 µl of cells were mixed with 0.5 µg of plasmid DNA or 5 µl of ligation reaction. After incubation for 20 min on ice, cells were subjected to a heat shock for 5 min at 37°C followed by incubation for 10 min on ice. Subsequently, cells were diluted in 1 ml LB medium and incubated at 37°C for 30 min. Cells were plated in a total volume of 100 µl on TB agar plates (Fluka). The plates were incubated at 37°C o/n and single colonies were picked for further cultivation in LB medium supplemented with 100 µg/ml ampicillin.

4.1.8 Construction of plasmids

For generation of retroviral expression vectors to establish the tetracycline-inducible expression system in hematopoietic cells pMOWS-puro (Ketteler et al., 2002) and pMOWSIN were used. pMOWSIN is a self-inactivating (SIN) retroviral vector that lacks the promoter and enhancer region of the U3 sequence in the 3'proviral longterminal repeats (LTRs). To yield pMOWS-rtTA-M2, cDNA of rtTA-M2 was amplified with primer sequences 5'-cgggatccatgtctagactggacaagagc-3' and 5'-cggaattcttagttagttatccggggagc-3' using pUHrT-62-1 as template (kindly provided by H. Bujard, ZMBH, University of Heidelberg). The PCR fragment was digested with *BamHI*/*EcoRI* and ligated into pMOWS. For generation of pMOWSIN-TRE-L, the TRE fragment in S2s-lMCg (kindly provided by R. Löw and H. Bujard, ZMBH, University of Heidelberg) was digested with *XhoI*, treated with T4 polymerase and subsequently digested with *HindIII*. The fragment was ligated into pMOWSIN that was

digested with *PmlI*/*EcoRI*. The TRE-L consists of the original heptamerized Tet-operator sequence P_{tet-1} with the CMV minimal promoter from position -53 to +75. The pMOWSIN-TRE-T vector was generated by ligating TRE in pTRE-tight (BD Bioscience Clontech) after digestion with *HindIII*, T4-polymerase treatment and EcoRI digestion in pMOWSIN treated with *PmlI*/*EcoRI*. The TRE-T sequence contains a modified Tet-operator sequence and a shortened CMV minimal promoter. GFP cDNA was cloned into pMOWSIN-TRE-T and pMOWSIN-TRE-L vectors using *BamHI*/*EcoRI* digestion. cDNA of SHP-1 was ligated into pMOWSIN-TRE-L after *NdeI/PmlI* digestion.

pMOWS-HA-EpoR (Becker et al., 2008) with a puromycin resistance cassette was used for retroviral infection of BaF3 cells to generate stable BaF3-EpoR cell lines.

pMOWSnr is a derivative of pMOWS where the puromycin resistance gene was replaced by the LNGFR cDNA (Miltenyi Biotech), so that transduced cells can be selected by magnetic beads. cDNA of SOCS3 and CIS were cloned into pMOWSnr to yield pMOWSnr-SOCS3 and pMOWSnr-CIS. Therefore, CIS cDNA and the pMOWSnr were digested with *EcoRI/NdeI*. SOCS3 was digested using *BamHI/NdeI* and ligated into the pMOWSnr also treated with *BamHI/NdeI*. pMOWSnr-SHP-1 was kindly provided by M. Schilling, DKFZ Heidelberg.

To generate pSBP-CIS, CIS cDNA was amplified using the primer sequences 5'-gaagatctatggtcctctgcgtacagggat-3' and 5'-cggaattctagagttggaaggggtac-3'. The PCR fragment was digested with *BglII*/*EcoRI* and cloned into pGEX-SBP treated with *BglII* and *EcoRI*.

All sequences were verified by sequencing analysis.

4.2 Mammalian cell lines, primary cells and cell culture techniques

If not stated otherwise, mammalian cell culture media and supplements were obtained from Gibco.

4.2.1 Cultivation of mammalian cell lines

The packaging cell line Phoenix eco was cultured in DMEM medium supplemented with 10% FCS and 1% antibiotics (10,000 U/ml penicillin and 10,000 µg/ml streptomycin sulfate). For selection of Phoenix eco cells stably expressing Gag-Pol-Env, cells were treated with 2 µg/ml Diphtheria toxin (Calbiochem) and 200 µg/ml Hygromycin B (Roche Diagnostics, Mannheim). Phoenix eco cells were subcultured by treatment with 0.5 mg/ml Trypsin and 0.2 mg/ml EDTA and never cultured longer than 2 weeks prior to transfection.

The IL-3 dependent murine pro B cell line BaF3 (Palacios and Steinmetz, 1985) was cultured in RPMI 1640 medium including 10% WEHI as a source of IL-3 and supplemented with 10% FCS and 1% antibiotics. Cells were subcultured after reaching a density of 5-8 x 10^5 cells/ml.

For long-term storage, BaF3 or Phoenix eco cells were frozen in liquid nitrogen in 90% serum and 10% DMSO at a density of 2.5x10^6.

4.2.2 Preparation of murine fetal liver cells

At E13.5 Balb/c mouse embryos were isolated from the uterus of sacrificed females. Fetal livers of embryos were dissected and resuspended in 500µl ice-cold phosphate-buffered saline (PBS) supplemented with 0.3% bovine serum albumin (BSA). After passing through a 40 µm cell strainer (BD Biosciences), cells were treated with 10 ml Red Blood Cell Lysing Buffer (Sigma-Aldrich) to remove erythrocytes. For negative depletion, fetal liver cells of 40 livers were incubated with 10 µl rat antibodies against the following surface markers: GR1, CD41, CD11b, CD14, CD45, CD45R/B220, CD4, CD8 (all purchased from BD Pharmingen), Ter119 (gift from Albrecht Müller, Julius-Maximilians-University, Würzburg, Germany) and with the rat monoclonal antibody YBM/42 (gift from Suzanne M. Watt, University of Oxford, Oxford, UK) for 30 min at 4°C. Cells were washed 3 times in PBS/ 0.3%BSA and were incubated for 30 min at 4°C with anti-rat antibody-coupled magnetic beads and negative sorted with MACS columns according to the manufacturer's instructions (Miltenyi Biotech). Sorted CFU-E were cultivated for 13 h in Iscove's Modified Dulbecco's Medium (IMDM) (Invitrogen), 30% fetal calf serum (FCS), and 50 µM β-mercaptoethanol supplemented with 0.5 U/ml Epo (Cilag-Jansen).

4.2.3 Preparation of WEHI-conditioned medium

To prepare IL-3 containing medium, WEHI-3B cells (Ralph and Nakoinz, 1977a; Ralph and Nakoinz, 1977b; Warner et al., 1969) were cultured in RPMI 1640 supplemented with 10% FCS and antibiotics until confluency. After expansion of the cells in a total volume of 50 ml, WEHI-conditioned medium was harvested every 5 days by centrifugation and subsequent filtration through a 0.2 µm filter in order to remove cell debris. The remaining adherent cells as well as the sedimented cells were further supplied with 50 ml of fresh medium and adherent cells were subcultured after 4-6 weeks.

4.2.4 Transient transfection of Phoenix eco cells

To produce virus supernatant for subsequent transductions, Phoenix eco packaging cells were transfected by the calcium-phosphate method. Transfections were performed either in small scale (6-well plates) or large scale (25 cm^2 dishes).

For small scale reactions, cells were seeded at a density of $8x10^5$ cells in 6-well plates 16-18 h prior to transfection. A mix of 10 µg plasmid DNA and 12.5 µl $CaCl_2$ (2.5 M) was added to 125 µl of 2x HBS (280 mM NaCl, 50 mM HEPES, 1.5 mM Na_2HPO_4, pH 7.05) to form the precipitate. For large scale reactions cells were seeded at a density of $12x10^6$ in 25 cm^2 dishes and a mix of 150 µg plasmid DNA and 187.5 µl $CaCl_2$ (2.5 M) was added to 1875 µl 2x HBS. The suspension was dropwise transferred to the cells. For efficient uptake of DNA, cells were incubated for 6-8 h in DMEM medium supplemented with 25 µM chloroquine. Subsequently, the medium was replaced by IMDM supplemented with 30% FCS, 1%

antibiotics and 50 µM β-mercaptoethanol. The retrovirus-containing supernatant was harvested after 16-18 h of incubation and filtered through a 0.45 µm filter (Millipore). Supernatants were either directly used for transduction or stored at -80°C for up to 3 months. Transfection efficiency was determined by measuring GFP expression in the FL-1 channel of a FACSCalibur (Becton Dickinson), in general yielding a GFP-positive population of 70-90%.

4.2.5 Retroviral transduction

To stably transduce BaF3 cells, 250 µl retroviral supernatant were supplemented with 8 µg/ml polybrene, mixed with $1x10^5$ BaF3 cells and centrifuged for 2 h at 340 g and 37°C in round bottom 2-ml microcentrifuge tubes. After centrifugation, cells were cultured for 48 h in standard medium, subsequently selected and further cultured with 1.5 µg/ml puromycin. Transduction efficiency was determined by measuring GFP expression in the FL-1 channel of a FACSCalibur (Becton Dickinson), in general yielding a GFP-positive population of 35-45%.

To transduce primary erythroid progenitor cells (CFU-E), 4.5 ml retroviral supernatants supplemented with 8 µg/ml polybrene were mixed with $3x10^6$ CFU-E cells in a 6-well plate and centrifuged for 3 h at 340 g and 37°C. Following spin-infection cells were cultivated for 12-14 h in IMDM (Invitrogen), 30% FCS, 1 % antibiotics and 50 µM β-mercaptoethanol supplemented with 0.5 U/ml Epo (Cilag-Jansen).

Successfully transduced cells were isolated using the MACSelect LNGFR selection kit (Miltenyi Biotech) according to the manufacturer's instructions. Briefly, $1x10^7$ washed cells were resuspended in 320 µl PBS/ 0.3% BSA and incubated with 80 µl MACS beads on ice for 15 min to magnetically label positively transduced cells. LS columns were placed in the magnetic field of a MACS Seperator and rinsed with 3 ml PBS/ 0.3% BSA. Cells were applied onto the column in 8 ml PBS/ 0.3% BSA and the flow through was collected as negative unlabeled cell fraction. The column was washed four times with 3 ml PBS/ 0.3% BSA. To elute the positive fraction, the column was removed from the magnetic field and transduced cells were flushed out with 4 ml PBS/ 0.3% BSA by firmly applying the plunger.

4.2.6 Flow cytometry

For the analysis of the induction efficiency of the Tet-system, GFP expression was determined by flow cytometry using the FL-1 channel of a FACSCalibur (Becton Dickinson). Therefore, cells were incubated with different doxycyline concentrations for 24 h and washed three times with PBS/0.3 % BSA before the flow cytometry analysis.

4.2.7 TUNEL assay

For detection and quantification of apoptosis at single cell level, the *In Situ* Cell Death Detection Kit (Roche Diagnostics, Mannheim) was used. The TUNEL (Terminal

deoxynucleotidyl Transferase-mediated dUTP nick end labeling) assay relies on the detection of single- and double-stranded DNA breaks that occur during the early stages of apoptosis. Apoptotic cells are identified by using TdT to transfer fluorescein-dUTP to these strand breaks of cleaved DNA. Briefly, $2x10^6$ CFU-E cells were fixed in freshly prepared 2% paraformaldehyde and permeabilised with 0.1% Triton X-100, 0.1% sodium citrate for 2 min. The positive control was treated with digestion buffer (DNaseI recombinant, DNaseI buffer, Roche Diagnostics, Mannheim) for 10 min. After washing with PBS/ 0.3% BSA, cells were resuspended in TUNEL reaction mixture (TdT, fluorescein-dUTP, reaction buffer) to label free 3'-OH groups of single- and double-stranded DNA. Fluorescein-dUTP incorporated in nucleotide polymers is detected and quantified by flow cytometry using the FL-2 channel of a FACSCalibur (Becton Dickinson). For statistical evaluation a two-sided, unpaired Student's *t*-test was performed with $P<0.05$ considered significant.

4.3 Biochemical and immunological protein analysis

4.3.1 Time-course experiments in BaF3-EpoR and CFU-E cells

BaF3-EpoR cells were washed three times with RPMI 1640 and starved for 3-5 h at 37°C in RPMI 1640 supplemented with 1 mg/ml BSA. CFU-E cells were washed three times and starved in Panserin 401 (PAN Biotech) supplemented with 50 µM β-mercaptoethanol and 1 mg/ml BSA (Sigma-Aldrich) for 1h. For time-course experiments BaF3 or CFU-E cells were preincubated for 5 min at 37°C and subsequently stimulated with 0.5-50 U/ml Epo (Janssen-Cilag) at 37°C. For each time point, $0.5x10^7$ CFU-E cells or $1x10^7$ BaF3-EpoR cells were taken from the pool of cells and lysed by adding 2x Nonidet P-40 lysis buffer, thereby terminating the reaction.

4.3.2 Preparation of cellular lysates

Detergent lysates of cells were prepared with 2x 1% NP40 buffer (1x buffer: 1% NP40, 150 mM NaCl, 20 mM Tris pH 7.4, 10 mM NaF, 1 mM EDTA pH 8.0, 1 mM $ZnCl_2$ pH 4.0, 1 mM $MgCl_2$, 1 mM Na_3VO_4, 10% Glycerol) supplemented with 2 µg/ml aprotinin and 200 µg/ml AEBSF. After 30 min of incubation at 4°C, the lysate was centrifuged for 10 min at 20,000 g and 4°C. The supernatant was either used directly, processed further by immunoprecipitation or total cellular lysates were stored at -80°C.

4.3.3 Immunoprecipitation

Immunoprecipitation was performed with an equivalent of $1x10^7$ BaF3-EpoR or $0.5x10^7$ CFU-E cells by adding the target-specific antibody and 25 µl of Protein A or Protein G sepharose (GE Healthcare) to the lysate for 2-8 h or o/n at 4°C. The immunoprecipitates were washed twice with 1x 1% NP40 lysis buffer and once with TNE buffer (10 mM Tris pH 7.4, 100 mM NaCl, 1 mM EDTA, pH 8.0, 100 µM Na_3VO_4) and were resuspended in 25 µl 2x SDS sample buffer (1x buffer: 2% SDS, 50 mM Tris pH 7.4, 10% glycerol, 5% β-mercaptoethanol, 100 mM DTT, 0.01% bromphenolblue). Immunoprecipitates were immediately subjected to protein gel electrophoresis or stored at -20°C. Immunoprecipitates of pulse-chase experiments were washed four times with 1x RIPA buffer and twice with TNE buffer.

Samples for time-course analysis of EpoR, JAK2, STAT5, CIS, SOCS3 or SHP-1 were prepared prior to immunoprecipitation by adding 40 ng of calibrator protein GST-EpoR (cytoplasmic domain), 18 ng of SBP-JAK2, 40 ng of GST-STAT5b, 2.3 ng SBP-CIS, and 1 ng SBP-SOCS3 to the lysates. Sample loading on SDS-PAGE was randomized to avoid correlated blotting errors (Schilling et al., 2005a).

4.3.4 SDS-PAGE

Proteins were separated according to their electrophoretic mobility in a denaturing SDS-PAGE (Laemmli, 1970). Protein samples were boiled for 3 min in SDS sample buffer. Protein samples were separated by 10% SDS-PAGE with low bis-acrylamide (GE Healthcare) (Table 2) and separated in a electric field in running buffer (192 mM glycine, 25 mM Tris, 0.1% SDS). Immunoprecipitates were centrifuged for 2 min at 15,700 g before loading. For total cellular lysates, an amount of 50-100 µg protein resuspended in 4x SDS sample buffer were separated by SDS-PAGE.

	Stacking gel (10 ml)	Separating gel 10% (20 ml)	Separating gel 15% (20 ml)
40% acrylamide	1 ml	5 ml	7.5 ml
2% w/v methylenebisacrylamide	0.5 ml	1.3 ml	0.88 ml
1M Tris-HCl, pH 6.8	1.25 ml	-	-
1.5M Tris-HCl, pH 8.8	-	5 ml	5 ml
10% SDS	0.1 ml	0.2 ml	0.2 ml
ddH_2O	7.15 ml	8.5 ml	6.42 ml
APS (10 %)	100 µl	200 µl	200 µl
Temed	10 µl	20 µl	20 µl

Table 2. SDS-Page for 10% and 15% polyacrylamide gels.

4.3.5 Coomassie staining

For Coomassie staining, gels were incubated in *Staining Solution* (0.25% Coomassie Brilliant Blue, 50% methanol, 12.5% acetic acid) for 10 min at room temperature. Subsequently, gels were incubated in *Destaining Solution 1* (45% methanol, 10% acetic acid) for 10 min and in *Destaining Solution 2* (5% methanol, 5% acetic acid) o/n at room temperature.

4.3.6 Immunoblot analysis

Immunoblotting was performed in semi-dry chambers (GE Healthcare) on nitrocellulose membranes with a pore size of 0.2 μm (Schleicher&Schuell).

Blotting was performed in transfer buffer (192 mM glycine, 25 mM Tris, 0.075% SDS, 0.5 mM Na_3VO_4, 15% methanol) for 1 h at approximately 1.3 mA/cm^2. Proteins were reversibly stained with Ponceau Red. After blocking unspecific antibody binding with 2-5% BSA diluted in TBS-T (10 mM Tris pH 7.4, 150 mM NaCl, 0.2% Tween-20), membranes were incubated with the appropriate first and secondary antibodies and proteins were visualized with the ECL or ECL Advance Western Blotting Detection Reagents (GE Healthcare) and subsequently detected on a Lumi-Imager F1^{TM} (Roche Diagnostics, Mannheim). Quantification was performed using the LumiAnalyst 3.1 software (Roche Diagnostics, Mannheim). To evaluate total protein levels, membranes were incubated in stripping buffer (62.5 mM Tris pH 6.8, 2% SDS, 100 mM β-mercaptoethanol) for 20-25 min at 65°C, blocked with 2-5 % BSA diluted in TBS-T, and reprobed with the appropriate first and secondary antibody.

4.3.7 Expression and purification of recombinant proteins in *E.coli*

For high-efficiency expression of calibrator constructs, expression plasmids were transformed into competent *E. coli* BL21(DE3)CodonPlusRIL cells (Stratagene) as described for DH5α cells. A single positive colony was cultured in 25 ml LB medium supplemented with 100 μg/ml ampicillin and 50 μg chloramphenicol at 37°C o/n. This o/n culture was then added to 225 ml fresh LB medium supplemented with ampicillin and chloramphenicol and cultured at 37°C for 90 min. After IPTG was added at a final concentration of 0.2 mM to induce protein expression, cells were cultured for another 3 h at 37°C. Cells were sedimented, washed with cold PBS and stored at -20°C o/n.

Upon thawing the cell pellet was resuspended in 15 ml bacterial lysis buffer (10 mM Tris pH 8.0, 100 mM NaCl, 1 mM EDTA) supplemented with 70 μl lysozyme solution (50 mg/ml) and 75 μl 1 M DTT, and lysed on ice for 20 min. After adding 2.25 ml 10% N-lauroylsarcosine the suspension was vortexed for 1 min and sonicated (Sonopuls, Bandelin) three times for 1 min on ice. The bacterial lysate was then centrifuged at 15,000 g for 15 min at 4°C to remove cell debris. The supernatant was carefully transferred to a fresh tube and 350 μl Triton X-100 were added. To bind GST- or SBP-tagged recombinant proteins, the supernatant was incubated with 500 μl glutathione sepharose beads or 500 μl streptavidin sepharose beads,

respectively, and rotated for 1 h at 4°C. Subsequently, beads were washed four times with cold 9% PBS, 1% NP40 supplemented with 5 mM DTT and once with cold PBS supplemented with 5 mM DTT. Beads were subsequently transferred to a 0,45 µm filter unit (Millipore) and recombinant proteins were eluted in fractions of 500 µl elution buffer (75 mM Tris pH 8.0, 150 mM NaCl, 0.1% SDS, 5 mM DTT) supplemented with 20 mM reduced glutathione or 2 mM biotin for GST- or SBP-tagged proteins, respectively. Protein aliquots were stored at -80°C.

4.3.8 Quantification of proteins

To determine protein concentrations of cellular lysates the BCA Protein Assay Kit (Pierce) was used according to the manufacturer's instructions.

For quantification of recombinant calibrator proteins, a dilution series of the respective recombinant calibrator protein and a BSA standard series were separated by SDS-PAGE. The gel was Coomassie stained and band intensities were quantified using a Lumi-Imager F1 (Roche Diagnostics, Mannheim) and the LumiAnalyst 3.1 software (Roche Diagnostics, Mannheim).

4.4 Antibodies

The following antibodies were used for immunoprecipitation (IP) and immunoblot analysis (IB).

primary antibodies	use	specification	company
mouse anti-phosphoTyr	IB (1:10000)	monoclonal, 4G10	UBI
rabbit anti-EpoR	IP (3 µl) IB (1:10000)	polyclonal, M-20	Santa Cruz
rabbit anti-JAK2	IB (1:10000)	monoclonal, 24B11	Cell Signaling
rabbit anti-JAK2	IP (1.5 µl)	polyclonal, serum	UBI
rabbit anti-STAT5	IP (5 µl) IB (1:10000)	polyclonal, C-17	Santa Cruz
rabbit anti-SOCS3	IB (1:1000)	polyclonal, 16030	Abcam
mouse anti-SOCS3	IP (8 µl)	monoclonal, 1B2	Zymed
rabbit anti-CIS	IP (3 µl)	polyclonal	serum from rabbit
goat anti-CIS	IB (1:10000)	polyclonal, N-19	Santa Cruz
rabbit anti-SHP-1	IP (3µl), IB (1:10000	polyclonal, c-19	Santa Cruz
rabbit anti-GFP	IB (1 : 10000)	polyclonal	serum from rabbit

Table 3. Primary antibodies.

conjugates	use	specification	company
donkey anti-rabbit IgG HRP	IB (1:10000)	polyclonal	GE Healthcare
sheep anti-mouse IgG HRP	IB (1:10000)	polyclonal	GE Healthcare
Protein A HRP	IB (1:10000)	-	GE Healthcare
donkey anti-goat IgG HRP	IB (1:10000)	ploYclonal	Santa Cruz

Table 4. Secondary antibody conjugates used for immunoblot analysis.

4.5 RNA analysis

4.5.1 Extraction of total RNA

Per time point total RNA from 3 x 10^6 primary erythroid progenitors was isolated using the RNeasy Mini Plus Kit (Qiagen). RNA was extracted according to the manufacturer's instructions for suspension cells. To eliminate traces of DNA, on-column digests using the RNAse-free DNAse Set (Qiagen) were performed. RNA was stored at -80°C or directly used for quantification and reverse transcription.

4.5.2 Quantification of RNA

The concentration of total RNA samples was determined by measuring the absorbance of diluted 1:50 in TRIS buffer pH 7.4 at 260 nm (Ultrospec 3100 pro, GE Healthcare).

4.5.3 Quantitative two-step RT-PCR

To generate cDNA 1 µg of total RNA was transcribed with the QuantiTect Reverse Transcription Kit (Qiagen) according to the manufacturer's instructions. Quantitative PCR (qPCR) was performed using a LightCycler 480 (Roche Diagnostics, Mannheim) in combination with the hydrolysis-based Universal ProbeLibrary (UPL) platform (Roche Diagnostics, Mannheim). In general, qPCR amplifications were performed in 96-well format in a 20 µl reaction volume containing 5 µl of 1:25 diluted template cDNA, 0.2 µM of forward and reverse primer, 0.2 µl of the appropriate UPL probe and 10 µl LightCycler 480 Probes Master solution (Roche Diagnostics, Mannheim) according to the manufacturer's manual. Primer pairs were generated using the automated UPL Assay Design Center (www.roche-applied-science.com).

Crossing point (CP) values were calculated using the Second Derivative Maximum method of the LightCycler 480 Basic Software (Roche Diagnostics, Mannheim). PCR efficiency correction was performed for each PCR setup individually based on a dilution series of template cDNA. Relative concentrations were normalized using HPRT as a reference gene.

PCR step		Temperature	Time
initial denaturation		95°C	5 min
50 cycles	melting	95°C	10 s
	primer annealing	60°C	30 s
	DNA synthesis and data acquisition	72°C	1 s
cooling		40°C	2 min

Table 5. PCR program for quantitative PCR.

4.5.4 Microarray analysis

The quality of total RNA samples, extracted from 3×10^6 CFU-E or 3×10^6 BaF3-EpoR cells was assessed with the Bioanalyzer 2100 (Agilent) to ensure that 28S/18S rRNA ratios were in the range of 1.5 to 2.0 and concentrations were comparable between samples. In total, 12 microarrays were used in the analysis comprising stimulations with 0.5 U/ml Epo for 0, 1, 2, 3, 4, 5, 6, 7, 8, 14, 19, 24 h and unstimulated control.

Raw microarray data were processed using the R environment (www.r-project.org) together with the Bioconductor toolbox (www.bioconductor.org). Normalization was performed using the variance stabilization algorithm (vsn) available in Bioconductor (Huber et al., 2002). Quality of the results has been assessed using made4, an R package for multivariate analysis of gene expression data (Culhane et al., 2005). Subsequent probe annotation was handled with the Bioconductor package annaffy. The logarithmic gene fold expression was calculated with respect to the gene expression at 0 hours. The gene expression kinetic from each experiment was ranked according to the absolute value of the combined mean and peak fold expression.

4.6 Mathematical modeling

4.6.1 Computational data processing

Randomized quantitative immunoblotting data was processed using GelInspector software (Schilling et al., 2005a). The addition of normalizers allowed for quality control and normalization of the raw data. The following normalizers were applied: GST-EpoR for EpoR and pEpoR, SBP-JAK2 for JAK2 and pJAK2, SPB-CIS for CIS and SBP-SOCS3 for SOCS3. For first estimates, cubic smoothing splines were used (MATLAB csaps function with smoothness parameter 0.3). For background correction, the lowest value of a time-course

was generally subtracted from all data points for all observed species. For estimation of the percentage of phosphorylated STAT5, the ratio of the shifted and the total fraction in the STAT5 immunoblot was determined.

4.6.2 Scaling factors and error estimation

Immunoblotting measurements typically yield relative concentrations, while the model is formulated in absolute concentrations. Therefore, immunoblotting data was scaled to numbers of molecules per cell. As the quality of a mathematical model is determined by its deviation from the data relative to the measurement error, the variability of the data had to be estimated. All stimulation experiments were performed at least twice with reproducible results. To estimate the error of the immunoblot results by a linear error model, the standard deviations of the replicates were plotted against the mean value of the respective data points. A linear regression was fitted yielding approximately a 15 % relative error and a 5 % absolute error. This error estimation confirms the approximately 20 % error of the immunoblotting technique determined in previous studies (Schilling et al., 2005a).

4.6.3 Parameter estimation

Parameter estimation was performed using the software PottersWheel (Maiwald et al., 2008). Each fit was performed with a deterministic trust region optimizer with χ^2 tolerance of 10^{-6} and fit parameters tolerance of 10^{-6}. All parameters were estimated with boundaries between 10^{-6} and 10^3, and none of the estimated parameters lay on these boundaries. Additionally, 5000 fits using random numbers as initial guesses for parameters, were computed to analyze the distribution of the parameter estimations. For this analysis only fits with comparable low χ^2 values (4% of 5000 fits) were used. This analysis confirmed a global parameter optimum for all parameters, showing identifiability of our model.

Confidence intervals on the parameters were calculated using a likelihood-based approach that systematically scans the profile likelihood in the parameter space to infer point-wise confidence intervals.

4.6.4 Sensitivity analysis

Sensitivity analysis was applied to investigate relative changes of derived system variables *K* as a result of relative changes in parameter values p_i

$$S_{p_i}^{K} = \frac{p_i}{K} \cdot \frac{\partial K}{\partial p_i} \qquad (1)$$

The control coefficients quantify the extent to which a characteristic of the dynamic time profile (such as the signalling amplitude, the duration, or the integrated output) is controlled by the processes in the mathematical model (Hornberg et al., 2005a). The software

PottersWheel (Maiwald et al., 2008) was used to calculate the control coefficients of the calibrated model.

5 References

Aaronson, D.S. & Horvath, C.M. A road map for those who don't know JAK-STAT. *Science* **296**, 1653-1655 (2002).

Aldridge, B.B., Burke, J.M., Lauffenburger, D.A. & Sorger, P.K. Physicochemical modelling of cell signalling pathways. *Nat Cell Biol* **8**, 1195-1203 (2006).

Altan-Bonnet, G. & Germain, R.N. Modeling T cell antigen discrimination based on feedback control of digital ERK responses. *PLoS Biol* **3**, e356 (2005).

Ariyoshi, K., Nosaka, T., Yamada, K., Onishi, M., Oka, Y., Miyajima, A. & Kitamura, T. Constitutive activation of STAT5 by a point mutation in the SH2 domain. *J Biol Chem* **275**, 24407-24413 (2000).

Backman, C.M., Zhang, Y., Hoffer, B.J. & Tomac, A.C. Tetracycline-inducible expression systems for the generation of transgenic animals: a comparison of various inducible systems carried in a single vector. *J Neurosci Methods* **139**, 257-262 (2004).

Baker, S.J., Rane, S.G. & Reddy, E.P. Hematopoietic cytokine receptor signaling. *Oncogene* **26**, 6724-6737 (2007).

Banga, J.R. Optimization in computational systems biology. *BMC Syst Biol* **2**, 47 (2008).

Banville, D., Stocco, R. & Shen, S.H. Human protein tyrosine phosphatase 1C (PTPN6) gene structure: alternate promoter usage and exon skipping generate multiple transcripts. *Genomics* **27**, 165-173 (1995).

Barber, D.L., Beattie, B.K., Mason, J.M., Nguyen, M.H., Yoakim, M., Neel, B.G., D'Andrea, A.D. & Frank, D.A. A common epitope is shared by activated signal transducer and activator of transcription-5 (STAT5) and the phosphorylated erythropoietin receptor: implications for the docking model of STAT activation. *Blood* **97**, 2230-2237 (2001).

Barclay, J.L., Anderson, S.T., Waters, M.J. & Curlewis, J.D. Regulation of suppressor of cytokine signaling 3 (SOC3) by growth hormone in pro-B cells. *Mol Endocrinol* **21**, 2503-2515 (2007).

Barde, I., Zanta-Boussif, M.A., Paisant, S., Leboeuf, M., Rameau, P., Delenda, C. & Danos, O. Efficient control of gene expression in the hematopoietic system using a single Tet-on inducible lentiviral vector. *Mol Ther* **13**, 382-390 (2006).

Barford, D. & Neel, B.G. Revealing mechanisms for SH2 domain mediated regulation of the protein tyrosine phosphatase SHP-2. *Structure* **6**, 249-254 (1998).

Barkai, N. & Leibler, S. Robustness in simple biochemical networks. *Nature* **387**, 913-917 (1997).

Baron, U. & Bujard, H. Tet repressor-based system for regulated gene expression in eukaryotic cells: principles and advances. *Methods Enzymol* **327**, 401-421 (2000).

Baxter, E.J., Scott, L.M., Campbell, P.J., East, C., Fourouclas, N., Swanton, S., Vassiliou, G.S., Bench, A.J., Boyd, E.M., Curtin, N., Scott, M.A., Erber, W.N. & Green, A.R. Acquired mutation of the tyrosine kinase JAK2 in human myeloproliferative disorders. *Lancet* **365**, 1054-1061 (2005).

Bazan, J.F. Structural design and molecular evolution of a cytokine receptor superfamily. *Proc Natl Acad Sci U S A* **87**, 6934-6938 (1990).

Becker, V., Sengupta, D., Ketteler, R., Ullmann, G.M., Smith, J.C. & Klingmuller, U. Packing density of the erythropoietin receptor transmembrane domain correlates with amplification of biological responses. *Biochemistry* **47**, 11771-11782 (2008).

Behar, M., Hao, N., Dohlman, H.G. & Elston, T.C. Mathematical and computational analysis of adaptation via feedback inhibition in signal transduction pathways. *Biophys J* **93**, 806-821 (2007).

Bouscary, D., Pene, F., Claessens, Y.E., Muller, O., Chretien, S., Fontenay-Roupie, M., Gisselbrecht, S., Mayeux, P. & Lacombe, C. Critical role for PI 3-kinase in the control

of erythropoietin-induced erythroid progenitor proliferation. *Blood* **101**, 3436-3443 (2003).
Bromberg, J.F., Wrzeszczynska, M.H., Devgan, G., Zhao, Y., Pestell, R.G., Albanese, C. & Darnell, J.E., Jr. Stat3 as an oncogene. *Cell* **98**, 295-303 (1999).
Bruggeman, F.J., Westerhoff, H.V., Hoek, J.B. & Kholodenko, B.N. Modular response analysis of cellular regulatory networks. *J Theor Biol* **218**, 507-520 (2002).
Cascante, M., Boros, L.G., Comin-Anduix, B., de Atauri, P., Centelles, J.J. & Lee, P.W. Metabolic control analysis in drug discovery and disease. *Nat Biotechnol* **20**, 243-249 (2002).
Chai, S.K., Nichols, G.L. & Rothman, P. Constitutive activation of JAKs and STATs in BCR-Abl-expressing cell lines and peripheral blood cells derived from leukemic patients. *J Immunol* **159**, 4720-4728 (1997).
Chaves, M., Sontag, ED., Dinerstein, RJ. Amplification in weakly activated signal transduction cascades. *J Phys Chem B* **108**, 15311-15320 (2004).
Chen, X., Vinkemeier, U., Zhao, Y., Jeruzalmi, D., Darnell, J.E., Jr. & Kuriyan, J. Crystal structure of a tyrosine phosphorylated STAT-1 dimer bound to DNA. *Cell* **93**, 827-839 (1998).
Chenuaud, P., Larcher, T., Rabinowitz, J.E., Provost, N., Joussemet, B., Bujard, H., Samulski, R.J., Favre, D. & Moullier, P. Optimal design of a single recombinant adeno-associated virus derived from serotypes 1 and 2 to achieve more tightly regulated transgene expression from nonhuman primate muscle. *Mol Ther* **9**, 410-418 (2004).
Cheong, R. & Levchenko, A. Wires in the soup: quantitative models of cell signaling. *Trends Cell Biol* **18**, 112-118 (2008).
Chim, C.S., Fung, T.K., Cheung, W.C., Liang, R. & Kwong, Y.L. SOCS1 and SHP1 hypermethylation in multiple myeloma: implications for epigenetic activation of the Jak/STAT pathway. *Blood* **103**, 4630-4635 (2004).
Cosman, D., Lyman, S.D., Idzerda, R.L., Beckmann, M.P., Park, L.S., Goodwin, R.G. & March, C.J. A new cytokine receptor superfamily. *Trends Biochem Sci* **15**, 265-270 (1990).
Cui, Y., Riedlinger, G., Miyoshi, K., Tang, W., Li, C., Deng, C.X., Robinson, G.W. & Hennighausen, L. Inactivation of Stat5 in mouse mammary epithelium during pregnancy reveals distinct functions in cell proliferation, survival, and differentiation. *Mol Cell Biol* **24**, 8037-8047 (2004).
Culhane, A.C., Thioulouse, J., Perriere, G. & Higgins, D.G. MADE4: an R package for multivariate analysis of gene expression data. *Bioinformatics* **21**, 2789-2790 (2005).
D'Andrea, A.D., Lodish, H.F. & Wong, G.G. Expression cloning of the murine erythropoietin receptor. *Cell* **57**, 277-285 (1989).
D'Andrea, A.D. & Zon, L.I. Erythropoietin receptor. Subunit structure and activation. *J Clin Invest* **86**, 681-687 (1990).
Damen, J.E., Cutler, R.L., Jiao, H., Yi, T. & Krystal, G. Phosphorylation of tyrosine 503 in the erythropoietin receptor (EpR) is essential for binding the P85 subunit of phosphatidylinositol (PI) 3-kinase and for EpR-associated PI 3-kinase activity. *J Biol Chem* **270**, 23402-23408 (1995).
Darnell, J.E., Jr. STATs and gene regulation. *Science* **277**, 1630-1635 (1997).
de la Chapelle, A., Traskelin, A.L. & Juvonen, E. Truncated erythropoietin receptor causes dominantly inherited benign human erythrocytosis. *Proc Natl Acad Sci U S A* **90**, 4495-4499 (1993).
Denson, L.A., Held, M.A., Menon, R.K., Frank, S.J., Parlow, A.F. & Arnold, D.L. Interleukin-6 inhibits hepatic growth hormone signaling via upregulation of Cis and Socs-3. *Am J Physiol Gastrointest Liver Physiol* **284**, G646-654 (2003).
Dolznig, H., Grebien, F., Deiner, E.M., Stangl, K., Kolbus, A., Habermann, B., Kerenyi, M.A., Kieslinger, M., Moriggl, R., Beug, H. & Mullner, E.W. Erythroid progenitor renewal versus differentiation: genetic evidence for cell autonomous, essential functions of EpoR, Stat5 and the GR. *Oncogene* **25**, 2890-2900 (2006).

Drexler, H.G., Matsuo, Y. & MacLeod, R.A. Malignant hematopoietic cell lines: in vitro models for the study of erythroleukemia. *Leuk Res* **28**, 1243-1251 (2004).

Dumon, S., Santos, S.C., Debierre-Grockiego, F., Gouilleux-Gruart, V., Cocault, L., Boucheron, C., Mollat, P., Gisselbrecht, S. & Gouilleux, F. IL-3 dependent regulation of Bcl-xL gene expression by STAT5 in a bone marrow derived cell line. *Oncogene* **18**, 4191-4199 (1999).

Ebert, B.L. & Bunn, H.F. Regulation of the erythropoietin gene. *Blood* **94**, 1864-1877 (1999).

Ehlting, C., Lai, W.S., Schaper, F., Brenndorfer, E.D., Matthes, R.J., Heinrich, P.C., Ludwig, S., Blackshear, P.J., Gaestel, M., Haussinger, D. & Bode, J.G. Regulation of suppressor of cytokine signaling 3 (SOCS3) mRNA stability by TNF-alpha involves activation of the MKK6/p38MAPK/MK2 cascade. *J Immunol* **178**, 2813-2826 (2007).

Elliott, J. & Johnston, J.A. SOCS: role in inflammation, allergy and homeostasis. *Trends Immunol* **25**, 434-440 (2004).

Endo, T.A., Masuhara, M., Yokouchi, M., Suzuki, R., Sakamoto, H., Mitsui, K., Matsumoto, A., Tanimura, S., Ohtsubo, M., Misawa, H., Miyazaki, T., Leonor, N., Taniguchi, T., Fujita, T., Kanakura, Y., Komiya, S. & Yoshimura, A. A new protein containing an SH2 domain that inhibits JAK kinases. *Nature* **387**, 921-924 (1997).

Feng, J., Witthuhn, B.A., Matsuda, T., Kohlhuber, F., Kerr, I.M. & Ihle, J.N. Activation of Jak2 catalytic activity requires phosphorylation of Y1007 in the kinase activation loop. *Mol Cell Biol* **17**, 2497-2501 (1997).

Funakoshi-Tago, M., Pelletier, S., Matsuda, T., Parganas, E. & Ihle, J.N. Receptor specific downregulation of cytokine signaling by autophosphorylation in the FERM domain of Jak2. *EMBO J* **25**, 4763-4772 (2006).

Garcon, L., Rivat, C., James, C., Lacout, C., Camara-Clayette, V., Ugo, V., Lecluse, Y., Bennaceur-Griscelli, A. & Vainchenker, W. Constitutive activation of STAT5 and Bcl-xL overexpression can induce endogenous erythroid colony formation in human primary cells. *Blood* **108**, 1551-1554 (2006).

Gobert, S., Chretien, S., Gouilleux, F., Muller, O., Pallard, C., Dusanter-Fourt, I., Groner, B., Lacombe, C., Gisselbrecht, S. & Mayeux, P. Identification of tyrosine residues within the intracellular domain of the erythropoietin receptor crucial for STAT5 activation. *EMBO J* **15**, 2434-2441 (1996).

Gossen, M. & Bujard, H. Tight control of gene expression in mammalian cells by tetracycline-responsive promoters. *Proc Natl Acad Sci U S A* **89**, 5547-5551 (1992).

Gossen, M., Freundlieb, S., Bender, G., Muller, G., Hillen, W. & Bujard, H. Transcriptional activation by tetracyclines in mammalian cells. *Science* **268**, 1766-1769 (1995).

Gregory, C.J. & Eaves, A.C. Human marrow cells capable of erythropoietic differentiation in vitro: definition of three erythroid colony responses. *Blood* **49**, 855-864 (1977).

Haan, S., Margue, C., Engrand, A., Rolvering, C., Schmitz-Van de Leur, H., Heinrich, P.C., Behrmann, I. & Haan, C. Dual role of the Jak1 FERM and kinase domains in cytokine receptor binding and in stimulation-dependent Jak activation. *J Immunol* **180**, 998-1007 (2008).

Hao, N., Behar, M., Parnell, S.C., Torres, M.P., Borchers, C.H., Elston, T.C. & Dohlman, H.G. A systems-biology analysis of feedback inhibition in the Sho1 osmotic-stress-response pathway. *Curr Biol* **17**, 659-667 (2007).

Haque, S.J., Harbor, P.C. & Williams, B.R. Identification of critical residues required for suppressor of cytokine signaling-specific regulation of interleukin-4 signaling. *J Biol Chem* **275**, 26500-26506 (2000).

He, T.C., Jiang, N., Zhuang, H. & Wojchowski, D.M. Erythropoietin-induced recruitment of Shc via a receptor phosphotyrosine-independent, Jak2-associated pathway. *J Biol Chem* **270**, 11055-11061 (1995).

Heinrich, R., Neel, B.G. & Rapoport, T.A. Mathematical models of protein kinase signal transduction. *Mol Cell* **9**, 957-970 (2002).

Higgins, D.G., Thompson, J.D. & Gibson, T.J. Using CLUSTAL for multiple sequence alignments. *Methods Enzymol* **266**, 383-402 (1996).

Ho, J.M., Beattie, B.K., Squire, J.A., Frank, D.A. & Barber, D.L. Fusion of the ets transcription factor TEL to Jak2 results in constitutive Jak-Stat signaling. *Blood* **93**, 4354-4364 (1999).

Hoffman, R., Benz, E., Shattil, S., Furie, B., Cohen, H., and Silberstein, L. Hematology, Basic Principles and Practice. *In: 2nd edition, Churchill Livingstone, New York, Edinburgh, London, Madrid, Melbourne, Milan, Tokyo.* (1995).

Hornberg, J.J., Binder, B., Bruggeman, F.J., Schoeberl, B., Heinrich, R. & Westerhoff, H.V. Control of MAPK signalling: from complexity to what really matters. *Oncogene* **24**, 5533-5542 (2005a).

Hornberg, J.J., Bruggeman, F.J., Binder, B., Geest, C.R., de Vaate, A.J., Lankelma, J., Heinrich, R. & Westerhoff, H.V. Principles behind the multifarious control of signal transduction. ERK phosphorylation and kinase/phosphatase control. *FEBS J* **272**, 244-258 (2005b).

Hortner, M., Nielsch, U., Mayr, L.M., Heinrich, P.C. & Haan, S. A new high affinity binding site for suppressor of cytokine signaling-3 on the erythropoietin receptor. *Eur J Biochem* **269**, 2516-2526 (2002).

Horvath, C.M. STAT proteins and transcriptional responses to extracellular signals. *Trends Biochem Sci* **25**, 496-502 (2000).

Huang, L.J., Constantinescu, S.N. & Lodish, H.F. The N-terminal domain of Janus kinase 2 is required for Golgi processing and cell surface expression of erythropoietin receptor. *Mol Cell* **8**, 1327-1338 (2001).

Huber, W., von Heydebreck, A., Sultmann, H., Poustka, A. & Vingron, M. Variance stabilization applied to microarray data calibration and to the quantification of differential expression. *Bioinformatics* **18 Suppl 1**, S96-104 (2002).

Ilangumaran, S., Ramanathan, S. & Rottapel, R. Regulation of the immune system by SOCS family adaptor proteins. *Semin Immunol* **16**, 351-365 (2004).

Irie-Sasaki, J., Sasaki, T., Matsumoto, W., Opavsky, A., Cheng, M., Welstead, G., Griffiths, E., Krawczyk, C., Richardson, C.D., Aitken, K., Iscove, N., Koretzky, G., Johnson, P., Liu, P., Rothstein, D.M. & Penninger, J.M. CD45 is a JAK phosphatase and negatively regulates cytokine receptor signalling. *Nature* **409**, 349-354 (2001).

James, C., Ugo, V., Le Couedic, J.P., Staerk, J., Delhommeau, F., Lacout, C., Garcon, L., Raslova, H., Berger, R., Bennaceur-Griscelli, A., Villeval, J.L., Constantinescu, S.N., Casadevall, N. & Vainchenker, W. A unique clonal JAK2 mutation leading to constitutive signalling causes polycythaemia vera. *Nature* **434**, 1144-1148 (2005).

Jegalian, A.G. & Wu, H. Differential roles of SOCS family members in EpoR signal transduction. *J Interferon Cytokine Res* **22**, 853-860 (2002).

Jelkmann, W. Molecular biology of erythropoietin. *Intern Med* **43**, 649-659 (2004).

Jiao, H., Berrada, K., Yang, W., Tabrizi, M., Platanias, L.C. & Yi, T. Direct association with and dephosphorylation of Jak2 kinase by the SH2-domain-containing protein tyrosine phosphatase SHP-1. *Mol Cell Biol* **16**, 6985-6992 (1996).

Johan, M.F., Bowen, D.T., Frew, M.E., Goodeve, A.C. & Reilly, J.T. Aberrant methylation of the negative regulators RASSFIA, SHP-1 and SOCS-1 in myelodysplastic syndromes and acute myeloid leukaemia. *Br J Haematol* **129**, 60-65 (2005).

Jones, M.L., Craik, J.D., Gibbins, J.M. & Poole, A.W. Regulation of SHP-1 tyrosine phosphatase in human platelets by serine phosphorylation at its C terminus. *J Biol Chem* **279**, 40475-40483 (2004).

Jost, E., do, O.N., Dahl, E., Maintz, C.E., Jousten, P., Habets, L., Wilop, S., Herman, J.G., Osieka, R. & Galm, O. Epigenetic alterations complement mutation of JAK2 tyrosine kinase in patients with BCR/ABL-negative myeloproliferative disorders. *Leukemia* **21**, 505-510 (2007).

Karnitz, L.M. & Abraham, R.T. Cytokine receptor signaling mechanisms. *Curr Opin Immunol* **7**, 320-326 (1995).

Kashii, Y., Uchida, M., Kirito, K., Tanaka, M., Nishijima, K., Toshima, M., Ando, T., Koizumi, K., Endoh, T., Sawada, K., Momoi, M., Miura, Y., Ozawa, K. & Komatsu, N. A member of Forkhead family transcription factor, FKHRL1, is one of the downstream

molecules of phosphatidylinositol 3-kinase-Akt activation pathway in erythropoietin signal transduction. *Blood* **96**, 941-949 (2000).
Ketteler, R., Glaser, S., Sandra, O., Martens, U.M. & Klingmüller, U. Enhanced transgene expression in primitive hematopoietic progenitor cells and embryonic stem cells efficiently transduced by optimized retroviral hybrid vectors. *Gene Ther* **9**, 477-487 (2002).
Ketteler, R., Moghraby, C.S., Hsiao, J.G., Sandra, O., Lodish, H.F. & Klingmüller, U. The cytokine-inducible Scr homology domain-containing protein negatively regulates signaling by promoting apoptosis in erythroid progenitor cells. *J Biol Chem* **278**, 2654-2660 (2003).
Kholodenko, B.N., Demin, O.V., Moehren, G. & Hoek, J.B. Quantification of short term signaling by the epidermal growth factor receptor. *J Biol Chem* **274**, 30169-30181 (1999).
Kholodenko, B.N. Cell-signalling dynamics in time and space. *Nat Rev Mol Cell Biol* **7**, 165-176 (2006).
Kholodenko, B.N. Untangling the signalling wires. *Nat Cell Biol* **9**, 247-249 (2007).
Khoury, J.D., Rassidakis, G.Z., Medeiros, L.J., Amin, H.M. & Lai, R. Methylation of SHP1 gene and loss of SHP1 protein expression are frequent in systemic anaplastic large cell lymphoma. *Blood* **104**, 1580-1581 (2004).
Khwaja, A. The role of Janus kinases in haemopoiesis and haematological malignancy. *Br J Haematol* **134**, 366-384 (2006).
Kisseleva, T., Bhattacharya, S., Braunstein, J. & Schindler, C.W. Signaling through the JAK/STAT pathway, recent advances and future challenges. *Gene* **285**, 1-24 (2002).
Klingmüller, U., Lorenz, U., Cantley, L.C., Neel, B.G. & Lodish, H.F. Specific recruitment of SH-PTP1 to the erythropoietin receptor causes inactivation of JAK2 and termination of proliferative signals. *Cell* **80**, 729-738 (1995).
Klingmüller, U., Bergelson, S., Hsiao, J.G. & Lodish, H.F. Multiple tyrosine residues in the cytosolic domain of the erythropoietin receptor promote activation of STAT5. *Proc Natl Acad Sci U S A* **93**, 8324-8328 (1996).
Klingmüller, U. The role of tyrosine phosphorylation in proliferation and maturation of erythroid progenitor cells--signals emanating from the erythropoietin receptor. *Eur J Biochem* **249**, 637-647 (1997).
Kolch, W., Calder, M. & Gilbert, D. When kinases meet mathematics: the systems biology of MAPK signalling. *FEBS Lett* **579**, 1891-1895 (2005).
Korf, U., Derdak, S., Tresch, A., Henjes, F., Schumacher, S., Schmidt, C., Hahn, B., Lehmann, W.D., Poustka, A., Beissbarth, T. & Klingmüller, U. Quantitative protein microarrays for time-resolved measurements of protein phosphorylation. *Proteomics* **8**, 4603-4612 (2008).
Kralovics, R., Indrak, K., Stopka, T., Berman, B.W., Prchal, J.F. & Prchal, J.T. Two new EPO receptor mutations: truncated EPO receptors are most frequently associated with primary familial and congenital polycythemias. *Blood* **90**, 2057-2061 (1997).
Kralovics, R., Passamonti, F., Buser, A.S., Teo, S.S., Tiedt, R., Passweg, J.R., Tichelli, A., Cazzola, M. & Skoda, R.C. A gain-of-function mutation of JAK2 in myeloproliferative disorders. *N Engl J Med* **352**, 1779-1790 (2005).
Krantz, S.B. Erythropoietin. *Blood* **77**, 419-434 (1991).
Lacronique, V., Boureux, A., Valle, V.D., Poirel, H., Quang, C.T., Mauchauffe, M., Berthou, C., Lessard, M., Berger, R., Ghysdael, J. & Bernard, O.A. A TEL-JAK2 fusion protein with constitutive kinase activity in human leukemia. *Science* **278**, 1309-1312 (1997).
Laemmli, U.K. Cleavage of structural proteins during the assembly of the head of bacteriophage T4. *Nature* **227**, 680-685 (1970).
Lee, Y.B., Glover, C.P., Cosgrave, A.S., Bienemann, A. & Uney, J.B. Optimizing regulatable gene expression using adenoviral vectors. *Exp Physiol* **90**, 33-37 (2005).
Legewie, S., Bluthgen, N. & Herzel, H. Quantitative analysis of ultrasensitive responses. *FEBS J* **272**, 4071-4079 (2005).

Legewie, S., Herzel, H., Westerhoff, H.V. & Bluthgen, N. Recurrent design patterns in the feedback regulation of the mammalian signalling network. *Mol Syst Biol* **4**, 190 (2008).

Levine, R.L. et al. The JAK2V617F activating mutation occurs in chronic myelomonocytic leukemia and acute myeloid leukemia, but not in acute lymphoblastic leukemia or chronic lymphocytic leukemia. *Blood* **106**, 3377-3379 (2005).

Levy, D.E. & Darnell, J.E., Jr. Stats: transcriptional control and biological impact. *Nat Rev Mol Cell Biol* **3**, 651-662 (2002).

Maiwald, T., Kreutz, C., Pfeifer, A.C., Bohl, S., Klingmüller, U. & Timmer, J. Dynamic pathway modeling: feasibility analysis and optimal experimental design. *Ann N Y Acad Sci* **1115**, 212-220 (2007).

Maiwald, T. & Timmer, J. Dynamical modeling and multi-experiment fitting with PottersWheel. *Bioinformatics* **24**, 2037-2043 (2008).

Mann, M. Functional and quantitative proteomics using SILAC. *Nat Rev Mol Cell Biol* **7**, 952-958 (2006).

Marg, A., Shan, Y., Meyer, T., Meissner, T., Brandenburg, M. & Vinkemeier, U. Nucleocytoplasmic shuttling by nucleoporins Nup153 and Nup214 and CRM1-dependent nuclear export control the subcellular distribution of latent Stat1. *J Cell Biol* **165**, 823-833 (2004).

Marine, J.C., McKay, C., Wang, D., Topham, D.J., Parganas, E., Nakajima, H., Pendeville, H., Yasukawa, H., Sasaki, A., Yoshimura, A. & Ihle, J.N. SOCS3 is essential in the regulation of fetal liver erythropoiesis. *Cell* **98**, 617-627 (1999).

Mason, J.M., Beattie, B.K., Liu, Q., Dumont, D.J. & Barber, D.L. The SH2 inositol 5-phosphatase Ship1 is recruited in an SH2-dependent manner to the erythropoietin receptor. *J Biol Chem* **275**, 4398-4406 (2000).

Matsumoto, A., Masuhara, M., Mitsui, K., Yokouchi, M., Ohtsubo, M., Misawa, H., Miyajima, A. & Yoshimura, A. CIS, a cytokine inducible SH2 protein, is a target of the JAK-STAT5 pathway and modulates STAT5 activation. *Blood* **89**, 3148-3154 (1997).

Matsumoto, A., Seki, Y., Kubo, M., Ohtsuka, S., Suzuki, A., Hayashi, I., Tsuji, K., Nakahata, T., Okabe, M., Yamada, S. & Yoshimura, A. Suppression of STAT5 functions in liver, mammary glands, and T cells in cytokine-inducible SH2-containing protein 1 transgenic mice. *Mol Cell Biol* **19**, 6396-6407 (1999).

Mattaj, I.W. & Englmeier, L. Nucleocytoplasmic transport: the soluble phase. *Annu Rev Biochem* **67**, 265-306 (1998).

Menon, M.P., Karur, V., Bogacheva, O., Bogachev, O., Cuetara, B. & Wojchowski, D.M. Signals for stress erythropoiesis are integrated via an erythropoietin receptor-phosphotyrosine-343-Stat5 axis. *J Clin Invest* **116**, 683-694 (2006).

Moucadel, V. & Constantinescu, S.N. Differential STAT5 signaling by ligand-dependent and constitutively active cytokine receptors. *J Biol Chem* **280**, 13364-13373 (2005).

Myers, M.P., Andersen, J.N., Cheng, A., Tremblay, M.L., Horvath, C.M., Parisien, J.P., Salmeen, A., Barford, D. & Tonks, N.K. TYK2 and JAK2 are substrates of protein-tyrosine phosphatase 1B. *J Biol Chem* **276**, 47771-47774 (2001).

Nagai, H., Kim, Y.S., Lee, K.T., Chu, M.Y., Konishi, N., Fujimoto, J., Baba, M., Matsubara, K. & Emi, M. Inactivation of SSI-1, a JAK/STAT inhibitor, in human hepatocellular carcinomas, as revealed by two-dimensional electrophoresis. *J Hepatol* **34**, 416-421 (2001).

Nagarajan, P. & Sinha, S. Development of an inducible gene expression system for primary murine keratinocytes. *J Dermatol Sci* **49**, 73-84 (2008).

Naka, T., Narazaki, M., Hirata, M., Matsumoto, T., Minamoto, S., Aono, A., Nishimoto, N., Kajita, T., Taga, T., Yoshizaki, K., Akira, S. & Kishimoto, T. Structure and function of a new STAT-induced STAT inhibitor. *Nature* **387**, 924-929 (1997).

Neel, B.G., Gu, H. & Pao, L. The 'Shp'ing news: SH2 domain-containing tyrosine phosphatases in cell signaling. *Trends Biochem Sci* **28**, 284-293 (2003).

Nelson, D.E., Ihekwaba, A.E., Elliott, M., Johnson, J.R., Gibney, C.A., Foreman, B.E., Nelson, G., See, V., Horton, C.A., Spiller, D.G., Edwards, S.W., McDowell, H.P., Unitt, J.F., Sullivan, E., Grimley, R., Benson, N., Broomhead, D., Kell, D.B. & White,

M.R. Oscillations in NF-kappaB signaling control the dynamics of gene expression. *Science* **306**, 704-708 (2004).

Neubauer, H., Cumano, A., Muller, M., Wu, H., Huffstadt, U. & Pfeffer, K. Jak2 deficiency defines an essential developmental checkpoint in definitive hematopoiesis. *Cell* **93**, 397-409 (1998).

Noe, G., Riedel, W., Kubanek, B. & Rich, I.N. An ELISA specific for murine erythropoietin. *Br J Haematol* **104**, 838-840 (1999).

Nosaka, T., Kawashima, T., Misawa, K., Ikuta, K., Mui, A.L. & Kitamura, T. STAT5 as a molecular regulator of proliferation, differentiation and apoptosis in hematopoietic cells. *EMBO J* **18**, 4754-4765 (1999).

O'Sullivan, L.A., Liongue, C., Lewis, R.S., Stephenson, S.E. & Ward, A.C. Cytokine receptor signaling through the Jak-Stat-Socs pathway in disease. *Mol Immunol* **44**, 2497-2506 (2007).

Oka, T., Ouchida, M., Koyama, M., Ogama, Y., Takada, S., Nakatani, Y., Tanaka, T., Yoshino, T., Hayashi, K., Ohara, N., Kondo, E., Takahashi, K., Tsuchiyama, J., Tanimoto, M., Shimizu, K. & Akagi, T. Gene silencing of the tyrosine phosphatase SHP1 gene by aberrant methylation in leukemias/lymphomas. *Cancer Res* **62**, 6390-6394 (2002).

Orkin, S.H. & Zon, L.I. Hematopoiesis: an evolving paradigm for stem cell biology. *Cell* **132**, 631-644 (2008).

Orton, R.J., Sturm, O.E., Vyshemirsky, V., Calder, M., Gilbert, D.R. & Kolch, W. Computational modelling of the receptor-tyrosine-kinase-activated MAPK pathway. *Biochem J* **392**, 249-261 (2005).

Palacios, R. & Steinmetz, M. Il-3-dependent mouse clones that express B-220 surface antigen, contain Ig genes in germ-line configuration, and generate B lymphocytes in vivo. *Cell* **41**, 727-734 (1985).

Pallen, C.J., Tan, Y.H. & Guy, G.R. Protein phosphatases in cell signalling. *Curr Opin Cell Biol* **4**, 1000-1007 (1992).

Pao, L.I., Badour, K., Siminovitch, K.A. & Neel, B.G. Nonreceptor protein-tyrosine phosphatases in immune cell signaling. *Annu Rev Immunol* **25**, 473-523 (2007a).

Pao, L.I., Lam, K.P., Henderson, J.M., Kutok, J.L., Alimzhanov, M., Nitschke, L., Thomas, M.L., Neel, B.G. & Rajewsky, K. B cell-specific deletion of protein-tyrosine phosphatase Shp1 promotes B-1a cell development and causes systemic autoimmunity. *Immunity* **27**, 35-48 (2007b).

Pei, D., Lorenz, U., Klingmüller, U., Neel, B.G. & Walsh, C.T. Intramolecular regulation of protein tyrosine phosphatase SH-PTP1: a new function for Src homology 2 domains. *Biochemistry* **33**, 15483-15493 (1994).

Pei, D., Wang, J. & Walsh, C.T. Differential functions of the two Src homology 2 domains in protein tyrosine phosphatase SH-PTP1. *Proc Natl Acad Sci U S A* **93**, 1141-1145 (1996).

Pellegrini, S. & Dusanter-Fourt, I. The structure, regulation and function of the Janus kinases (JAKs) and the signal transducers and activators of transcription (STATs). *Eur J Biochem* **248**, 615-633 (1997).

Pezet, A., Favre, H., Kelly, P.A. & Edery, M. Inhibition and restoration of prolactin signal transduction by suppressors of cytokine signaling. *J Biol Chem* **274**, 24497-24502 (1999).

Pircher, T.J., Geiger, J.N., Zhang, D., Miller, C.P., Gaines, P. & Wojchowski, D.M. Integrative signaling by minimal erythropoietin receptor forms and c-Kit. *J Biol Chem* **276**, 8995-9002 (2001).

Pluta, K., Luce, M.J., Bao, L., Agha-Mohammadi, S. & Reiser, J. Tight control of transgene expression by lentivirus vectors containing second-generation tetracycline-responsive promoters. *J Gene Med* **7**, 803-817 (2005).

Poole, A.W. & Jones, M.L. A SHPing tale: perspectives on the regulation of SHP-1 and SHP-2 tyrosine phosphatases by the C-terminal tail. *Cell Signal* **17**, 1323-1332 (2005).

Radtke, S., Haan, S., Jorissen, A., Hermanns, H.M., Diefenbach, S., Smyczek, T., Schmitz-Vandeleur, H., Heinrich, P.C., Behrmann, I. & Haan, C. The Jak1 SH2 domain does

not fulfill a classical SH2 function in Jak/STAT signaling but plays a structural role for receptor interaction and up-regulation of receptor surface expression. *J Biol Chem* **280**, 25760-25768 (2005).

Rakesh, K. & Agrawal, D.K. Controlling cytokine signaling by constitutive inhibitors. *Biochem Pharmacol* **70**, 649-657 (2005).

Ralph, P. & Nakoinz, I. Antibody-dependent killing of erythrocyte and tumor targets by macrophage-related cell lines: enhancement by PPD and LPS. *J Immunol* **119**, 950-954 (1977a).

Ralph, P. & Nakoinz, I. Direct toxic effects of immunopotentiators on monocytic, myelomonocytic, and histiocytic or macrophage tumor cells in culture. *Cancer Res* **37**, 546-550 (1977b).

Ravichandran, K.S., Lorenz, U., Shoelson, S.E. & Burakoff, S.J. Interaction of Shc with Grb2 regulates association of Grb2 with mSOS. *Mol Cell Biol* **15**, 593-600 (1995).

Reich, N.C. & Liu, L. Tracking STAT nuclear traffic. *Nat Rev Immunol* **6**, 602-612 (2006).

Richmond, T.D., Chohan, M. & Barber, D.L. Turning cells red: signal transduction mediated by erythropoietin. *Trends Cell Biol* **15**, 146-155 (2005).

Rottapel, R., Ilangumaran, S., Neale, C., La Rose, J., Ho, J.M., Nguyen, M.H., Barber, D., Dubreuil, P. & de Sepulveda, P. The tumor suppressor activity of SOCS-1. *Oncogene* **21**, 4351-4362 (2002).

Saharinen, P. & Silvennoinen, O. The pseudokinase domain is required for suppression of basal activity of Jak2 and Jak3 tyrosine kinases and for cytokine-inducible activation of signal transduction. *J Biol Chem* **277**, 47954-47963 (2002).

Saharinen, P., Vihinen, M. & Silvennoinen, O. Autoinhibition of Jak2 tyrosine kinase is dependent on specific regions in its pseudokinase domain. *Mol Biol Cell* **14**, 1448-1459 (2003).

Sarna, M.K., Ingley, E., Busfield, S.J., Cull, V.S., Lepere, W., McCarthy, D.J., Wright, M.J., Palmer, G.A., Chappell, D., Sayer, M.S., Alexander, W.S., Hilton, D.J., Starr, R., Watowich, S.S., Bittorf, T., Klinken, S.P. & Tilbrook, P.A. Differential regulation of SOCS genes in normal and transformed erythroid cells. *Oncogene* **22**, 3221-3230 (2003).

Sasaki, A., Yasukawa, H., Suzuki, A., Kamizono, S., Syoda, T., Kinjyo, I., Sasaki, M., Johnston, J.A. & Yoshimura, A. Cytokine-inducible SH2 protein-3 (CIS3/SOCS3) inhibits Janus tyrosine kinase by binding through the N-terminal kinase inhibitory region as well as SH2 domain. *Genes Cells* **4**, 339-351 (1999).

Sasaki, A., Yasukawa, H., Shouda, T., Kitamura, T., Dikic, I. & Yoshimura, A. CIS3/SOCS-3 suppresses erythropoietin (EPO) signaling by binding the EPO receptor and JAK2. *J Biol Chem* **275**, 29338-29347 (2000).

Schilling, M., Maiwald, T., Bohl, S., Kollmann, M., Kreutz, C., Timmer, J. & Klingmüller, U. Computational processing and error reduction strategies for standardized quantitative data in biological networks. *FEBS J* **272**, 6400-6411 (2005a).

Schilling, M., Maiwald, T., Bohl, S., Kollmann, M., Kreutz, C., Timmer, J. & Klingmüller, U. Quantitative data generation for systems biology: the impact of randomisation, calibrators and normalisers. *Syst Biol (Stevenage)* **152**, 193-200 (2005b).

Schilling, M., Pfeifer, A.C., Bohl, S. & Klingmüller, U. Standardizing experimental protocols. *Curr Opin Biotechnol* **19**, 354-359 (2008).

Schindler, C., Shuai, K., Prezioso, V.R. & Darnell, J.E., Jr. Interferon-dependent tyrosine phosphorylation of a latent cytoplasmic transcription factor. *Science* **257**, 809-813 (1992).

Schindler, C. & Darnell, J.E., Jr. Transcriptional responses to polypeptide ligands: the JAK-STAT pathway. *Annu Rev Biochem* **64**, 621-651 (1995).

Schmidt, A., Kellermann, J. & Lottspeich, F. A novel strategy for quantitative proteomics using isotope-coded protein labels. *Proteomics* **5**, 4-15 (2005).

Schwaller, J., Frantsve, J., Aster, J., Williams, I.R., Tomasson, M.H., Ross, T.S., Peeters, P., Van Rompaey, L., Van Etten, R.A., Ilaria, R., Jr., Marynen, P. & Gilliland, D.G. Transformation of hematopoietic cell lines to growth-factor independence and

induction of a fatal myelo- and lymphoproliferative disease in mice by retrovirally transduced TEL/JAK2 fusion genes. *EMBO J* **17**, 5321-5333 (1998).

Shudo, E., Yang, J., Yoshimura, A. & Iwasa, Y. Robustness of the signal transduction system of the mammalian JAK/STAT pathway and dimerization steps. *J Theor Biol* **246**, 1-9 (2007).

Shultz, L.D., Schweitzer, P.A., Rajan, T.V., Yi, T., Ihle, J.N., Matthews, R.J., Thomas, M.L. & Beier, D.R. Mutations at the murine motheaten locus are within the hematopoietic cell protein-tyrosine phosphatase (Hcph) gene. *Cell* **73**, 1445-1454 (1993).

Shultz, L.D., Rajan, T.V. & Greiner, D.L. Severe defects in immunity and hematopoiesis caused by SHP-1 protein-tyrosine-phosphatase deficiency. *Trends Biotechnol* **15**, 302-307 (1997).

Siewert, E., Muller-Esterl, W., Starr, R., Heinrich, P.C. & Schaper, F. Different protein turnover of interleukin-6-type cytokine signalling components. *Eur J Biochem* **265**, 251-257 (1999).

Silva, M., Benito, A., Sanz, C., Prosper, F., Ekhterae, D., Nunez, G. & Fernandez-Luna, J.L. Erythropoietin can induce the expression of bcl-x(L) through Stat5 in erythropoietin-dependent progenitor cell lines. *J Biol Chem* **274**, 22165-22169 (1999).

Simoncic, P.D., Lee-Loy, A., Barber, D.L., Tremblay, M.L. & McGlade, C.J. The T cell protein tyrosine phosphatase is a negative regulator of janus family kinases 1 and 3. *Curr Biol* **12**, 446-453 (2002).

Singh, A., Jayaraman, A. & Hahn, J. Modeling regulatory mechanisms in IL-6 signal transduction in hepatocytes. *Biotechnol Bioeng* **95**, 850-862 (2006).

Socolovsky, M., Fallon, A.E., Wang, S., Brugnara, C. & Lodish, H.F. Fetal anemia and apoptosis of red cell progenitors in Stat5a-/-5b-/- mice: a direct role for Stat5 in Bcl-X(L) induction. *Cell* **98**, 181-191 (1999).

Socolovsky, M., Nam, H., Fleming, M.D., Haase, V.H., Brugnara, C. & Lodish, H.F. Ineffective erythropoiesis in Stat5a(-/-)5b(-/-) mice due to decreased survival of early erythroblasts. *Blood* **98**, 3261-3273 (2001).

Soebiyanto, R.P., Sreenath, S.N., Qu, C.K., Loparo, K.A. & Bunting, K.D. Complex systems biology approach to understanding coordination of JAK-STAT signaling. *Biosystems* **90**, 830-842 (2007).

Sourjik, V. & Berg, H.C. Receptor sensitivity in bacterial chemotaxis. *Proc Natl Acad Sci U S A* **99**, 123-127 (2002).

Starr, R., Willson, T.A., Viney, E.M., Murray, L.J., Rayner, J.R., Jenkins, B.J., Gonda, T.J., Alexander, W.S., Metcalf, D., Nicola, N.A. & Hilton, D.J. A family of cytokine-inducible inhibitors of signalling. *Nature* **387**, 917-921 (1997).

Stelling, J., Sauer, U., Szallasi, Z., Doyle, F.J., 3rd & Doyle, J. Robustness of cellular functions. *Cell* **118**, 675-685 (2004).

Swameye, I., Muller, T.G., Timmer, J., Sandra, O. & Klingmüller, U. Identification of nucleocytoplasmic cycling as a remote sensor in cellular signaling by databased modeling. *Proc Natl Acad Sci U S A* **100**, 1028-1033 (2003).

Tauchi, T., Damen, J.E., Toyama, K., Feng, G.S., Broxmeyer, H.E. & Krystal, G. Tyrosine 425 within the activated erythropoietin receptor binds Syp, reduces the erythropoietin required for Syp tyrosine phosphorylation, and promotes mitogenesis. *Blood* **87**, 4495-4501 (1996).

ten Hoeve, J., de Jesus Ibarra-Sanchez, M., Fu, Y., Zhu, W., Tremblay, M., David, M. & Shuai, K. Identification of a nuclear Stat1 protein tyrosine phosphatase. *Mol Cell Biol* **22**, 5662-5668 (2002).

Tsuji-Takayama, K., Otani, T., Inoue, T., Nakamura, S., Motoda, R., Kibata, M. & Orita, K. Erythropoietin induces sustained phosphorylation of STAT5 in primitive but not definitive erythrocytes generated from mouse embryonic stem cells. *Exp Hematol* **34**, 1323-1332 (2006).

Ungureanu, D., Saharinen, P., Junttila, I., Hilton, D.J. & Silvennoinen, O. Regulation of Jak2 through the ubiquitin-proteasome pathway involves phosphorylation of Jak2 on Y1007 and interaction with SOCS-1. *Mol Cell Biol* **22**, 3316-3326 (2002).

Ungureanu, D., Vanhatupa, S., Gronholm, J., Palvimo, J.J. & Silvennoinen, O. SUMO-1 conjugation selectively modulates STAT1-mediated gene responses. *Blood* **106**, 224-226 (2005).

Urlinger, S., Baron, U., Thellmann, M., Hasan, M.T., Bujard, H. & Hillen, W. Exploring the sequence space for tetracycline-dependent transcriptional activators: novel mutations yield expanded range and sensitivity. *Proc Natl Acad Sci U S A* **97**, 7963-7968 (2000).

Valentino, L. & Pierre, J. JAK/STAT signal transduction: regulators and implication in hematological malignancies. *Biochem Pharmacol* **71**, 713-721 (2006).

Van Zant, G. & Shultz, L. Hematologic abnormalities of the immunodeficient mouse mutant, viable motheaten (mev). *Exp Hematol* **17**, 81-87 (1989).

Vandesompele, J., De Preter, K., Pattyn, F., Poppe, B., Van Roy, N., De Paepe, A. & Speleman, F. Accurate normalization of real-time quantitative RT-PCR data by geometric averaging of multiple internal control genes. *Genome Biol* **3**, RESEARCH0034 (2002).

Vera, J., Bachmann, J., Pfeifer, A.C., Becker, V., Hormiga, J.A., Darias, N.V., Timmer, J., Klingmüller, U. & Wolkenhauer, O. A systems biology approach to analyse amplification in the JAK2-STAT5 signalling pathway. *BMC Syst Biol* **2**, 38 (2008).

Verdier, F., Chretien, S., Muller, O., Varlet, P., Yoshimura, A., Gisselbrecht, S., Lacombe, C. & Mayeux, P. Proteasomes regulate erythropoietin receptor and signal transducer and activator of transcription 5 (STAT5) activation. Possible involvement of the ubiquitinated Cis protein. *J Biol Chem* **273**, 28185-28190 (1998a).

Verdier, F., Rabionet, R., Gouilleux, F., Beisenherz-Huss, C., Varlet, P., Muller, O., Mayeux, P., Lacombe, C., Gisselbrecht, S. & Chretien, S. A sequence of the CIS gene promoter interacts preferentially with two associated STAT5A dimers: a distinct biochemical difference between STAT5A and STAT5B. *Mol Cell Biol* **18**, 5852-5860 (1998b).

Walrafen, P., Verdier, F., Kadri, Z., Chretien, S., Lacombe, C. & Mayeux, P. Both proteasomes and lysosomes degrade the activated erythropoietin receptor. *Blood* **105**, 600-608 (2005).

Ward, A.C., Oomen, S.P., Smith, L., Gits, J., van Leeuwen, D., Soede-Bobok, A.A., Erpelinck-Verschueren, C.A., Yi, T. & Touw, I.P. The SH2 domain-containing protein tyrosine phosphatase SHP-1 is induced by granulocyte colony-stimulating factor (G-CSF) and modulates signaling from the G-CSF receptor. *Leukemia* **14**, 1284-1291 (2000).

Warmuth, M., Kim, S., Gu, X.J., Xia, G. & Adrian, F. Ba/F3 cells and their use in kinase drug discovery. *Curr Opin Oncol* **19**, 55-60 (2007).

Warner, N.L., Moore, M.A. & Metcalf, D. A transplantable myelomonocytic leukemia in BALB-c mice: cytology, karyotype, and muramidase content. *J Natl Cancer Inst* **43**, 963-982 (1969).

Weissman, I.L. Stem cells: units of development, units of regeneration, and units in evolution. *Cell* **100**, 157-168 (2000).

Westerhoff, H.V. Signalling control strength. *J Theor Biol* **252**, 555-567 (2008).

Wickrema, A. & Crispino, J.D. Erythroid and megakaryocytic transformation. *Oncogene* **26**, 6803-6815 (2007).

Wormald, S., Zhang, J.G., Krebs, D.L., Mielke, L.A., Silver, J., Alexander, W.S., Speed, T.P., Nicola, N.A. & Hilton, D.J. The comparative roles of suppressor of cytokine signaling-1 and -3 in the inhibition and desensitization of cytokine signaling. *J Biol Chem* **281**, 11135-11143 (2006).

Wu, C., Sun, M., Liu, L. & Zhou, G.W. The function of the protein tyrosine phosphatase SHP-1 in cancer. *Gene* **306**, 1-12 (2003).

Wu, H., Liu, X., Jaenisch, R. & Lodish, H.F. Generation of committed erythroid BFU-E and CFU-E progenitors does not require erythropoietin or the erythropoietin receptor. *Cell* **83**, 59-67 (1995).

Xu, X., Sun, Y.L. & Hoey, T. Cooperative DNA binding and sequence-selective recognition conferred by the STAT amino-terminal domain. *Science* **273**, 794-797 (1996).

Yamada, S., Shiono, S., Joo, A. & Yoshimura, A. Control mechanism of JAK/STAT signal transduction pathway. *FEBS Lett* **534**, 190-196 (2003).

Yi, T., Mui, A.L., Krystal, G. & Ihle, J.N. Hematopoietic cell phosphatase associates with the interleukin-3 (IL-3) receptor beta chain and down-regulates IL-3-induced tyrosine phosphorylation and mitogenesis. *Mol Cell Biol* **13**, 7577-7586 (1993).

Yi, T., Zhang, J., Miura, O. & Ihle, J.N. Hematopoietic cell phosphatase associates with erythropoietin (Epo) receptor after Epo-induced receptor tyrosine phosphorylation: identification of potential binding sites. *Blood* **85**, 87-95 (1995).

Yoshikawa, H., Matsubara, K., Qian, G.S., Jackson, P., Groopman, J.D., Manning, J.E., Harris, C.C. & Herman, J.G. SOCS-1, a negative regulator of the JAK/STAT pathway, is silenced by methylation in human hepatocellular carcinoma and shows growth-suppression activity. *Nat Genet* **28**, 29-35 (2001).

Yoshimura, A., Ohkubo, T., Kiguchi, T., Jenkins, N.A., Gilbert, D.J., Copeland, N.G., Hara, T. & Miyajima, A. A novel cytokine-inducible gene CIS encodes an SH2-containing protein that binds to tyrosine-phosphorylated interleukin 3 and erythropoietin receptors. *EMBO J* **14**, 2816-2826 (1995).

Zhang, Q., Raghunath, P.N., Vonderheid, E., Odum, N. & Wasik, M.A. Lack of phosphotyrosine phosphatase SHP-1 expression in malignant T-cell lymphoma cells results from methylation of the SHP-1 promoter. *Am J Pathol* **157**, 1137-1146 (2000).

Zhang, Z., Shen, K., Lu, W. & Cole, P.A. The role of C-terminal tyrosine phosphorylation in the regulation of SHP-1 explored via expressed protein ligation. *J Biol Chem* **278**, 4668-4674 (2003).

Zi, Z., Cho, K.H., Sung, M.H., Xia, X., Zheng, J. & Sun, Z. In silico identification of the key components and steps in IFN-gamma induced JAK-STAT signaling pathway. *FEBS Lett* **579**, 1101-1108 (2005).

6 Appendix

6.1 Ordinary differential equations model to study JAK2/STAT5 amplification

Ordinary differential equations (in power law terms)

$$\frac{d}{dt}EJ = \gamma_1 - \gamma_2 \cdot EJ^{g_1} \cdot Epo^{g_2} - \gamma_1 \cdot EJ^{g_3} \quad (1)$$

$$\frac{d}{dt}pEpJ = \gamma_2 \cdot EJ^{g_1} \cdot Epo^{g_2} - \gamma_3 \cdot pEpJ^{g_4} \quad (2)$$

$$\frac{d}{dt}S = 2 \cdot \gamma_4 \cdot \left(DpS_{nc}(t-\tau)\right)^{g_5} - 2 \cdot \gamma_5 \cdot S^{g_6} \cdot pEpJ^{g_7} \quad (3)$$

$$\frac{d}{dt}DpS = \gamma_5 \cdot S^{g_6} \cdot pEpJ^{g_7} - \gamma_6 \cdot DpS^{g_8} \quad (4)$$

$$\frac{d}{dt}DpS_{nc} = \gamma_6 \cdot DpS^{g_8} - \gamma_4 \cdot \left(DpS_{nc}(t-\tau)\right)^{g_5} \quad (5)$$

Logarithmic amplification factor

To analyze how the Epo-induced signal is amplified through the JAK2/STAT5 pathway, the logarithmic amplification factor (*LA*) between the two activated intermediates *X** and *Y** was defined.

$$LA = \log\left(\frac{\int_0^T V^+_{Y^*}(t)dt}{\int_0^T V^+_{X^*}(t)dt}\right) \quad (6)$$

T is the duration of stimulation and *LA* is the logarithm of the ratio between the production of the two intermediates. The total production of an intermediate is described by the integral of the net activation rate during the stimulation process. Considering this definition, a system amplifies between two steps in the pathway when *LA* is higher than zero (Vera, Bachmann et al, 2008).

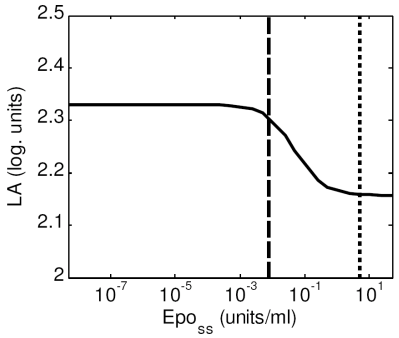

Fig. S1. Logarithmic amplification (LA) for different values of sustained Epo simuli. The LA was determined to analyze the amplification between the phosphorylated EpoR/JAK2 complex and phosphorylated STAT5 in the nucleus. The physiological serum concentration of Epo, (7.9×10^{-3} U/ml: long-dashed line) and the concentration of Epo used in the experiments (5 U/ml: short-dashed line) are indicated. Epo_{ss}: Epo (Vera et al., 2008).

6.2 Validation of time-resolved mRNA induction of SOCS3 and CIS by RT-PCR

Results from expression profiling by microarray analysis were validated for CIS and SOCS3 mRNA levels in CFU-E cells using quantitative RT-PCR. After stimulation of CFU-E cells with 5 U/ml Epo fold changes in CIS and SOCS3 mRNA levels were analysed for different timepoints. Relative concentrations were normalized using the second generation housekeeper HPRT as a reference (Vandesompele et al., 2002). The fold induction was calculated with respect to the expression at 0 h.

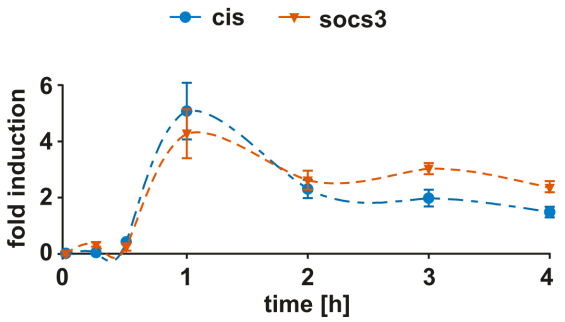

Fig. S2. Induction of Epo-induced mRNA levels of CIS and SOCS3 in CFU-E cells using quantitative RT-PCR. Fold changes in CIS and SOCS3 mRNA levels after stimulation of CFU-E cells with 5 U/ml Epo were analysed for different timepoints. Relative concentrations were normalized with HPRT and the fold induction was calculated with respect to the expression at 0 h.

6.3 Ordinary differential equation model of the JAK2/STAT5 pathway in CFU-E cells

Ordinary differential equations (ODE) are shown for the dynamic JAK2/STAT5 pathway model in primary CFU-E cells. Parameter values of the best fit including 1σ confidence intervals are displayed.

Ordinary differential equations

JAK2	$\dot{x}_1 = -k_1 \cdot u_1 \cdot x_1 / (1 + k_2 \cdot x_8) + k_5 \cdot x_2 \cdot x_6$
pJAK2	$\dot{x}_2 = +k_1 \cdot u_1 \cdot x_1 / (1 + k_2 \cdot x_8) + k_5 \cdot x_2 \cdot x_6$
EpoR	$\dot{x}_3 = -k_3 \cdot u_2 \cdot x_3 / (1 + k_2 \cdot x_8) + k_4 \cdot x_7) + k_6 \cdot x_4 \cdot x_6$
pEpoR	$\dot{x}_4 = +k_3 \cdot x_2 \cdot x_3 / (1 + k_2 \cdot x_8 + k_4 \cdot x_7) - k_6 \cdot x_4 \cdot x_6$
SHP1	$\dot{x}_5 = -1/(k_7 + x_5) \cdot x_5 \cdot x_4) + k_8 \cdot x_6$
SHP1_active	$\dot{x}_6 = +1/(k_7 + x_5) \cdot x_5 \cdot x_4) + k_8 \cdot x_6$
CIS	$\dot{x}_7 = +k_{14} \cdot x_{12} \cdot 0.275 / 0.4 - k_{15} \cdot x_7$
SOCS3	$\dot{x}_8 = +k_{16} \cdot x_{13} \cdot 0.275 / 0.4 - k_{17} \cdot x_8$
STAT5	$\dot{x}_9 = -k_9 \cdot x_2 \cdot x_9 \cdot (1 + k_{10} \cdot x_4 / (1 + k_{11} \cdot x_7)) / (1 + k_2 \cdot x_8) + k_{13} \cdot x_{11} \cdot 0.275) / 0.4$
pSTAT5	$\dot{x}_{10} = +k_9 \cdot x_2 \cdot x_9 \cdot (1 + k_{10} \cdot x_4 / (1 + k_{11} \cdot x_7)) / (1 + k_2 \cdot x_8) - k_{12} \cdot x_{10}$
npSTAT5	$\dot{x}_{11} = +k_{12} \cdot x_{10}) \cdot 0.4 / 0.275 - k_{13} \cdot x_{11}$
CIS_RNA	$\dot{x}_{12} = +(k_{14} \cdot x_{11} \cdot (1 - u_2)) / 0.275 - k_{14} \cdot x_{12}$
SOCS3_RNA	$\dot{x}_{13} = +(k_{16} \cdot x_{11} \cdot (1 - u_2)) / 0.275 - k_{16} \cdot x_{13}$

Parameters

k_1 JAK2 activation
k_2 inhibition by SOCS3
k_3 EpoR activation
k_4 EpoR inhibition by CIS
k_5 JAK2 deactivation by SHP-1
k_6 EpoR deactivation by SHP-1
k_7 SHP1 activation
k_8 SHP1 deactivation
k_9 STAT5 activation by JAK2
k_{10} STAT5 activation via EpoR
k_{11} STAT5 inhibition by CIS
k_{12} STAT5 import
k_{13} STAT5 export
k_{14} CIS expression
k_{15} CIS degradation
k_{16} SOCS3 expression
k_{17} SOCS3 degradation

Parameter values and confidence interval profile likelihood pointwise

Parameter	Best fit	
k_1 (pM^{-1} min^{-1})	0.0225	(0.0175 - 0.0321)
k_2 (min^{-1})	0.0624	(0.0532 - 0.0746)
k_3 (min^{-1})	0.0104	(7.7e-3 - 0.0139)
k_4 (min^{-1})	0.0440	(0.0314 - 0.0611)
k_5 (min^{-1})	0.1629	(0.0804 - 0.3610)
k_6 (min^{-1})	0.0380	(0.0224 - 0.0802)
k_7 (min^{-1})	97.837	(42.838 - 269.95)
k_8 (min^{-1})	0.0134	(9.7e-3 - 0.0176)
k_9 (min^{-1})	2.4e-4	(3.0e-5 - 4.43e-4)
k_{10} (min^{-1})	17.039	(91034 - 158.48)
k_{11} (min^{-1})	0.0166	(0.0104 - 0.0260)
k_{12} (min^{-1})	0.0628	(0.0520 - 0.0774)
k_{13} (min^{-1})	0.1280	(0.0904 - 0.1945)
k_{14} (min^{-1})	0.0126	(0.0111 - 0.0148)
k_{15} (min^{-1})	5.17e-3	(2.7e-3 - 7.852e-3)
k_{16} (min^{-1})	0.0107	(9.1e-3 - 0.0127)
k_{17} (min^{-1})	0.0216	(0.0157 - 0.0297)

6.4 Identifiability analysis

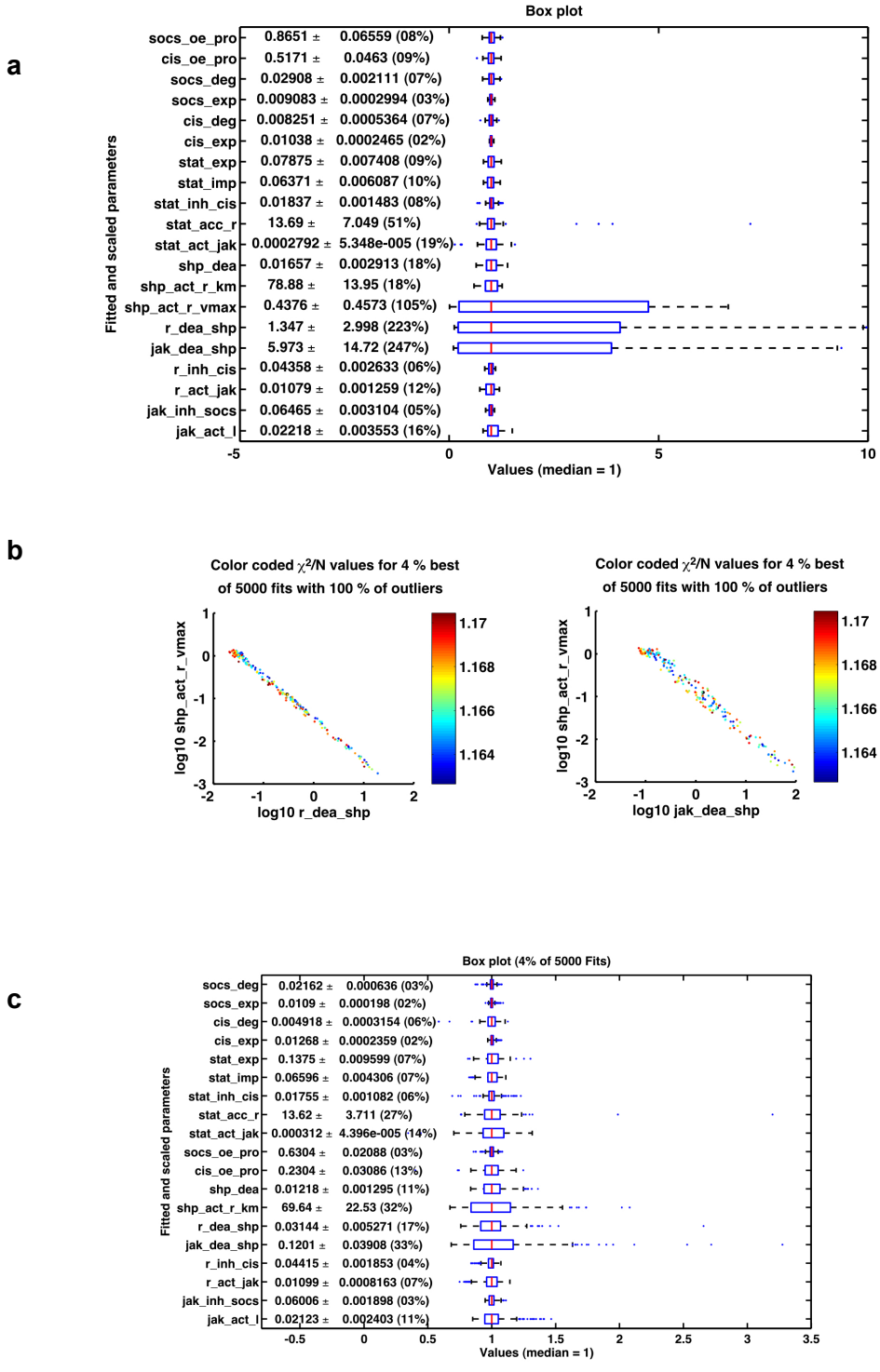

Fig. S3. Identifiablity analysis by fit sequence analysis. (a) Box plots of all estimated parameters are shown for the best 4% of 5000 fits. Three parameters have a standard deviation larger than 25%. **(b)** Non-parametric bootstrap-based algorithm for identifiability testing (NBI) revealed parameter dependencies for a set of two and three parameters, respectively. *SHP-1 activation by EpoR_vmax (shp_act_r_vmax)* show a linear relationship to *EpoR deactivation by SHP-1 (r_dea_shp) as well as to JAK2 deactivation by SHP-1 (jak_dea_shp).* **(c)** The parameter *SHP1 activation by EpoR_vmax* was fixed and parameter estimation was repeated. Box plots of all estimated parameters are shown for the best 4% of 5000 fits. All parameters show a standard deviation smaller than 35% (data provided by M.Schilling, DKFZ, Heidelberg).

6.5 Abbreviations

7-AAD	7-aminoactinomycin D
BFU-E	burst forming unit-erythroid
bp	base pairs
BSA	bovine serum albumin
CD	cluster of differentiation
cDNA	complementary DNA
CFU-E	colony forming unit-erythroid
CFU-GEMM	colony forming unit-granulocytes, erythrocytes, monocytes, macrophages
CIS	cytokine-inducible SH2 domain-containing protein
d	days postconception
DMEM	Dulbecco's modified eagle medium
DMSO	dimethyl sulfoxide
DNA	deoxyribonucleic acid
dNTP	deoxyribonucleotide triphosphate
Dox	doxycycline
DTT	dithiothreitol
E. coli	Escherichia coli
ECL	enhanced chemiluminescence
EDTA	ethylenediaminetetraacetic acid
EGFR	epidermal growth factor receptor
EGFP	enhanced green fluorescent protein
Epo	erythropoietin
EpoR	erythropoietin receptor
ER	endoplasmic reticulum
FACS	fluorescence activated cell sorter
FCS	fetal calf serum
FLC	fetal liver cells
g	g force
G418	geneticin
Gab	Grb2-associated binder
G-CSF	granulocyte colony-stimulating factor
GFP	green fluorescent protein
GHR	growth hormone receptor
Grb	growth factor receptor-bound protein
h	hours
HA	hemagglutinin

HBS	hepes buffered saline
HEPES	4-(2-Hydroxyethyl)piperazine-1-ethanesulfonic acid
HIF	hypoxia-inducible transcription factor
HRP	horseradish peroxidase
HSC	hematopoietic stem cell
IB	immunoblot
Ig	immunglobulin
IL	interleukin
IMDM	Isocove's modified Dulbecco's medium
IP	immunoprecipitation
JAK	Janus kinase
kDa	kilodalton
LB	Luria Bertani broth
M	molarity
MAPK	mitogen-activated protein kinase
min	minutes
ml	milliliter
µl	microliter
neo	neomycin resistance gene
nm	nanometer
o/n	over night
ODE	ordinary differential equations
PAGE	polyacrylamide gel electrophoresis
PBS	phosphate buffered saline
PCR	polymerase chain reaction
PDGFR	platelet-derived growth factor receptor
PE	phycoerythrin
Pfu	*Pyrococcus furiosus*
PI3K	phosphatidylinositol 3-kinase
PKB	protein kinase B
PKC	protein kinase C
puro	puromycin
rhEpo	recombinant human erythropoietin
rpm	rounds per minute
RT	room temperature
SBP	streptavidin-binding peptide
SCF	stem cell factor

SDS	sodium dodecyl sulfate
SH	Src homology
SHP	SH2 domain-containing protein tyrosine phosphatase
SOCS	suppressor of cytokine signaling
Sos	son of sevenless
STAT	signal transducer and activator of transcription
strep	streptavidin
TAE	Tris-acetate-EDTA
Taq	*Thermus aquaticus*
TB	Terrific broth
TBS	Tris buffered saline
TBST	Tris buffered saline with Tween-20
TE	Tris-EDTA
Tet	tetracycline
TfR	transferrin receptor
TM	transmembrane
TPO	thrombopoietin
Tris	Tris(hydroxymethyl)-aminomethane
U	unit of enzyme activity
WEHI	Walter and Eliza Hall Institute
w/v	weight per volume

6.6 Erklärung

Ich erkläre hiermit, dass ich die vorgelegte Dissertation selbst verfasst und mich dabei keiner anderen als der von mir ausdrücklich bezeichneten Quellen und Hilfen bedient habe.
Weiterhin erkläre ich hiermit, dass ich an keiner anderen Stelle ein Prüfungsverfahren beantragt bzw. die Dissertation in dieser oder anderer Form bereits anderweitig als Prüfungsarbeit verwendet oder einer anderen Fakultät als Dissertation vorgelegt habe.

Heidelberg, den 19.01.2009

Julie Bachmann